

2m4

NASA CONTRACTOR
REPORT

NASA CR-129019

CALCULATION OF EDDY VISCOSITY IN A
COMPRESSIBLE TURBULENT BOUNDARY
LAYER WITH MASS INJECTION AND
CHEMICAL REACTION

Volume I

By Satoaki Omori
University of Alabama Huntsville
Huntsville, Alabama

December 1973

Final Report



NASA-CR-129019-Vol-1) CALCULATION OF EDDY
VISCOSITY IN A COMPRESSIBLE TURBULENT
BOUNDARY LAYER WITH MASS INJECTION AND
CHEMICAL REACTION, VOLUME (Alabama Univ.,
Huntsville.) ~~102~~ p HC \$8.25 CSCL 20D

N74-17017

Unclas
29941

94
Prepared for

NASA-GEORGE C. MARSHALL SPACE FLIGHT CENTER
Marshall Space Flight Center, Alabama 35812

1. REPORT NO. NASA CR-129019		2. GOVERNMENT ACCESSION NO.		3. RECIPIENT'S CATALOG NO.	
4. TITLE AND SUBTITLE CALCULATION OF EDDY VISCOSITY IN A COMPRESSIBLE TURBULENT BOUNDARY LAYER WITH MASS INJECTION AND CHEMICAL REACTION Vol. I				5. REPORT DATE December 1973	
				6. PERFORMING ORGANIZATION CODE	
7. AUTHOR(S) Satoaki Omori				8. PERFORMING ORGANIZATION REPORT #	
9. PERFORMING ORGANIZATION NAME AND ADDRESS University of Alabama Huntsville Huntsville, Alabama				10. WORK UNIT NO.	
				11. CONTRACT OR GRANT NO. NCA 8-68; Mod. 7	
12. SPONSORING AGENCY NAME AND ADDRESS National Aeronautics and Space Administration Washington, D. C. 20546				13. TYPE OF REPORT & PERIOD COVERED Contractor; Final	
				14. SPONSORING AGENCY CODE	
15. SUPPLEMENTARY NOTES This research work was supported by NASA-George C. Marshall Space Flight Center UAH-MSFC Cooperative Agreement Modification No. 7.					
16. ABSTRACT <p>The turbulent kinetic energy equation is coupled with boundary layer equations to solve the characteristics of compressible turbulent boundary layers with mass injection and combustion. The Reynolds stress is related to the turbulent kinetic energy using the Prandtl-Wieghardt formulation. When a lean mixture of hydrogen and nitrogen is injected through a porous plate into the subsonic turbulent boundary layer of air flow and ignited by external means, the turbulent kinetic energy increases twice as much as that of noncombusting flow with the same mass injection rate of nitrogen. The magnitudes of eddy viscosity between combusting and noncombusting flows with injection, however, are almost the same due to temperature effects, while the distributions are different. The velocity profiles are significantly affected by combustion; that is, combustion alters the velocity profile as if the mass injection rate is increased, reducing the skin-friction as a result of a smaller velocity gradient at the wall.</p> <p>If pure hydrogen as a transpiration coolant is injected into a rocket nozzle boundary layer flow of combustion products, the temperature drops significantly across the boundary layer due to the high heat capacity of hydrogen. At a certain distance from the wall, hydrogen reacts with the combustion products, liberating an extensive amount of heat. The resulting large increase in temperature reduces the eddy viscosity in this region.</p>					
17. KEY WORDS			18. DISTRIBUTION STATEMENT Unclassified-unlimited <i>Klaus W. Gross</i>		
19. SECURITY CLASSIF. (of this report) Unclassified		20. SECURITY CLASSIF. (of this page) Unclassified		21. NO. OF PAGES 101 94	
				22. PRICE 8.25 NTIS	

FOREWORD

The present report is part of a two volume set which describes the calculation of eddy viscosity for boundary layer flows with mass injection and chemical reaction. Volume I contains the theoretical analysis and a discussion of the results obtained to date. Volume II includes the computer program and sample cases.

The concept and computer program can perform the calculations of the eddy viscosity for any case provided the boundary layer edge conditions and the wall temperature distribution are given. Primarily, however, the program was adopted for problems occurring in a regeneratively or transpiration cooled rocket thrust chamber.

Volumes I and II have been distributed according to the attached distribution lists.

This work was conducted under the Cooperative Agreement between the University of Alabama in Huntsville and the Marshall Space Flight Center, National Aeronautics and Space Administration, Modification 7, NCA 8-68.

The author gratefully acknowledges the supply of data and helpful discussions with Mr. Klaus W. Gross, and the assistance in computer programming and checking of Mr. Alfred N. Krebsbach, George C. Marshall Space Flight Center.

TABLE OF CONTENTS

INTRODUCTION	2
BASIC EQUATIONS	3
TURBULENT KINETIC ENERGY EQUATION	5
SOLUTION METHOD	8
EFFECT OF CHEMICAL REACTION IN THE SUBSONIC BOUNDARY LAYER DUE TO 4% HYDROGEN INJECTION	12
EFFECT OF PURE HYDROGEN INJECTION INTO THE SUPERSONIC BOUNDARY LAYER	18
CONCLUSIONS	22
SYMBOLS	24
REFERENCES	27
FIGURES	30
TABLE	61
APPENDIX A - TURBULENT BOUNDARY LAYER EQUATIONS	62
APPENDIX B - TURBULENT KINETIC ENERGY EQUATION	80
DISTRIBUTION LIST	89

LIST OF ILLUSTRATIONS

Figure	Title	Page
1.	Eddy Viscosity Profiles for Muzzy's Experiments.....	30
2.	Eddy Viscosity Profiles for Klebanoff's Experiments.....	31
3.	Relation between the Constant γ and Mass Injection Ratio F	32
4.	Eddy Viscosity Profiles for Squire's Experiments.....	33
5.	Turbulent Kinetic Energy and Boundary Layer Thicknesses for Squire's Experiments.....	34
6.	Air Flow with Combustion due to Injection of a Mixture of Hydrogen and Nitrogen	35
7.	Velocity, Momentum, and Displacement Thicknesses.....	36
8.	Eddy Viscosity Profiles.....	37
9.	Non-Dimensionalized Eddy Viscosity Profiles with Combustion	38
10.	Non-Dimensionalized Eddy Viscosity Profiles without Combustion	39
11.	Temperature and Velocity Profiles with Combustion.....	40
12.	Velocity and Density Profiles.....	41
13.	Mass Flow Profiles	42
14.	Turbulent Kinetic Energy Profiles.....	43
15.	Friction Profiles	44
16.	Distributions of Element Mass Fraction at the Wall.....	45
17.	Mixture Ratio Profiles	46
18.	Species Mass Fraction Profiles.....	47
19.	Distributions of Skin Friction and Its Coefficient.....	48

LIST OF ILLUSTRATIONS

Figure	Title	Page
20.	250K Thrust Chamber Geometry of Pratt & Whitney Aircraft.....	49
21.	Input Distributions of Gas-side Wall Temperature and Pressure.....	50
22.	Input Distribution of Mass Injection Rate.....	51
23.	Calculated Distributions of Velocity Thickness.....	52
24.	Calculated Distributions of Momentum and Displacement Thicknesses	53
25.	Comparison of Eddy Viscosities with and without Hydrogen Injection.....	54
26.	Velocity Profiles with Hydrogen Injection.....	55
27.	Temperature Profiles with Hydrogen Injection.....	56
28.	Comparison of Velocity Profiles with and without Hydrogen Injection at $M = 2.8$	57
29.	Comparison of Temperature Profiles with and without Hydrogen Injection at $M = 2.8$	58
30.	Comparison of Turbulent Kinetic Energy Profiles with and without Hydrogen Injection at $M = 2.35$ and 2.8	59
31.	Comparison of Eddy Viscosity Profiles with and without Hydrogen Injection at $M = 2.35$ and 2.8	60

LIST OF TABLES

Table	Title	Page
I	Effects of Mass Injection and Combustion on Boundary Layer Characteristics at $x = 76.2$ cm.....	61

CALCULATION OF EDDY VISCOSITY IN A COMPRESSIBLE TURBULENT
BOUNDARY LAYER WITH MASS INJECTION AND CHEMICAL REACTION

Volume I

Introduction

This paper presents the results of recent efforts to calculate the eddy viscosity and the effect of mass injection into the boundary layer including chemical reactions.

Although the modified van Driest-Clauser eddy viscosity model by Cebeci et al.¹ provides good results for external air flow, the adequacy of this model for nozzle flow with combustion products and a strongly cooled wall has not yet been verified due to limited experimental data. Even for nozzle air flow the modified van Driest-Clauser eddy viscosity model does not show the experienced relaminarization tendency in the nozzle convergent section and exhibits an unrealistic decrease of eddy viscosity downstream of the throat toward the nozzle exit.²

In order to include the effects of the past history of flow and the strong temperature variation across the boundary layer due to chemical reaction or wall cooling, the turbulent kinetic energy equation has been introduced for the solution of the Reynolds stress in this study. A kinetic energy approach was conducted for incompressible flow by Rotca³, Glushko⁴, Bradshaw et al.⁵, Donaldson⁶, Maise and McDonald⁷, and Beckwith and Bushnell⁸. Patankar and Spalding⁹ calculated compressible turbulent boundary layer flow with a similar method but could not attain satisfactory agreements of the skin friction and the heat transfer results with experimental measure-

ments.

In this analysis, the Reynolds stress and the turbulent kinetic energy are related with the gradient of mean velocity according to Prandtl and Wieghardt¹⁰. The turbulent kinetic energy equation, derived from the Navier-Stokes equations, is simplified according to Rotta^{3,11}. The constants in the reduced form of the turbulent kinetic energy equation are obtained from iterations of numerical calculations and comparisons of results with available experimental data for incompressible flow with or without mass injection, assuming the compressibility effects hidden in these constants to be negligible. The profile of the eddy viscosity across boundary layers and boundary layer thicknesses calculated for supersonic flow of $M = 2.5$ are in good agreement with experimental data by Squire^{12,13}. Calculations are also performed for subsonic air flow with injection of pure nitrogen or a mixture of 4% hydrogen mixed with nitrogen, and for the hydrogen-oxygen combustion product flow in a nozzle with hydrogen injection. The effects of wall cooling and heating are also investigated for the flow without mass injection.

The solution method was based on the Crank-Nicolson implicit finite difference technique¹⁴ and the chemical reaction was assumed to be in local shifting equilibrium.

Basic Equations

The compressible turbulent boundary layer equations² for steady state and two-dimensional and axisymmetric flows are presented in a

curvilinear coordinate system, neglecting the transverse-curvature effect. The derivation of equations is shown in Appendix A and B.

Continuity

$$\frac{\partial}{\partial x} (\bar{\rho} \bar{u} r_w^j) + \frac{\partial}{\partial y} \left[(\bar{\rho} \bar{v} + \overline{\rho' v'}) r_w^j \right] = 0 \quad (1)$$

Momentum

$$\bar{\rho} \bar{u} \frac{\partial \bar{u}}{\partial x} + (\bar{\rho} \bar{v} + \overline{\rho' v'}) \frac{\partial \bar{u}}{\partial y} = - \frac{dP}{dx} + \frac{\partial}{\partial y} \left[(\mu + \epsilon) \frac{\partial \bar{u}}{\partial y} \right] \quad (2)$$

Energy

$$\begin{aligned} \bar{\rho} \bar{u} \frac{\partial \bar{H}}{\partial x} + (\bar{\rho} \bar{v} + \overline{\rho' v'}) \frac{\partial \bar{H}}{\partial y} = \frac{\partial}{\partial y} \left\{ \left(\frac{\mu}{Pr} + \frac{\epsilon}{Pr_T} \right) \frac{\partial \bar{H}}{\partial y} + \left[\mu \left(1 - \frac{1}{Pr} \right) \right. \right. \\ \left. \left. + \epsilon \left(1 - \frac{1}{Pr_T} \right) \right] \bar{u} \frac{\partial \bar{u}}{\partial y} + \sum_{i=1}^n \left[\frac{\mu}{Pr} (Le-1) + \frac{\epsilon}{Pr_T} (Le_T-1) \right] \bar{h}_i \frac{\partial \bar{Y}_i}{\partial y} \right\} \quad (3) \end{aligned}$$

Element

$$\bar{\rho} \bar{u} \frac{\partial \bar{\alpha}_m}{\partial x} + (\bar{\rho} \bar{v} + \overline{\rho' v'}) \frac{\partial \bar{\alpha}_m}{\partial y} = \frac{\partial}{\partial y} \left[\left(\frac{\mu L}{Pr} + \frac{\epsilon Le_T}{Pr_T} \right) \frac{\partial \bar{\alpha}_m}{\partial y} \right] \quad (4)$$

where $j = 0$ for two-dimensional flow and $j = 1$ for axisymmetric flow.

The eddy viscosity, ϵ , is defined as

$$\epsilon = - \overline{(\rho v)' u'} / (\partial \bar{u} / \partial y). \quad (5)$$

The flow is assumed to be calorically perfect and obeys the equation of state,

$$\bar{P} = \frac{\bar{\rho} \bar{R} \bar{T}}{M} \quad (6)$$

where the time mean of the correlation between fluctuating density and temperature, $\overline{\rho' T'}$, is neglected because of its small order of magnitude as stated by Harvey et al.¹⁵

Turbulent Kinetic Energy Equation

Considering the continuity and momentum equations for compressible turbulent boundary layers, the system of turbulent fluctuation equations is written² in the cartesian tensor notation as

$$\begin{aligned}
 & \overline{(\rho u_k)' u_j'} \frac{\partial \bar{u}_i}{\partial x_k} + \overline{(\rho u_k)' u_i'} \frac{\partial \bar{u}_j}{\partial x_k} + (\bar{\rho} \bar{u}_k + \overline{\rho' u_k'}) \frac{\partial \overline{u_i' u_j'}}{\partial x_k} + \frac{\partial \overline{(\rho u_i' u_j' u_k')}}{\partial x_k} \\
 & = - \left(\frac{\partial \overline{p' u_i'}}{\partial x_i} + \frac{\partial \overline{p' u_j'}}{\partial x_j} \right) + \overline{p'} \left(\frac{\partial \bar{u}_i}{\partial x_i} + \frac{\partial \bar{u}_j}{\partial x_j} \right) \\
 & + \frac{\partial}{\partial x_k} \left(\mu \frac{\partial \overline{u_i' u_j'}}{\partial x_k} \right) - 2\mu \frac{\partial \bar{u}_i}{\partial x_k} \frac{\partial \bar{u}_j}{\partial x_k} \quad (7)
 \end{aligned}$$

Introducing the previous three equations in Eq. (7) for $i = j = 1, 2$, and 3 , and defining the turbulent kinetic energy as $K = \overline{u' u'} + \overline{v' v'} + \overline{w' w'}$, the following turbulent kinetic energy equation is obtained², using Rotta's assumptions,^{3, 11} to model the turbulent diffusion and dissipation terms.

$$\begin{aligned}
 \bar{\rho} \bar{u} \frac{\partial K}{\partial x} + (\bar{\rho} \bar{v} + \overline{\rho' v'}) \frac{\partial K}{\partial y} & = - 2 \overline{(\rho v)' u'} \frac{\partial \bar{u}}{\partial y} + \frac{\partial}{\partial y} \left[(\mu + \alpha \rho \Lambda K^{1/2}) \frac{\partial K}{\partial y} \right] \\
 & - \bar{\rho} \mu \beta \frac{K}{\Lambda^2} - \gamma \frac{\bar{\rho} K^{3/2}}{\Lambda} \quad (8)
 \end{aligned}$$

In Eq. (8) α , β , and γ are constants, and Λ is the dissipation length.

In order to relate the Reynolds stress, $-\overline{(\rho v)' u'}$, with the kinetic energy, K , the Prandtl-Wieghardt formula¹⁰ is utilized

$$-\overline{(\rho v)' u'} = k \bar{\rho} \Lambda K^{1/2} \left| \frac{\partial \bar{u}}{\partial y} \right| \quad (9)$$

The equations can be solved in closed form, when the previous three constants, the constant, k , and the dissipation length, Λ , which is a function of the distance from a wall, are known.

For the ideal (one component) gas, only the equations of continuity, momentum, energy, turbulent kinetic energy, and state must be considered, and terms including the species gradient can be deleted from Eq. (3). In calculating air flow without chemically reactive mass injection the Prandtl number is assumed to be constant, and the molecular viscosity is considered to follow the Sutherland law:

$$\mu = 2.27 \times 10^{-8} T^{1/2} (1 + 198.6/T)^{-1} \quad (10)$$

The turbulent Prandtl number is calculated based on the formula by Cebeci:¹⁶

$$Pr_T = \frac{0.4}{0.44} \frac{[1 - \exp(-y^+/\Lambda^+)]}{[1 - \exp(-y^+ Pr_r^{1/2}/B^+)]} \quad (11)$$

At the wall, $y = 0$, Eq. (11) reduces to

$$Pr_T = \frac{0.4}{0.44} \frac{B^+}{\Lambda^+} Pr_r^{-1/2} \quad (12)$$

For a combustible gas mixture the molecular viscosity, μ , is calculated from Wilke's semi-empirical formula;¹⁷

$$\mu = \sum_{i=1}^{n_s} \mu_i \left(1 + \sum_{\substack{j=1 \\ j \neq i}}^{n_s} \varphi_{ij} X_j/X_i \right)^{-1} \quad (13)$$

and the thermal conductivity is obtained according to Mason and Saxena,¹⁸

$$\lambda = \sum_{i=1}^{n_s} \lambda_i \left(1 + 1.065 \sum_{j=1}^{n_s} \varphi_{ij} X_j / X_i \right)^{-1} \quad (14)$$

where the viscosity of each specie, μ_i , is taken from Svehla¹⁹ as in Reference 14. The laminar Prandtl number is internally obtained from

$$P_r = \mu \left(\sum_{i=1}^n \bar{Y}_i \bar{C}_{P_i} \right) / \lambda \quad (15)$$

and the turbulent Prandtl number is calculated as in the ideal gas case. To simplify the calculation the laminar and turbulent Lewis numbers are assumed to be unity. The system of equations (1) through (8) is solved including the locally shifting chemical equilibrium calculation²⁰ to relate element and species mass fraction, enthalpy, specific heat, and temperature for a given pressure and assigned enthalpies, h_i° .

The boundary conditions are:

at the wall, $y = 0$;

$$\bar{u}(x, 0) = 0$$

$$\bar{\rho} \bar{v} + \overline{\rho' v'} = \dot{m}_w(x)$$

$$\bar{T}(x, 0) = \bar{T}_w(x)$$

$$\left(\partial \bar{\alpha}_m / \partial y \right)_{y=0} = \dot{m}_w (\bar{\alpha}_{m_w} - \bar{\alpha}_{m_I}) P_{r_w} / \mu_w Le_w$$

$$K(x, 0) = 0 \quad (16)$$

at the outer edge of boundary layer, $y \rightarrow \infty$;

$$\bar{u}(x, \infty) = U_e(x)$$

$$\bar{T}(x, \infty) = \bar{T}_e(x)$$

$$\bar{\alpha}_m(x, \infty) = \bar{\alpha}_{me}(x)$$

$$K(x, \infty) = 0 \quad (17)$$

Solution Method

In reference to experiments by Bradshaw and Ferriss²¹ for incompressible flow, and assuming the compressibility effect on the dissipation length to be negligible, the dissipation length, Λ , is modeled as

$$\Lambda / \delta = 0.205 (y/\delta)^3 - 0.586 (y/\delta)^2 + 0.431 (y/\delta) \quad (18)$$

To avoid occasional negative results of the turbulent kinetic energy K in the vicinity of the wall, the boundary layer is subdivided into a region very close to the wall and the wake region, since the turbulent dissipation terms exceed the remaining terms in Eq. (8) due to the combination of constants close to the wall. Considering the effect of the molecular viscosity in Eq. (8) to be small, the following term can be neglected:

$$\frac{\partial}{\partial y} \left(\mu \frac{\partial K}{\partial y} \right) - \bar{\rho} \mu \beta \frac{K}{\Lambda^2}$$

The eddy viscosity for the wake region results obtained from Eqs. (5) and (9) is:

$$\epsilon_0 = k \bar{\rho} \Lambda K^{1/2} \left| \frac{\partial \bar{u}}{\partial y} \right| / \left(\frac{\partial \bar{u}}{\partial y} \right) \quad (19)$$

Close to the wall the modified van Driest model¹ based upon the Prandtl mixing length theory is applied, and the inner eddy viscosity yields:

$$\epsilon_i = \bar{\rho} \ell^2 \left| \frac{\partial \bar{u}}{\partial y} \right| \quad (20)$$

with the mixing length,

$$\ell = 0.40 y [1 - \exp(-y/\Lambda)] \quad (21)$$

The van Driest "Damping factor, Λ ," includes the effect of suction or mass addition and pressure gradient as indicated by Cebeci¹.

The inner eddy viscosity, ϵ_i , is used adjacent to the wall until the height at which $\epsilon_0 = \epsilon_i$ is reached at each axial station. From that point to the boundary layer edge, the outer eddy viscosity formulation is utilized.

The three remaining constants in the system of equations are assigned the following values:

$$\alpha = 0.1/K$$

$$k = 0.6$$

$$\gamma = 0.36$$

After relating α and k by the indicated formulation² the constant values for k and γ were obtained from numerical calculations, based upon a trial and error iteration, which matched experimental data

by Muzzy²² for subsonic air flow without mass addition, especially the measured eddy viscosity (Fig. 1). Calculation was initiated 150 cm upstream of the measurement location to match the given velocity thickness 90 cm downstream of the computation start point which was considered to be the virtual origin of the non-blowing turbulent boundary layer. In Muzzy's experiment²² the large-scale disturbances were artificially created by sandpaper upstream in the test section.

In order to assess the validity of the present concept, calculations were performed for comparisons with Klebanoff's experiments.²³ He also used artificial thickening of the turbulent boundary layer by covering the first 60 cm of a vertically mounted flat plate with sandpaper. Comparison of the measured data and the calculated results were made 315 cm downstream from the leading edge. According to Klebanoff²³ the turbulent boundary layer virtually originates 430 cm upstream of the test station. Thus computation was started at this virtual origin. The experimental free stream velocity and momentum Reynolds number are $U_e = 10.67\text{m/sec}$, and $R_\theta = 6900$, respectively. The calculated Reynolds number is $R_\theta = 6960$. The analytically calculated eddy viscosities and their corresponding measured values²³ are presented in Fig. 2. The agreement with Klebanoff's data is satisfactory.

Since Muzzy's experiments²² include uniform nitrogen gas injection from a 60 cm long porous wall, calculations were conducted to obtain the relation between the constant, γ , and the non-dimensionalized

mass injection rate, $F = \dot{m}_w / \rho_e U_e$. As shown in Figs. 1 and 3, variation of the constant γ for a given mass injection rate provided good simulations of measured values.

So far subsonic flow was considered. Verifying the assumption that compressibility effects on the dissipation length and the constants are negligible, analytical results were compared with data^{12, 13} for compressible flow of $M = 2.5$. As Figs. 4 and 5 indicate, the calculated results are in good agreement with measured values by Squire.^{12, 13} Differences between the calculated and measured eddy viscosities non-dimensionalized with the boundary layer thickness $\delta_{0.995}$ are within experimental tolerances (Fig. 4). In using the displacement thickness δ^* in the non-dimensionalized eddy viscosity term, it becomes evident that the effect of mass injection disappears. This, however, is only true for a constant wall temperature, which was present in Squire's case ($T_w = 295^\circ\text{K}$). Different constant wall temperatures would indicate a pronounced effect, since the displacement thickness is strongly affected by the wall temperature. In Fig. 5, calculated boundary layer thicknesses are compared with measured values by Squire for a case without mass injection. The agreements are remarkably good. The curve shows the profile of the turbulent kinetic energy calculated.

Effect of Chemical Reaction in the Subsonic Boundary

Layer Due to 4% Hydrogen Injection

To investigate the effect of combustion on the turbulent intensity, the eddy viscosity, and other boundary layer profiles, hydrogen gas diluted by nitrogen gas is uniformly injected from a porous wall into the turbulent boundary layer, outside of which dry air is flowing with the constant velocity of 10.67m/sec. Wooldrige and Muzzy,²⁴ and Jones and Isaacson²⁵ conducted such experiments, in which the hydrogen gas injected is diluted to 4% by nitrogen gas. The severe environment, high temperatures due to strong chemical reaction in the boundary layer, prevented them to measure eddy viscosities. In their experiments the virtual origin of turbulent boundary layer is far upstream of the porous plate and depends on the mass injection rate.

In order to understand the effects of mass injection and combustion on the boundary layer characteristics well and save computation time, the present study analyzes the flow without mass injection and the case that the mass, $\bar{m}_w = 0.0044\text{g}/(\text{sec. cm}^2)$ is evenly injected through a 76.2 cm long porous plate, with a leading edge. Two modes of mass injection are considered the injectants are 100% nitrogen gas and a mixture of 4% hydrogen and 96% nitrogen gases by weight. The free stream velocity, U_e , is 10.67m/sec, the pressure, $P_e = 1 \text{ atm}$, and the temperature, $T_e = 295^\circ\text{K}$. Thus, the mass injection ratio if $F = \bar{m}_w / \rho_e U_e = 0.0035$.

The wall temperature distribution shown in Fig. 6, is almost the same as measured by Wooldrige and Muzzy.²⁴ For the chemical reaction calculation, the following nine species are considered as combustion products: H, H₂, H₂O, O, OH, O₂, N, NO, and N₂.

Calculated results of boundary layer thicknesses are shown in Fig. 7. At $x = 60$ cm the 100% nitrogen injection increases the velocity thickness, δ , to approximately 70% of the non-blowing velocity thickness, while the combustion due to 4% hydrogen injection causes an additional 70% increase in velocity thickness compared with the case of 100% nitrogen injection. Combustion significantly increases the velocity thickness.

The momentum thicknesses, θ , for the flows with and without combustion differ but are in a close range, while the displacement thickness, δ^* , in the combusting flow is twice as thick as the corresponding non-combustion value. The momentum thickness, θ , is reduced due to combustion.

The eddy viscosity profiles are shown in Fig. 8 at three axial stations for combusting and non-combusting flows. The magnitudes of eddy viscosity for both flows are almost the same. The distributions, however, are different. The eddy viscosity profile without mass injection at $x = 76.2$ cm illustrates that both the magnitude and distribution are quite different from those of the other two cases with mass injection. The peak values of eddy viscosity with

mass injection, with or without combustion, is twice as great as the value without injection. If the eddy viscosity is shown in a non-dimensional coordinate system, such as Figs. 9 and 10, the effect of combustion on the eddy viscosity profile is almost concealed. Profiles of temperature and velocity are shown in Fig. 11. In this graph, the non-combusting flow has negative gradients of temperature and higher velocity gradients at the wall than those of combusting flow. It is evident that combustion in the boundary layer plays a similar role as injection of mass at the wall, reducing the eddy viscosity close to the wall (Figs. 9 and 10). The eddy viscosity close to the wall, Fig. 10, is large for non-combusting case, but smaller for combusting flow, Fig. 9. This means temperature affects the eddy viscosity. Comparing the temperature profiles in Fig. 11 with those measured by Wooldrige and Muzzy²⁴ and Jones and Isaacson,²⁵ one can deduce that the shifting equilibrium assumption is valid for the combustion of hydrogen with air. The flame zone shown by their experiments is very thin.

The difference between the velocity and density profiles in a combusting layer and those for a non-combusting layer are illustrated in Fig. 12. The second derivative of velocity for the combusting flow is positive below and around the flare sheet, while that for the non-combusting flow is negative across the boundary layer. This result coincides with the experimental velocity profile by Jones and Isaacson.²⁵ Downstream at the axial distance of $x = 50.8$ cm the velocity profiles of the combusting flow tend to collapse

towards a single curve, but the density profiles are still non-similar. The three velocity curves in Fig. 12 for the cases without injection show that heating of the wall is equivalent to injecting mass at the wall.

To understand the great difference of displacement thickness, δ^* , between the combusting and non-combusting flows, mass flow profiles are exhibited in Fig. 13. It is obvious that the mass flow profiles differ significantly for two cases with injection due mainly to the difference of density profiles (Fig. 12). Temperature increase due to the combustion is a cause of thickening the displacement thickness, δ^* . The velocity distribution, as shown in Fig. 11, is effected by both the distributions of eddy viscosity and density, increasing the velocity thickness (Fig. 7). Thus the mass flow profile has a dual effect of density, directly and indirectly. The curve without mass injection, which is below the profile with 100% nitrogen injection, shows that the displacement thickness increases due to mass injection considering the definition of displacement thickness. Effects of mass injection and combustion on boundary layer characteristics are summarized at $x = 76.2$ cm in Table I.

In Figs. 8, 9, and 10, the magnitudes of eddy viscosity for combusting and non-combusting flows are very close while the distributions were different. This seems to indicate that combustion does not increase the eddy viscosity. The turbulent kinetic energy, however, increases significantly due to mass injection and combustion as shown in Fig. 14.

This figure indicates that the mass injection increases the turbulent intensity by 50% and combustion with 4% hydrogen injection enhances it almost three times as much as the peak intensity without injection. Thus, it may be concluded that in spite of the increase of turbulent kinetic energy due to combustion the decrease of density prohibits the increase of eddy viscosity. Considering Eq. (19), the eddy viscosity is proportional to the density and the square root of the turbulent kinetic energy. Thus, the effect of the density distribution is more significant than the turbulent kinetic energy. Comparing curves without mass injection in Fig. 14, we notice that the heated wall decreases the turbulent kinetic energy close to the wall.

The friction profiles at $x = 76.2$ cm are compared for the combusting and non-combusting flows in Fig. 15. The skin friction of combusting flow is only 16% compared with non-combusting flow, because the velocity gradient at the wall of combusting flow is much smaller than that of non-combusting flow as shown in Fig. 11. The value of skin friction, τ_w , for flow without injection of course has the largest value as shown in Fig. 15. In Table I and Fig. 12, the skin-friction τ_w , is also reduced when the wall temperature increased.

It requires a long distance for the combusting flow to reach an almost equilibrium profile. As shown in Fig. 12, velocity profiles were almost equilibrium downstream of $x = 50.8$ cm, but density profiles were still non-equilibrium. The distributions of element mass fractions

at the wall are shown in Fig. 16. The equilibrium condition at the wall is attained around $x = 50$ cm. The small change downstream of $x = 50$ cm is due to the wall temperature distribution.

The profiles of mixture ratio, F/θ , are shown in Fig. 17, where the mixture ratio is defined as the ratio of hydrogen element to the sum of oxygen and nitrogen elements by weight. Fig. 18 shows the species mass fraction profiles at $x = 76.2$ cm. The mass fractions of H_2 , H_2O , and N_2 at the wall are $Y_{H_2} = 0.012$, $Y_{H_2O} = 0.228$, and $Y_{N_2} = 0.760$, respectively.

Fig. 19 shows the distributions of skin friction coefficient, C_f , and skin friction, τ_w , in flow direction. As known already from the velocity profiles, the skin friction is reduced significantly due to combustion in the boundary layer. Table I also indicates that the skin friction with 100% N_2 injection drops to about one-third of the value of isothermal flow without injection. The skin friction of combusting flow is less than 10% of the value of the isothermal case without injection. Even without mass injection, the skin friction becomes smaller for higher wall temperatures and increases for cooled walls. The effects of cooler walls on velocity profiles are shown in Fig. 12, that is, the velocity curve indicates that the cold wall has a similar effect on the velocity profile as suction at the wall. We have already known that a hot wall plays a similar role to mass injection. Referring to Fig. 14 again and the velocity thickness shown in Table I, the turbulent kinetic energy has a smaller value close to the wall for a hot wall compared with a cold wall. The same can be said of eddy viscosities, Fig. 8,

where the eddy viscosity without injection and with a cold wall is larger close to the wall than for a hot wall. Thus, the velocity gradient at the cold wall is steeper than for the hot wall (Fig. 12). As mentioned previously the velocity profile is affected through both the eddy viscosity and density profile.

If the weight percentage of hydrogen in the gas mixture injected increases to 8% or more using the same mass injection rate as before, the boundary layer is blown off as a result of zero velocity gradient at the wall at a certain distance from the leading edge.

Effect of Pure Hydrogen Injection into the Supersonic Boundary Layer

The flow characteristics in nozzles with divergent half angles of 10° and 15° and with uniform hydrogen injection at the wall were investigated by Omori.² The present study was performed on the boundary layer flow in a rocket nozzle with the divergent half angle of 31.5° and the variable mass injection rate of pure hydrogen along the nozzle contour.

The thrust chamber geometry, a nozzle built by Pratt & Whitney Aircraft, is shown in Fig. 20. The chamber stagnation pressure, P_0 , is $2.135 \times 10^7 \text{ N/m}^2$ (3097 Psia); the temperature, $T_0 = 3680^\circ\text{K}$, and the mixture ratio of oxygen to hydrogen, $O/F = 6.29$. The experimental distributions of the static pressure and the wall temperature with hydrogen injection are shown along the nozzle axis in Fig. 21. As shown in Fig. 22, the

hydrogen injection rate is uneven in axial direction with the highest rate around the nozzle throat. Using these distributions and the chamber initial conditions outlined above, calculated results of the boundary layer velocity, momentum, and displacement thicknesses are illustrated in Figs. 23 and 24 for two cases with and without injection, where the same wall temperature distribution in Fig. 21 was assumed even in the case without injection.

For the flow without injection, the velocity boundary layer thickness (Fig. 23) decreases in the nozzle convergent section due to the reduction of eddy viscosity in flow direction for reasons shown in Fig. 25. The velocity boundary layer thickness with hydrogen injection in Fig. 23, however, has an irregular distribution because of the uneven mass injection. In the nozzle divergent section the velocity thickness without injection increases in flow direction except for a small disturbance which is caused by the wall temperature distribution. It is noted from Fig. 23 that the effects of hydrogen injection and upstream history on the velocity boundary layer thickness are significant. Fig. 24 indicates that both momentum and displacement thicknesses are greatly affected by hydrogen injection. The reason for the momentum thickness to become negative with hydrogen injection, Fig. 22, is explained below. With injection, the temperature across the boundary layer decreases due to the high heat capacity of hydrogen. The hydrogen injected reacts with combustion products generating heat. This heat energy is consumed to accelerate the flow with an over-

shoot in the boundary layer as well as to increase the temperature gradient over a certain distance from the wall (Figs. 26, 27, and 28). This velocity overshoot shown in Figs. 26 and 28 is caused by the combined effects of the favorable pressure gradient of the free-stream and the chemical reaction due to hydrogen injection in the boundary layer (Jones and Isaacson²⁵). As Fig. 28 shows, the skin friction coefficient increases with hydrogen injection and chemical reaction in the flow with a favorable pressure gradient. The velocity gradient at the wall in Figs. 26 and 28 is greater for the flow with injection than without injection. Fig. 27 shows temperature profiles in the subsonic region, and Fig. 29 in the supersonic region.

Profiles of the turbulent kinetic energy are shown in Fig. 30. The turbulent kinetic energy without injection has a smaller value than that with hydrogen injection except in the immediate vicinity of the wall. It is evident from Figs. 29 and 30 that the turbulent kinetic energy distribution is related to temperature. Fig. 5 showed results of a nozzle air flow with wall temperatures at room condition and lower free-stream temperature. The curves in Fig. 30 are the results of the accelerated nozzle flow with the wall temperature of 1056°K and the free-stream temperature 2376°K.

Eddy viscosity profiles in the supersonic region are shown in Fig. 31. Both the magnitude and the distribution of eddy viscosities differ considerably between the flows with hydrogen injection and without injection. The magnitude of eddy viscosity increases due to

hydrogen injection. This result is contrary to a previous report by this author,² where the mass injection rate was even. The present nozzle, however, has a peak injection rate of $\dot{m}_w = 2.2\text{g}/(\text{cm}^2 \cdot \text{sec})$ around the throat (Fig. 22) and a larger nozzle half angle. This uneven injection and the difference of nozzle geometry, which causes the different favorable pressure gradient in flow direction, are believed to increase the eddy viscosity. The eddy viscosity profile with hydrogen injection has a minimum point in the middle of the boundary layer, where the temperature increases sharply due to the chemical reaction of injected hydrogen with combustion products.

Conclusions

Coupling the turbulent kinetic energy equation with boundary layer equations, the characteristics of compressible turbulent boundary layer flows are solved for cases with or without mass injection and combustion. The mechanism of turbulence has been considered in such a way that the variation of turbulent production, diffusion, dissipation terms in the turbulent kinetic energy equation were examined by changing the constants until the results would simulate Muzzy's experimental data. After obtaining the relations for each term in the turbulent kinetic energy equation as mentioned above, this modeling of the turbulent kinetic energy equation was verified, comparing the calculated results with subsonic and supersonic experimental data by Klebanoff and Squire, respectively.

To investigate the effect of combustion in subsonic flow, a calculation was performed for air flow with mass injection of 4% hydrogen. It was found that combustion significantly induces turbulence. The magnitude of eddy viscosity in the combusting flow is almost the same as that in non-combusting flow with the same mass injection rate of pure nitrogen, while the distribution of eddy viscosity differs. This is attributed to the difference in temperature profiles between combusting and non-combusting flows. Combustion has a similar effect on the velocity profile as if the mass injection rate is increased. That is, the combusting flow has a smaller velocity gradient at the wall than the

non-combusting flow with the same mass injection rate. As a result, the skin friction of combusting flow is much smaller than that of non-combusting flow, for a case without pressure gradient in flow direction.

Calculations were also conducted for combustion product flows in a rocket thrust chamber with pure hydrogen injection from the wall simulating transpiration cooling. The injected hydrogen decreases the temperature in the boundary layer due to its high heat capacity. When the mass injection rate is varying in axial direction, the eddy viscosity becomes larger than for the case without injection although nozzle geometry has an affect also. The distortion of eddy viscosity occurs, when the temperature increases sharply due to the chemical reaction of injected hydrogen with combustion products in the boundary layer. The velocity gradient at the wall for the case with pure hydrogen injection and chemical reaction is larger than that without mass injection for a flow with favorable pressure gradient as prevalent in a nozzle. Thus, the skin friction of the flow with hydrogen injection is larger than that without injection, when a favorable pressure gradient exists. This result is contrary to constant free stream flow conditions. Therefore, the pressure gradient in flow direction exerts a significant influence on the boundary layer characteristics.

The effects of wall temperature on the boundary characteristics were also examined for a flow without wall mass injection. When the free stream velocity is constant in flow direction and subsonic, heating of the wall is equivalent to injecting mass at the wall, and cooling the wall has the opposite effect.

SYMBOLS

A	van Driest's Damping factor
B	Mass transfer number: $2F/C_f$
C_f	Skin friction coefficient
C_p	Specific heat at constant pressure
D	Diffusion coefficient
F	Mass injection ratio, $\dot{m}_w / \rho_e U_e$
H	Total enthalpy, $H = \bar{H} + H' = h + u^2/2$
h	Enthalpy, $h = \bar{h} + h' = \sum_{i=1}^n h_i Y_i$
h_i	Enthalpy of species i, $h_i = \bar{h}_i + h'_i = \int_{T^0}^T C_{pi} dT + h_i^0$
K	Turbulent kinetic energy per unit density, $K = \overline{u'u'} + \overline{v'v'} + \overline{w'w'}$
k	Constant
Le	Lewis number
ℓ	Prandtl mixing length
M	Mean molecular weight
\dot{m}_w	Mass addition rate from the wall
n	Number of species
P, p	Pressure
P_c	Chamber stagnation pressure
P_r	Prandtl number
\dot{q}_w	Heat transfer rate into the wall
R	Universal gas constant
r_{mi}	Mass ratio of element m in species i
r_w	Nozzle radius

St	Stanton number
T	Temperature
u	velocity in x direction
v	Velocity in y direction
X_i	Mole fraction of species i
x	Distance along the contour
Y_i	Mass fraction of species i
y	Normal distance from the wall
z	Axial distance
α	Constant
α_m	Element mass fraction, $\alpha_m = \sum_{i=1}^n r_{m_i} Y_i$
β	Constant
γ	Constant
$\delta_{.990}$	Velocity thickness, $\delta = y$ at $u/u_e = 0.990$
$\delta_{.995}$	Velocity thickness, $\delta = y$ at $u/u_e = 0.995$
δ^*	Displacement thickness, $\delta^* = \int_0^{\infty} (1 - \rho u / \rho_e U_e) dy$
ϵ	Eddy viscosity
θ	Momentum thickness, $\theta = \int_0^{\infty} (\rho u / \rho_e U_e) (1 - u/u_e) dy$
Λ	Dissipation length
λ	Thermal conductivity
μ	Molecular viscosity
ρ	Density
τ	Shear stress

Subscripts

e	Boundary layer edge
I	Transpiration coolant
i	Species
m	Element
T	Turbulent
w	Wall

Superscripts

()' Fluctuating term

$\overline{(\quad)}$ Time averaged quantity

Notations in Eq. (11) through Eq. (14) should be consulted with Ref. 14.

References

1. Cebeci, T., Smith, A.M.O., and Mosinskis, G., "Calculation of Compressible Adiabatic Turbulent Boundary Layers," AIAA Paper 69-687, 1969.
2. Omori, S., "Eddy Viscosity Calculation Along the Chemical Rocket Thrust Chamber Wall Using Turbulent Kinetic Energy," Combustion Science and Technology, 1973, Vol. , pp.
3. Rotta, J. C., "Recent Attempts to Develop a Generally Applicable Calculation Method for Turbulent Shear Flow Layers," AGARD Report CP-93, 1972.
4. Glushko, G. S., "Turbulent Boundary-Layer on a Plane Plate in Incompressible Liquid," Izvestiya Akademik Nauk, SSSR, Mekhanika, No. 4, 1965, pp. 12-23.
5. Bradshaw, P., Ferriss, D. H., and Atwell, N. P., "Calculation of Boundary-Layer Development Using the Turbulent Energy Equation," Journal of Fluid Mechanic, Vol. 28, 1967, pp.593-616.
6. Donaldson, C., "A Progress Report on an Attempt to Construct an Invariant Model of Turbulent Shear Flows," AGARD CP-93, 1972.
7. Maise, G., and McDonald, H., "Mixing Length and Kinematic Eddy Viscosity in a Compressible Boundary Layer," AIAA Journal, Vol. 6, 1968, pp. 73-80.
8. Beckwith, I.E. and Bushnell, D. M., "Calculation of Mean and Fluctuating Properties of the Incompressible Turbulent Boundary Layer," Proceedings of the 1968 AFOSR-IFP-STANFORD Conference on Computation of Turbulent Boundary Layers, Stanford University, 1969, pp. 275-299.
9. Patankar, S. V. and Spalding, D. B., "A Finite-Difference Procedure for Solving the Equations of the Two-Dimensional Boundary Layer," Int. J. Heat Mass Transfer, Vol. 10, 1967, pp. 1389-1411.
10. Prandtl, L. and Wieghardt, K., "Ueber Ein Neues Formel System Fur Die Ausgebildete Turbulenz," Nachr. Akad. Wiss., Gottingen, Mathematik-Phys., 1945, Kl. 6-19.
11. Rotta, J. C., "Statistische Theori Nichthomogener Turbulenz," Zeitschrift fur Physik, Bd. 129, 1951, pp. 547-572.

12. Squire, L.C., "Further Experimental Investigations of Compressible Turbulent Boundary Layers with Air Injection," Cambridge University Engineering Department, R&M 3627, 1970.
13. Squire, L.C., "Eddy Viscosity Distributions in Compressible Turbulent Boundary Layers with Injection," The Aeronautical Quarterly, Vol. XXII, Part 2, 1971, pp. 169-182.
14. Levine, J. N., "Transpiration and Film Cooling Boundary Layer Computer Program," SN-230, 1971, Dynamic Science, A Division of Marshall Industries.
15. Harvey, W. D., Bushnell, D. N., and Beckwith, I.E., "Fluctuating Properties of Turbulent Boundary Layers for Mach Numbers up to 9," NASA TND-5496, 1969.
16. Cebeci, T., "Calculation of Compressible Turbulent Boundary Layers with Heat Transfer and Mass Transfer," AIAA Paper 70-741, 1970.
17. Bird, R. B., Stewart, U.E., and Lightfoot, E.N., Transport Phenomena, John Wiley & Sons, 1960.
18. Mason, E. A. and Saxena, S. C., Physics of Fluids, 1, 5, 1958, pp. 361-369.
19. Svehla, R. A., "Estimated Viscosities and Thermal Conductivities of Gases at High Temperatures," NASA TR-132, 1962.
20. Frey, H. M. and Nickerson, G. R., "Two-Dimensional Kinetic Reference Program," 1970, Dynamic Science, A Division of Marshall Industries.
21. Bradshaw, P. and Ferriss, D. H., "Derivation of a Shear-Stress Transport Equation from the Turbulent Energy Equation," Proceedings of the 1968 AFOSR-IFP-STANFORD Conference on Computation of Turbulent Boundary Layers, Stanford University, 1969, pp. 264-274.
22. Muzzy, R. J., "Surface Mass Addition into a Turbulent Boundary Layer," AIAA Journal, Vol. 5, No. 5, May 1967, pp. 1029-1032.
23. Klebanoff, P. S., "Characteristics of Turbulence in a Boundary Layer with Zero Pressure Gradient," NACA-TR1247, 1955.
24. Wooldridge, C. E. and Muzzy, R. J., "Boundary-Layer Turbulence Measurements with Mass Addition and Combustion," AIAA Journal, Vol. 4, No. 11, November 1966, pp. 2009-2016.

25. Jones, J. W. and Isaacson, L. K., "A Turbulent Boundary Layer with Mass Addition, Combustion, and Pressure Gradients," AFOSR Scientific Report, AFOSR-70-1428TR, College of Engineering, University of Utah, Salt Lake City, Utah.

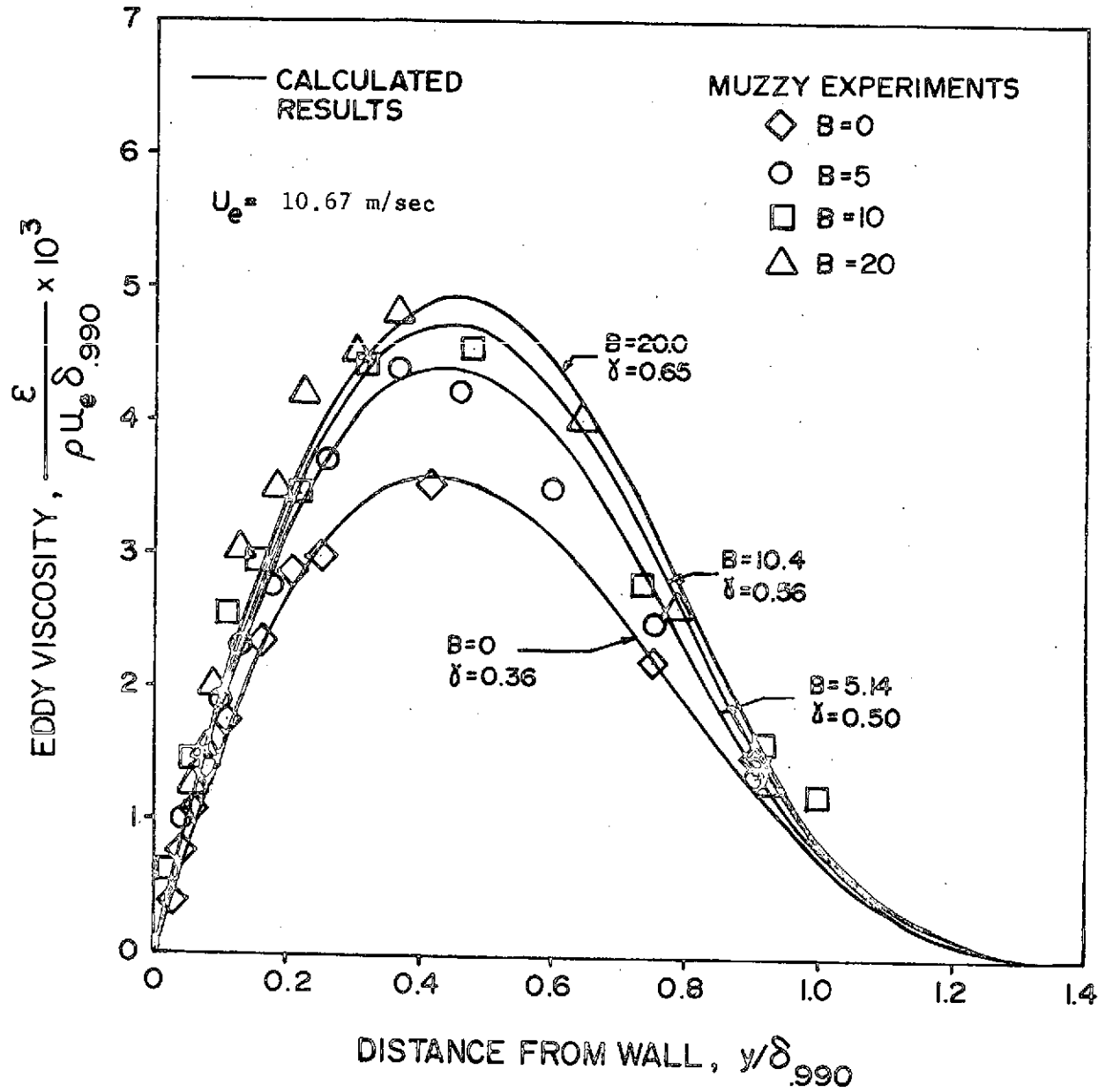


Figure 1. Eddy Viscosity Profiles for Muzzy's Experiments

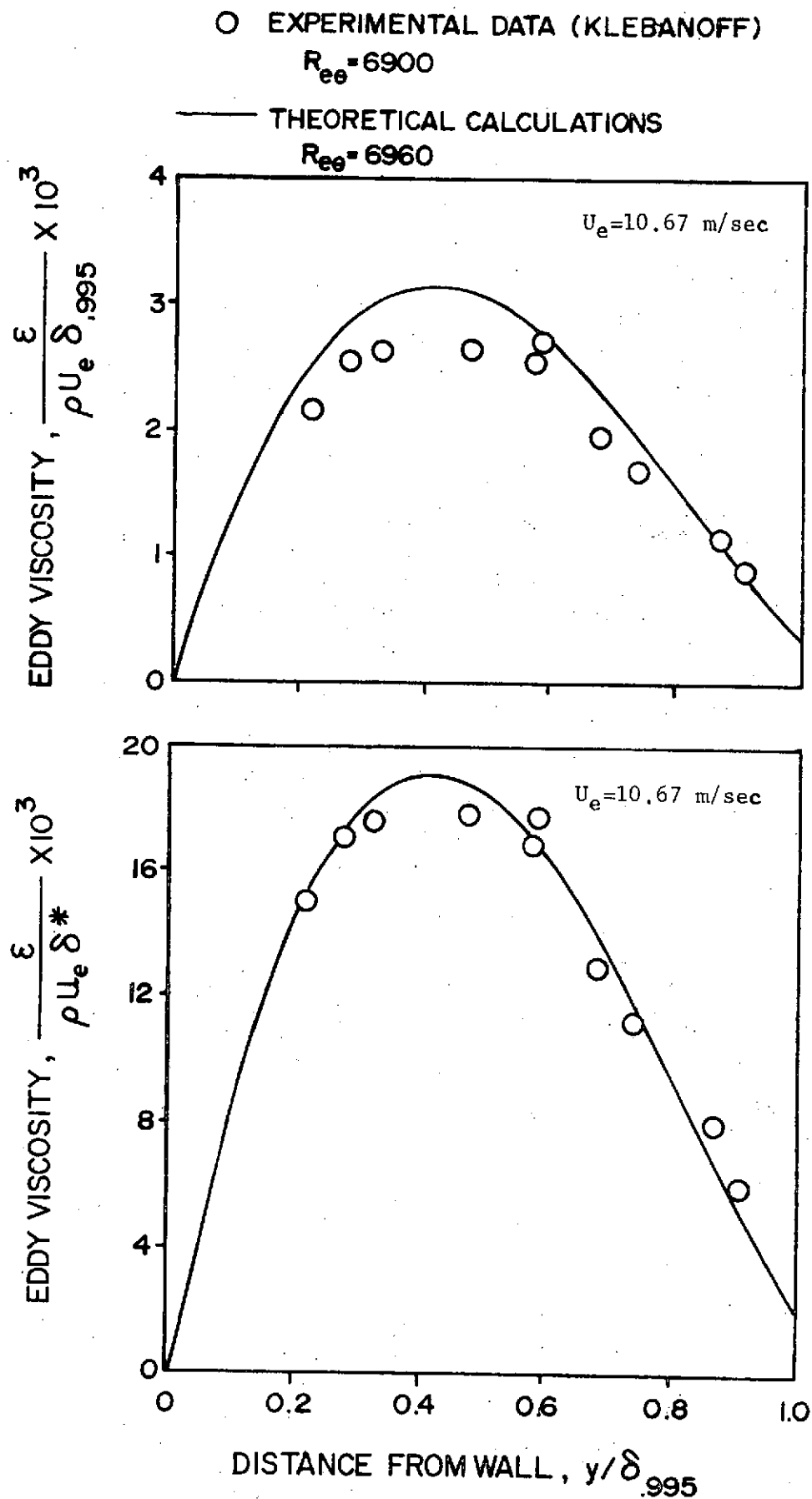


Figure 2. Eddy Viscosity Profiles for Klebanoff's Experiments

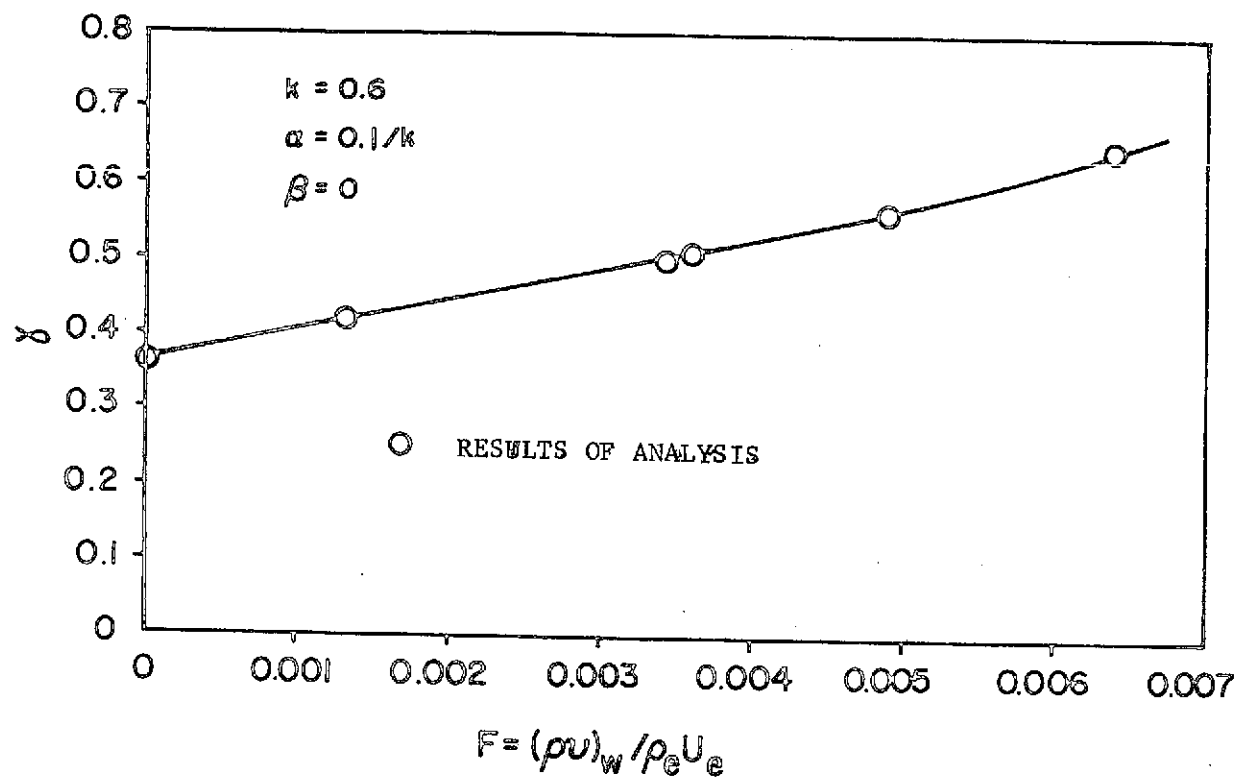


Figure 3. Relation Between the Constant γ and Mass Injection Ratio F

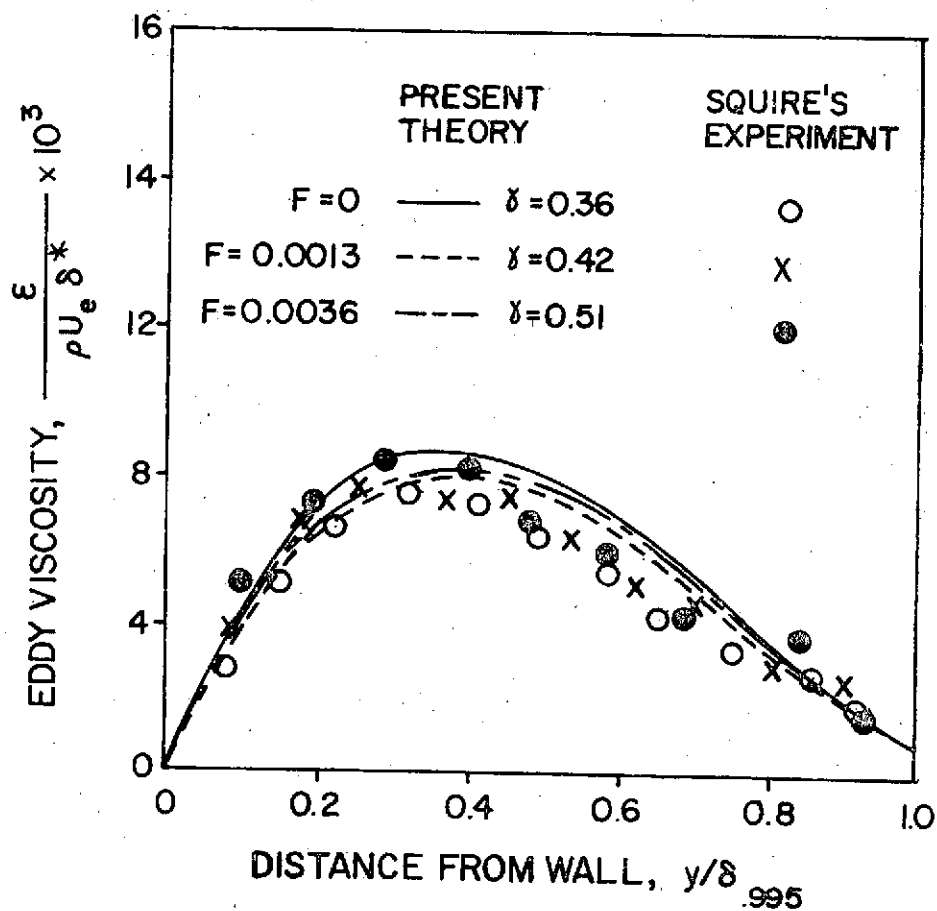
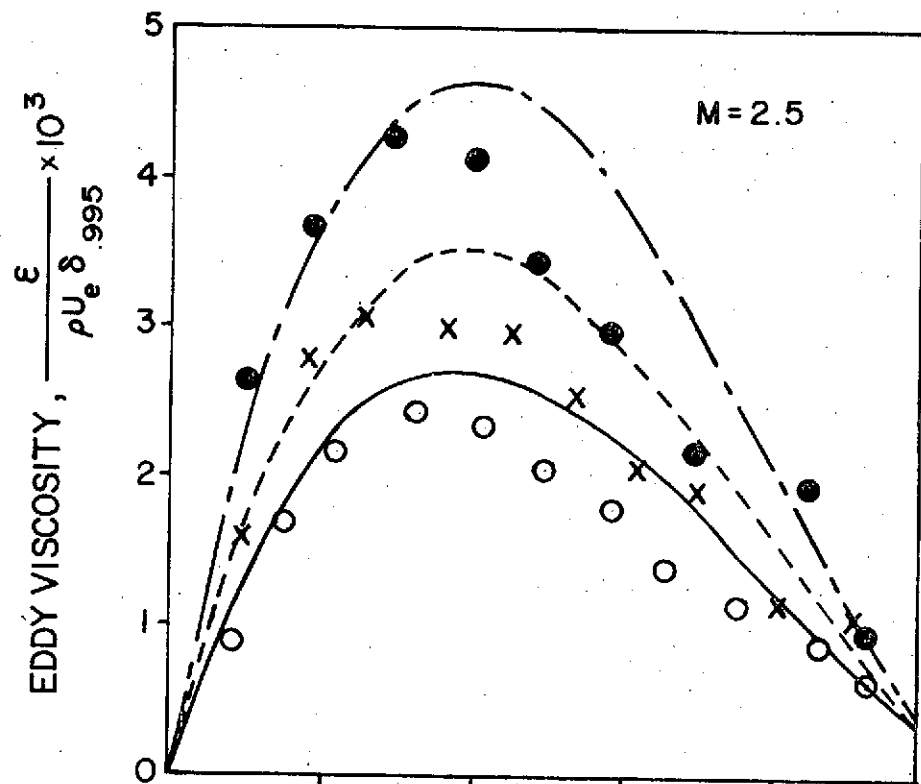
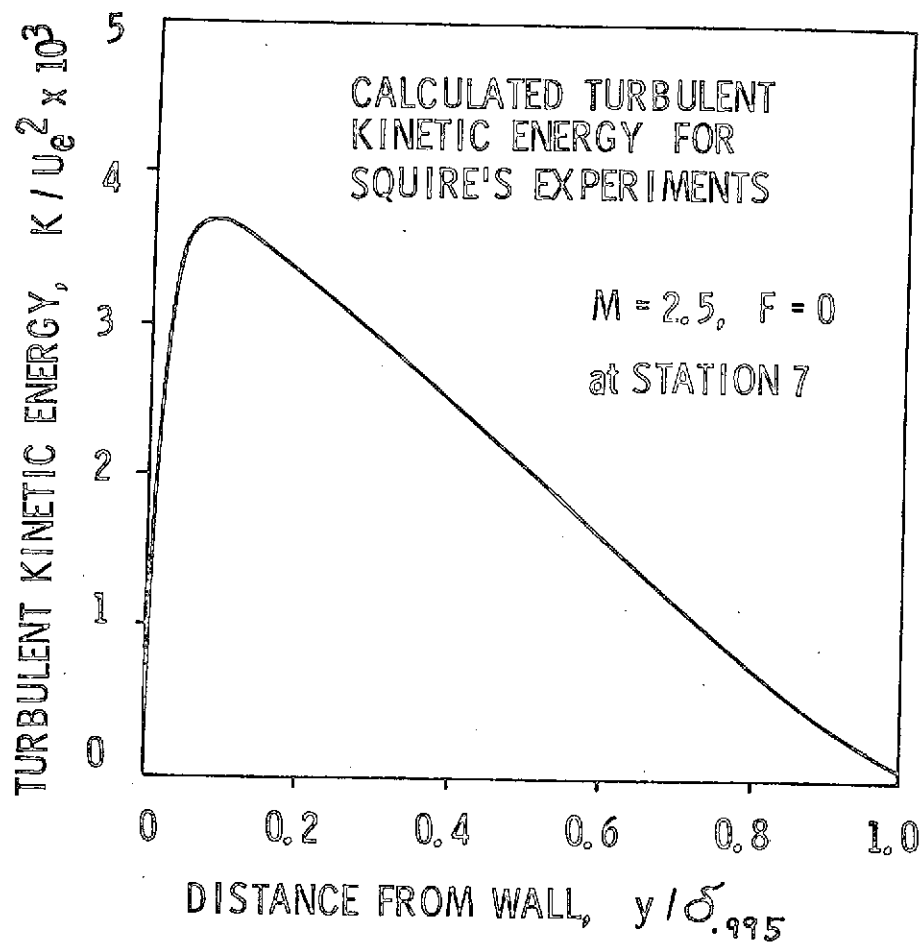


Figure 4. Eddy Viscosity Profiles for Squire's Experiments



$$P_0 = 3.082 \times 10^5 \text{ N/m}^2$$

(44.7 psia)

$$T_0 = 295 \text{ }^\circ\text{K}$$

	PRESENT CALCULATION	EXPERIMENT BY SQUIRE
$\delta_{.995}$	5.10 mm	5.20 mm
θ	0.39 mm	0.40 mm
δ^*	1.61 mm	1.69 mm
C_f	0.00164	0.00167

$$\rho_e U_e = 33.9 \text{ g / (sec} \cdot \text{cm}^2)$$

Calculated at Station 7.

Figure 5. Turbulent Kinetic Energy and Boundary Layer Thicknesses for Squire's Experiments

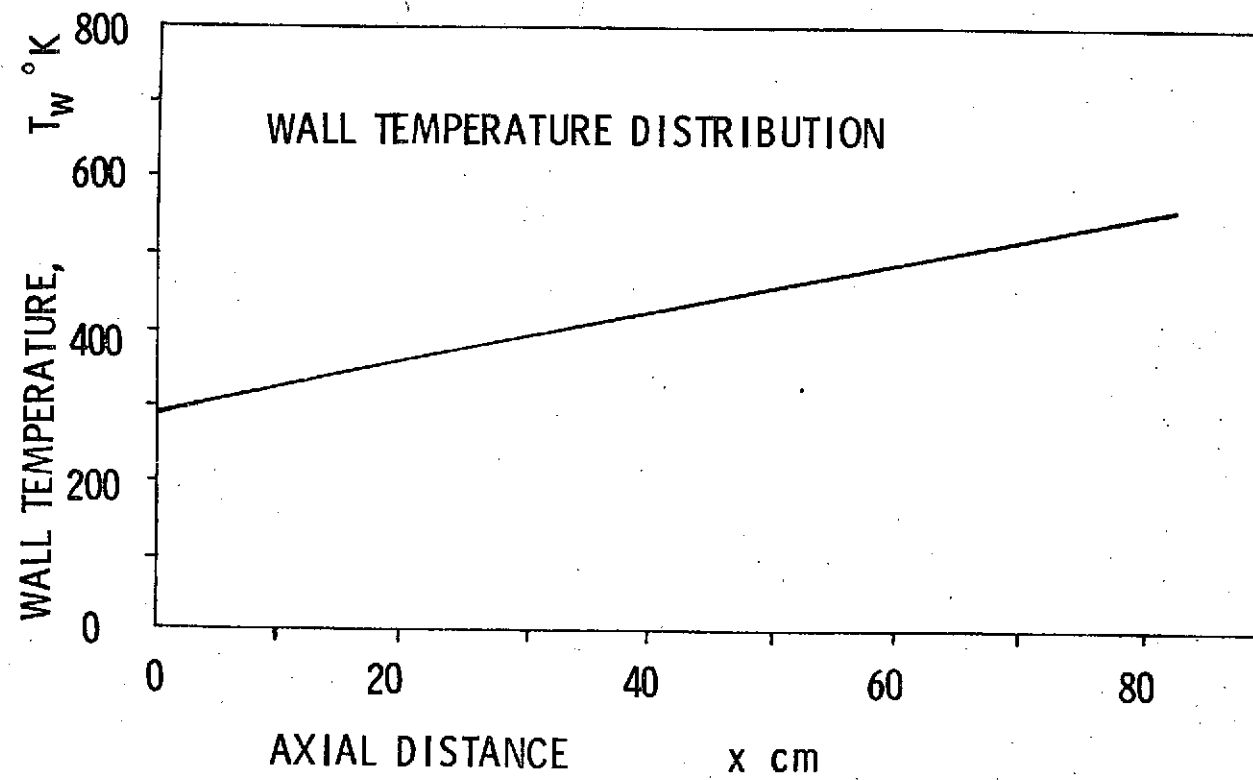
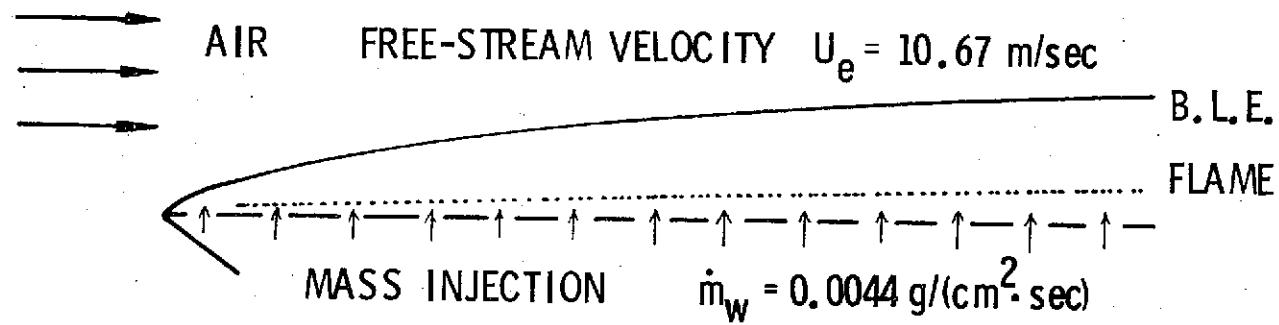


Figure 6. Air Flow with Combustion due to Injection of a Mixture of Hydrogen and Nitrogen

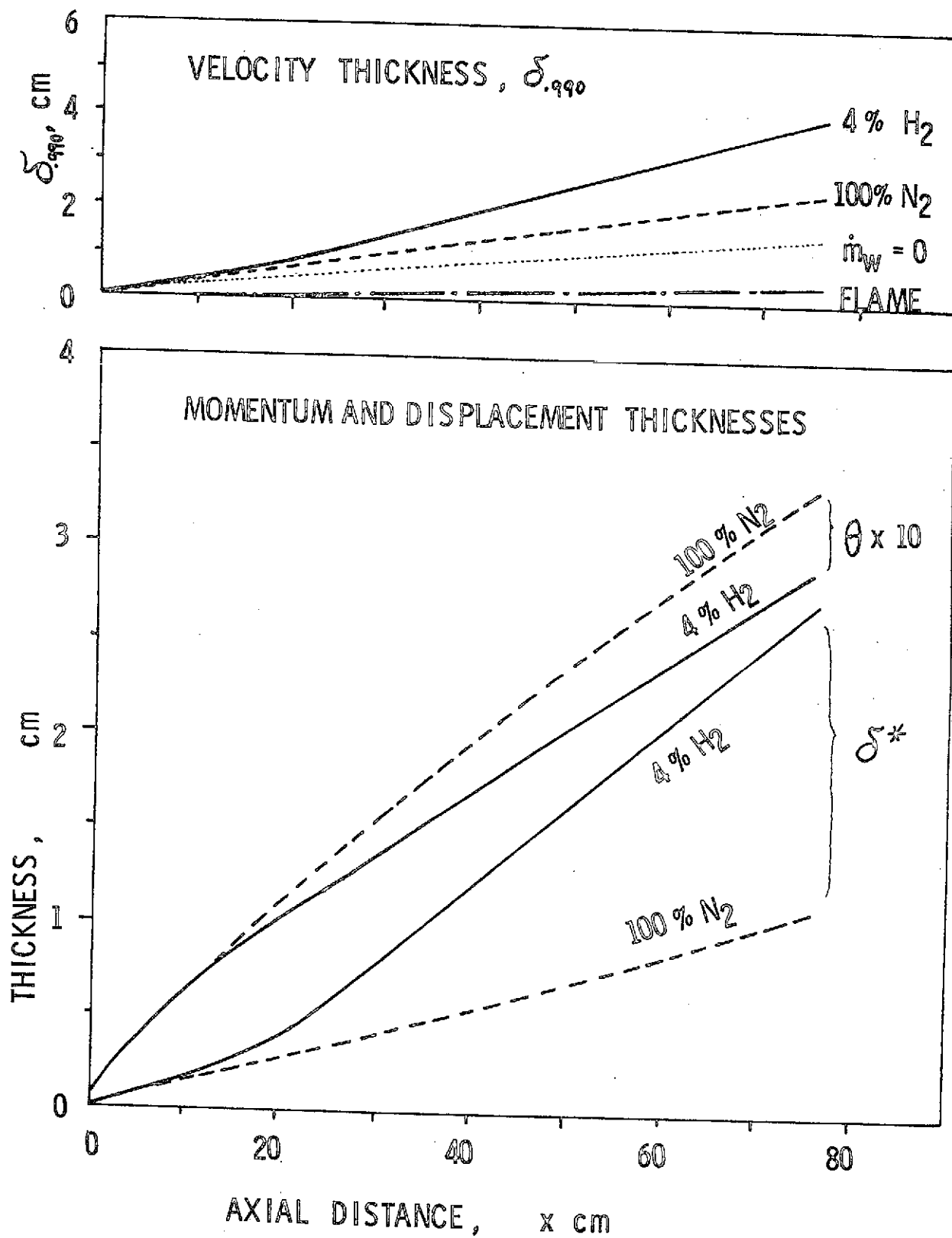


Figure 7. Velocity, Momentum, and Displacement Thicknesses

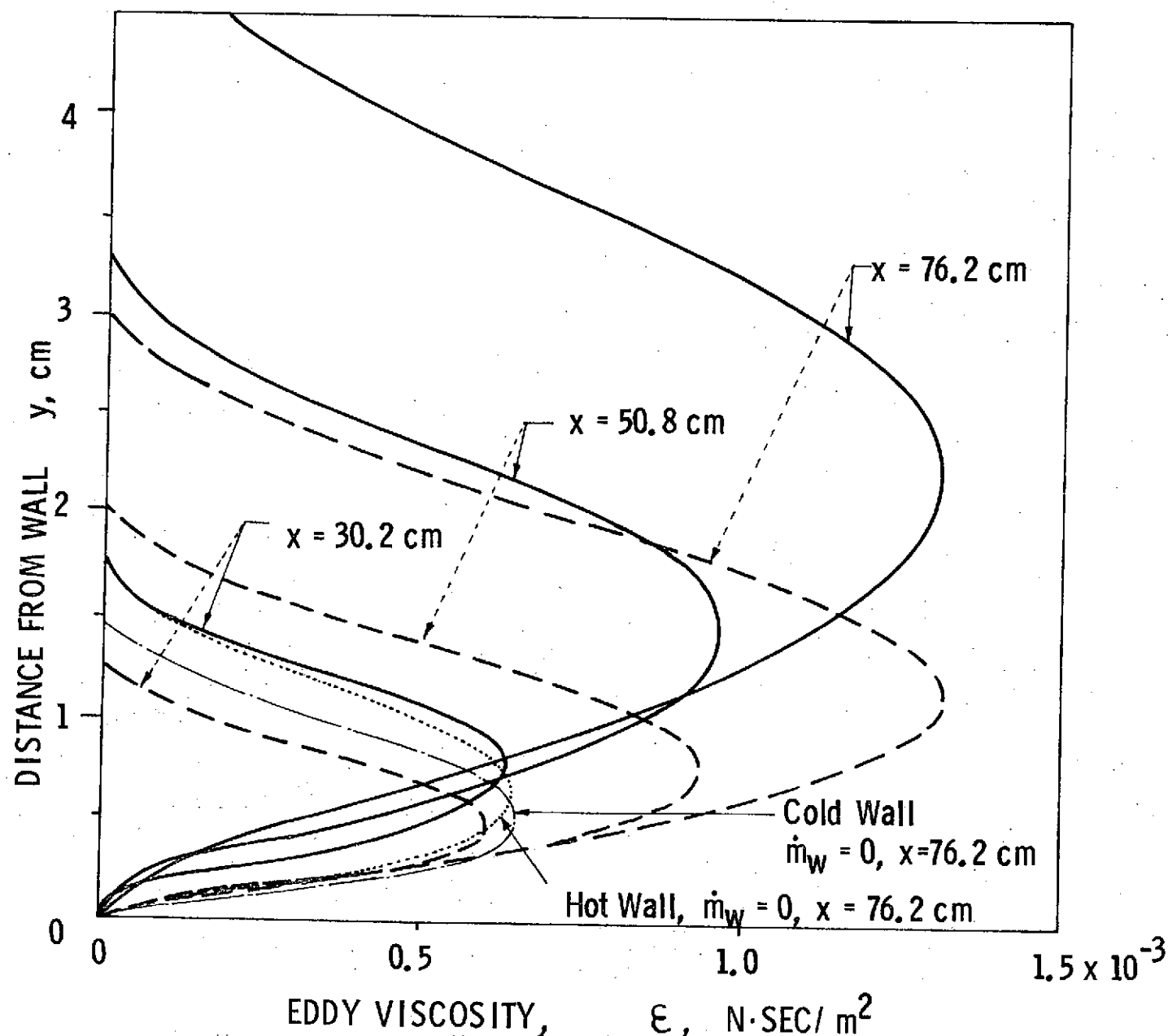


Figure 8. Eddy Viscosity Profiles

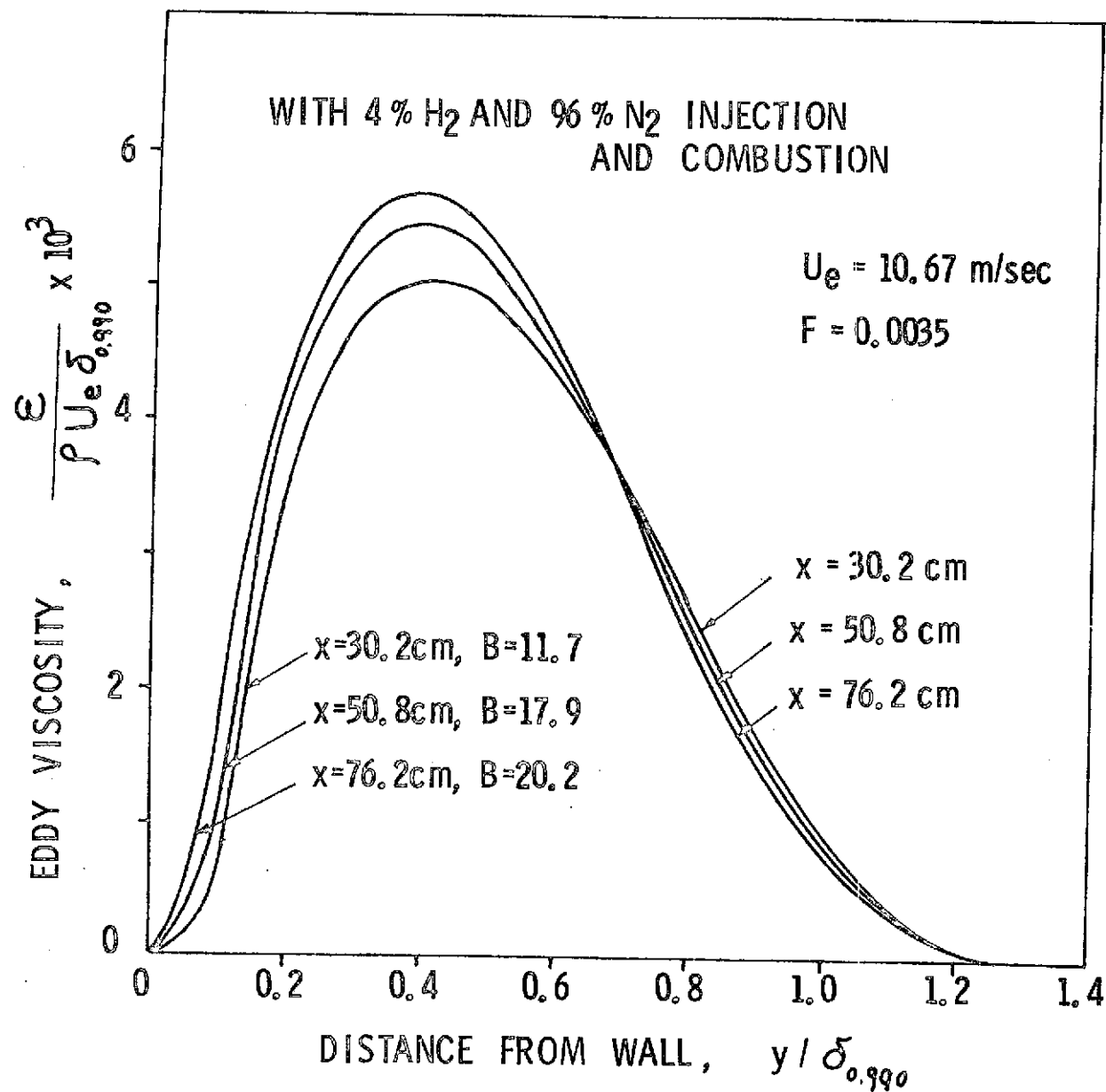


Figure 9. Non-Dimensionalized Eddy Viscosity Profiles with Combustion

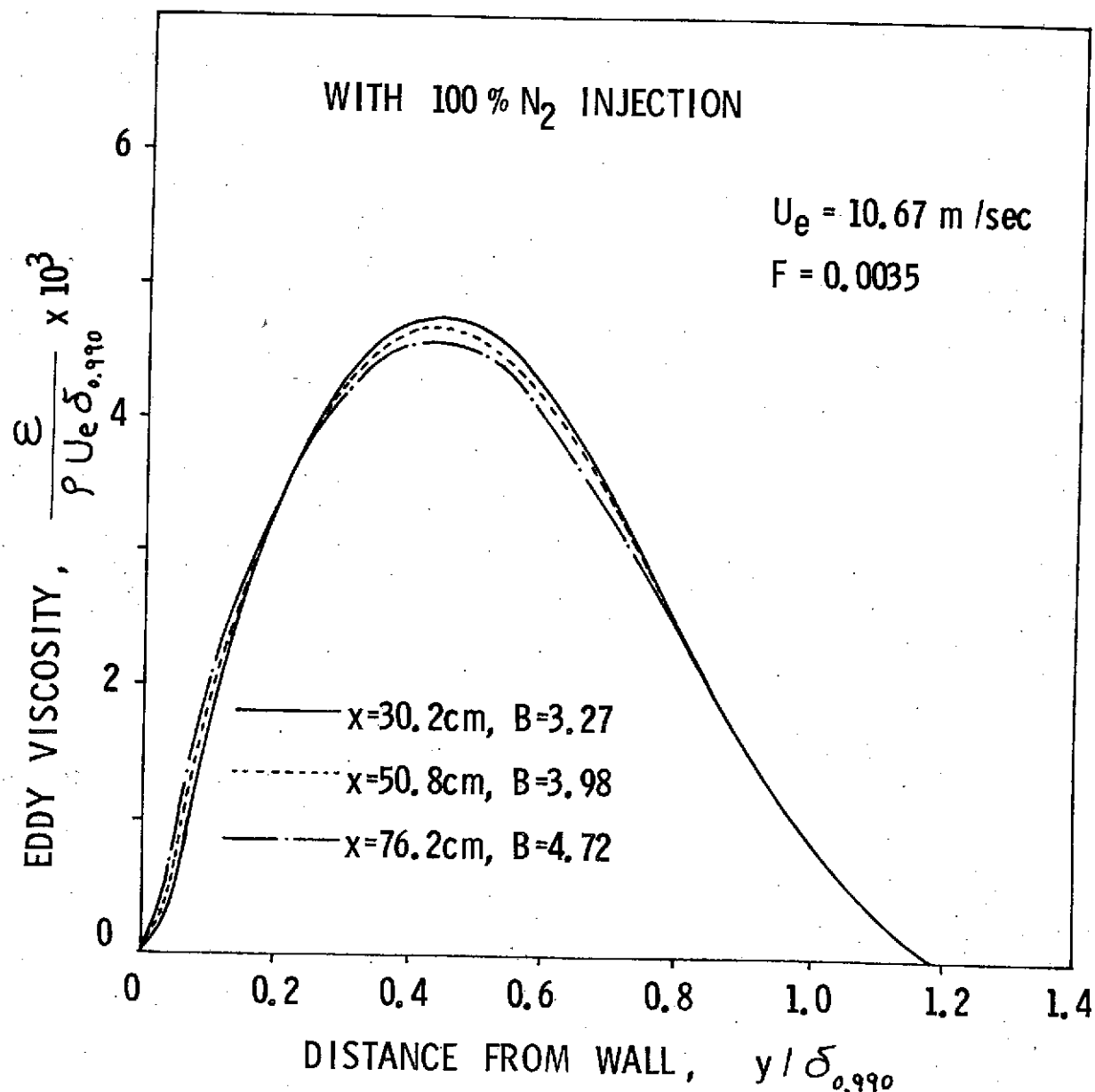


Figure 10. Non-Dimensionalized Eddy Viscosity Profiles without Combustion

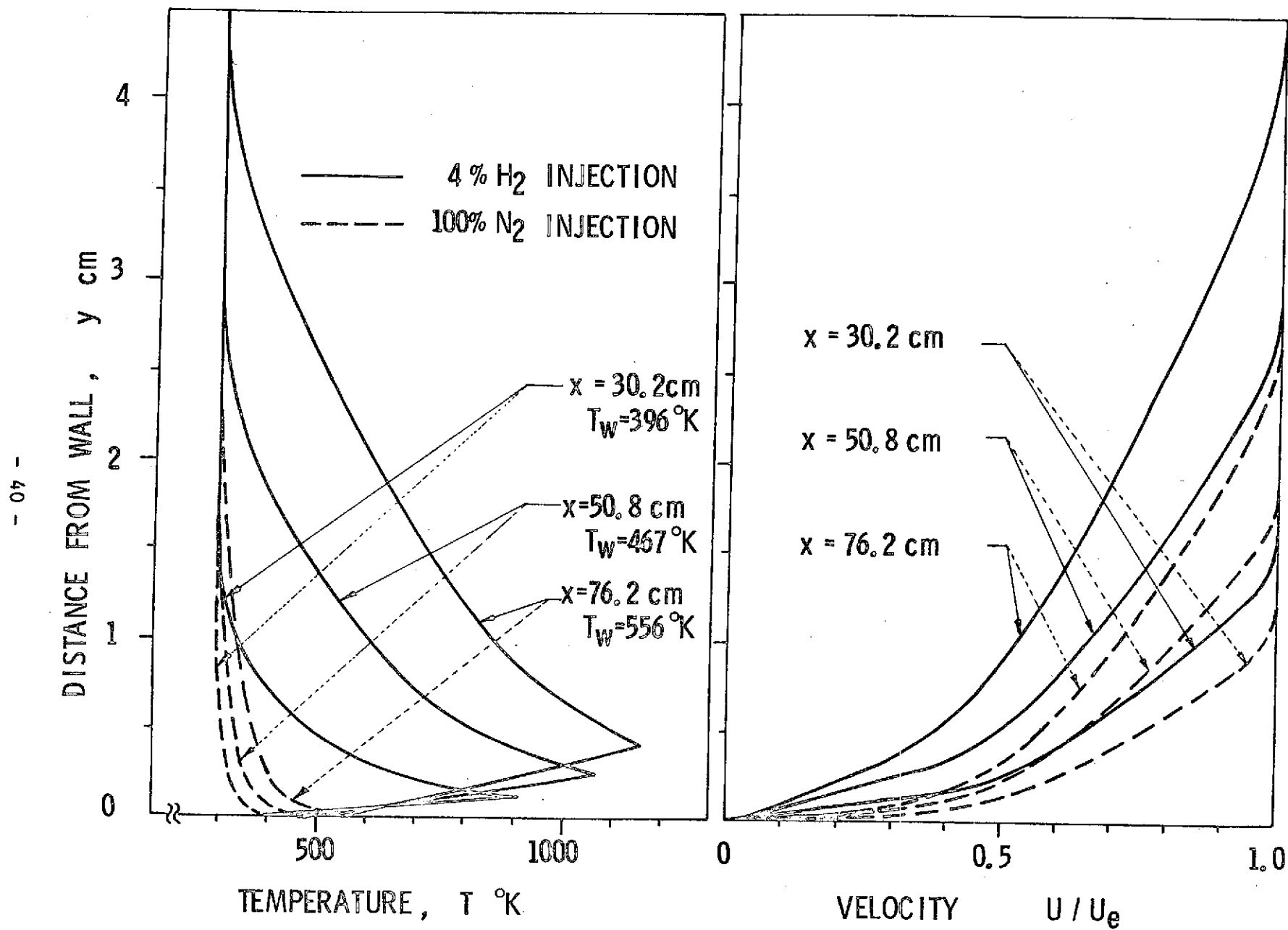


Figure 11. Temperature and Velocity Profiles with Combustion

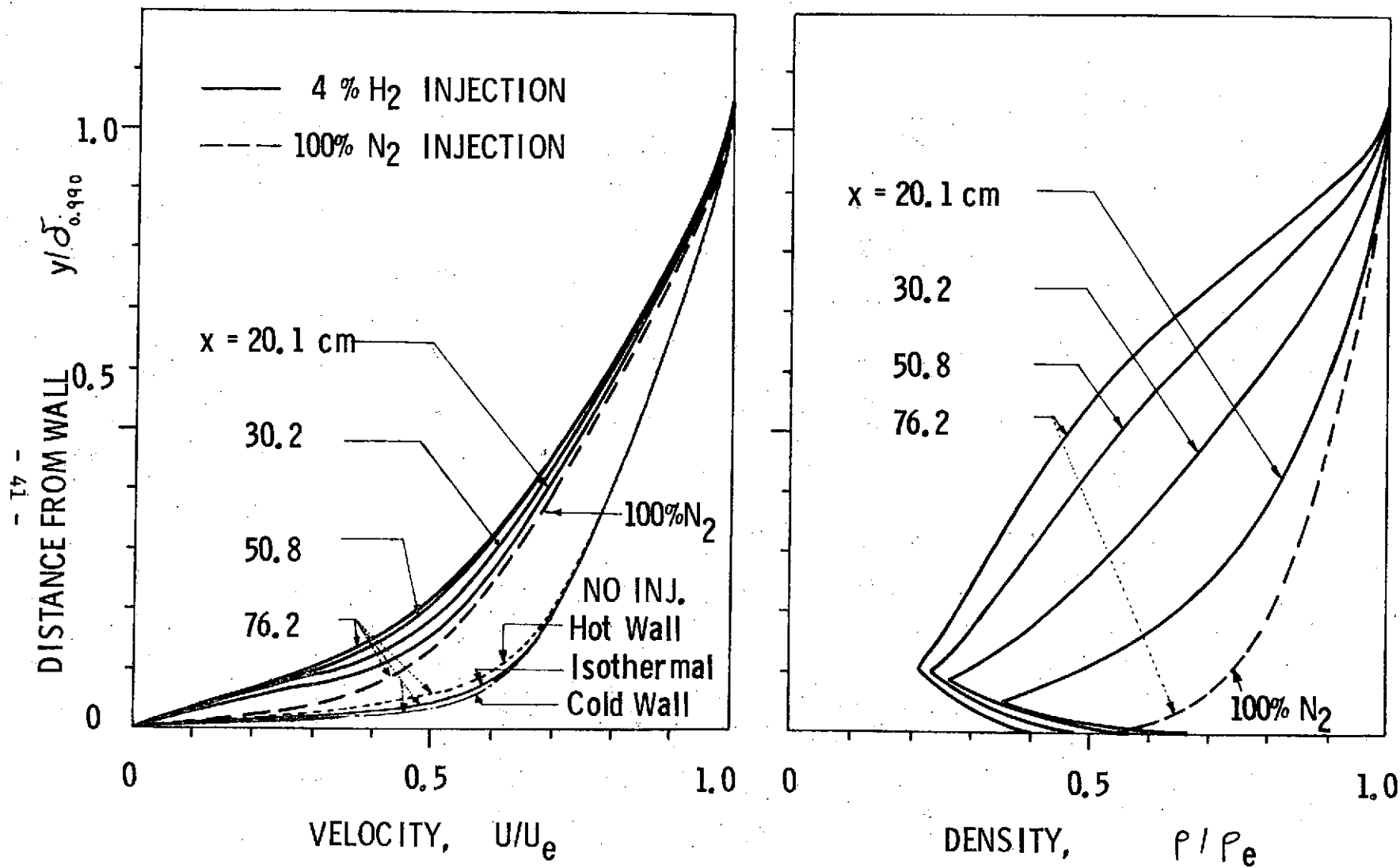


Figure 12. Velocity and Density Profiles

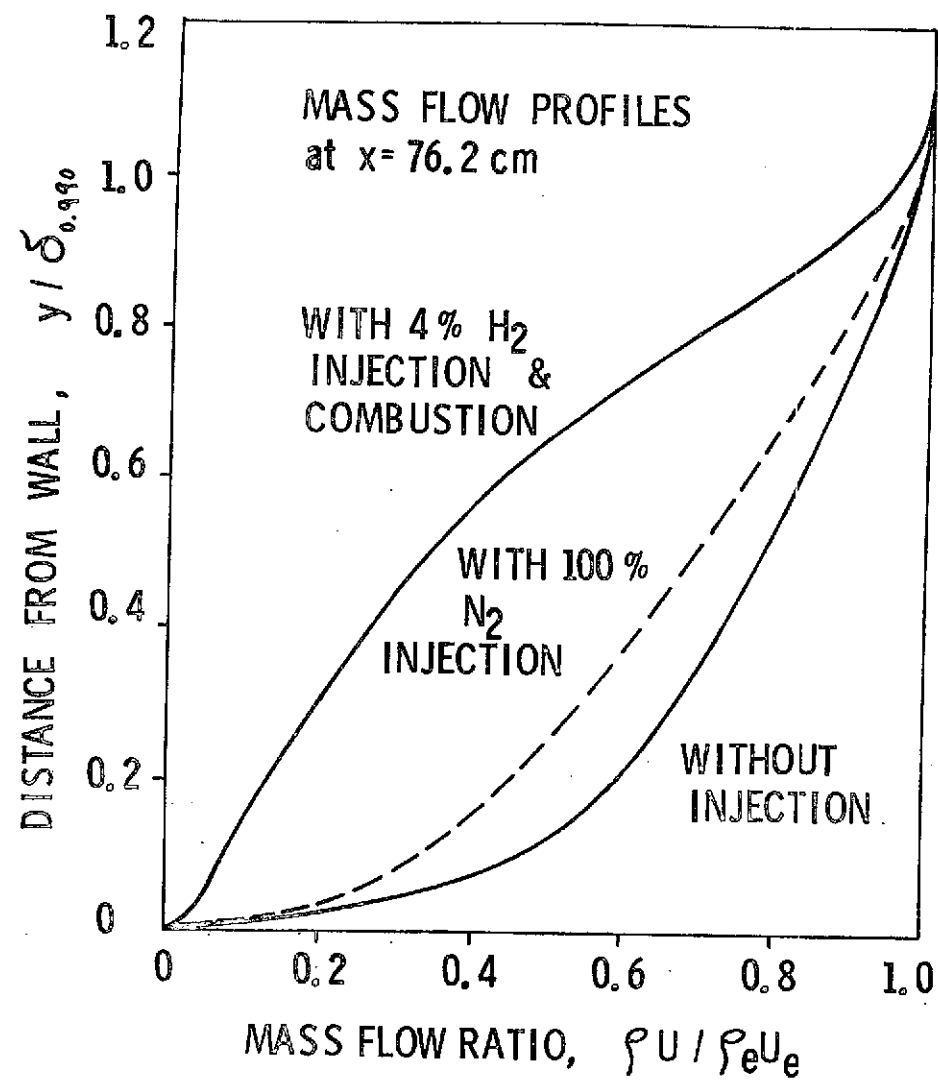


Figure 13. Mass Flow Profiles

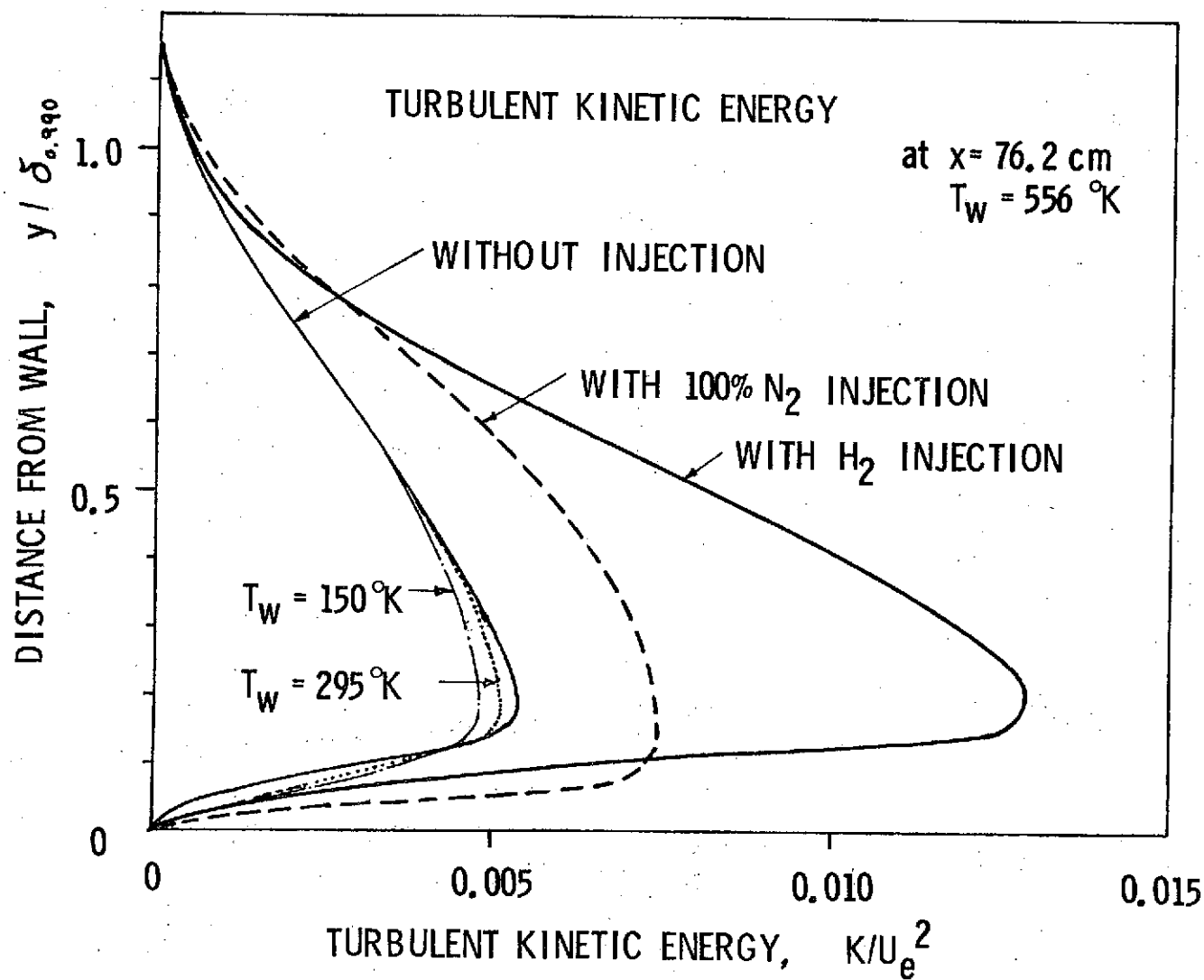


Figure 14. Turbulent Kinetic Energy Profiles

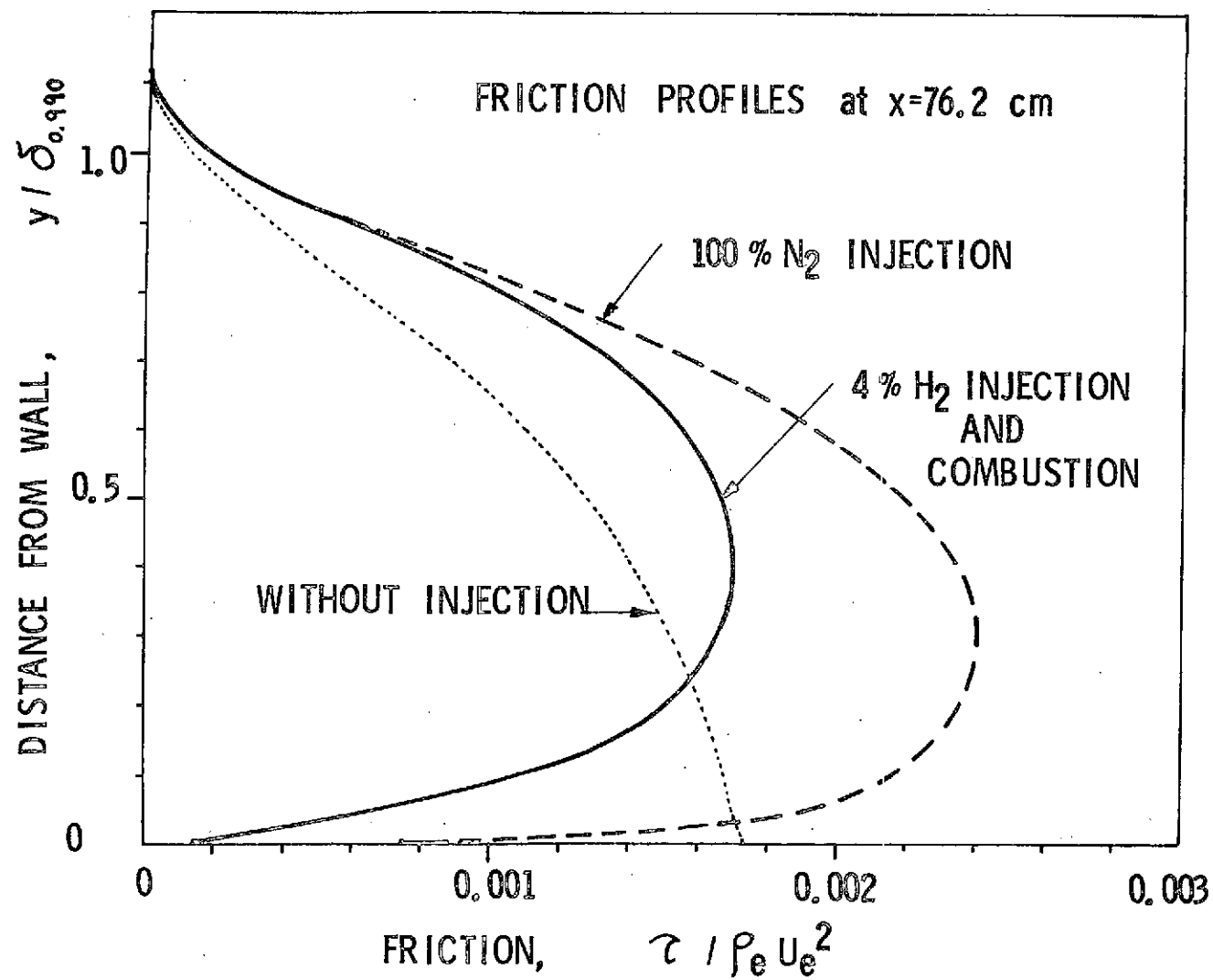


Figure 15. Friction Profiles

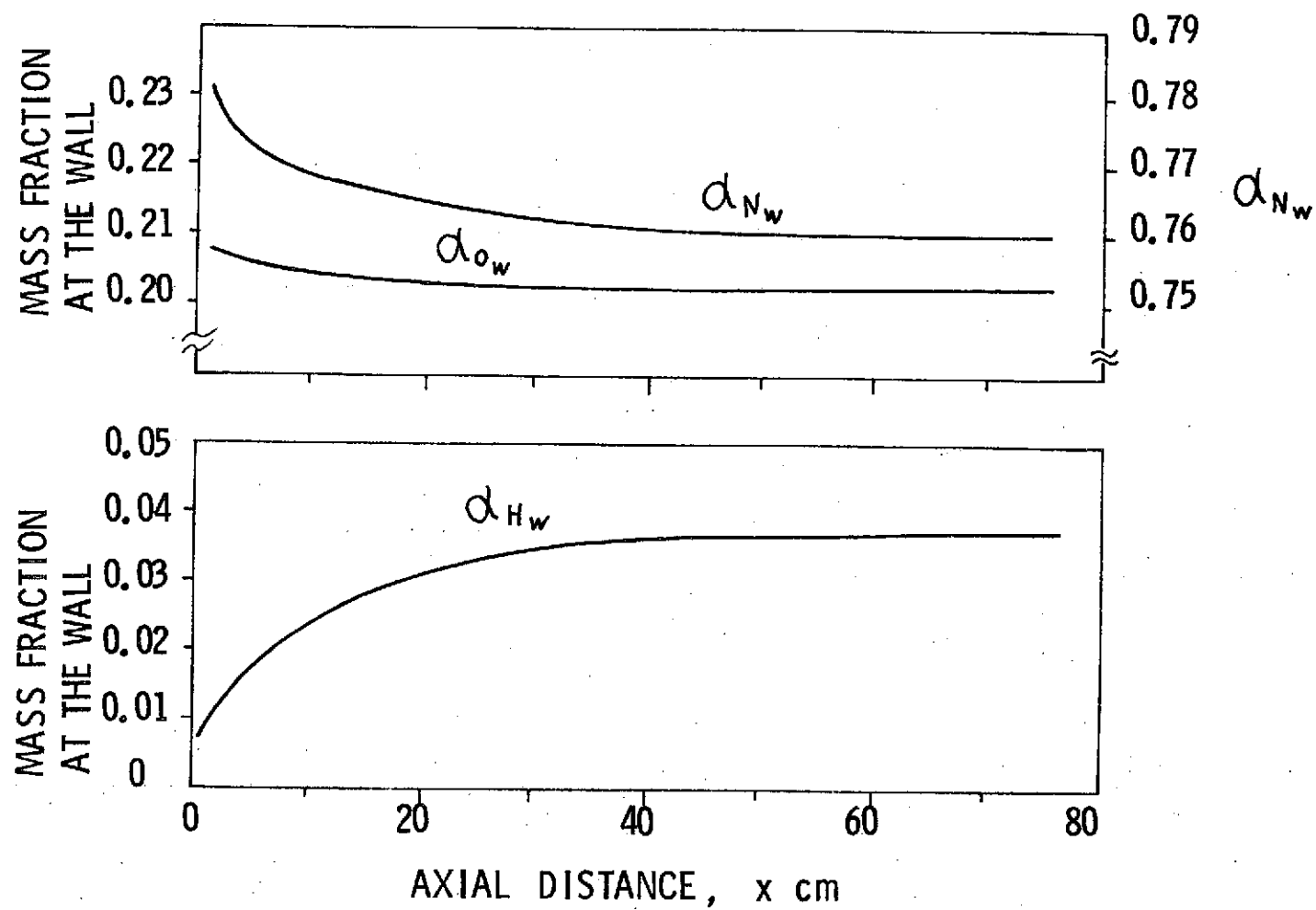


Figure 16. Distributions of Element Mass Fraction at the Wall

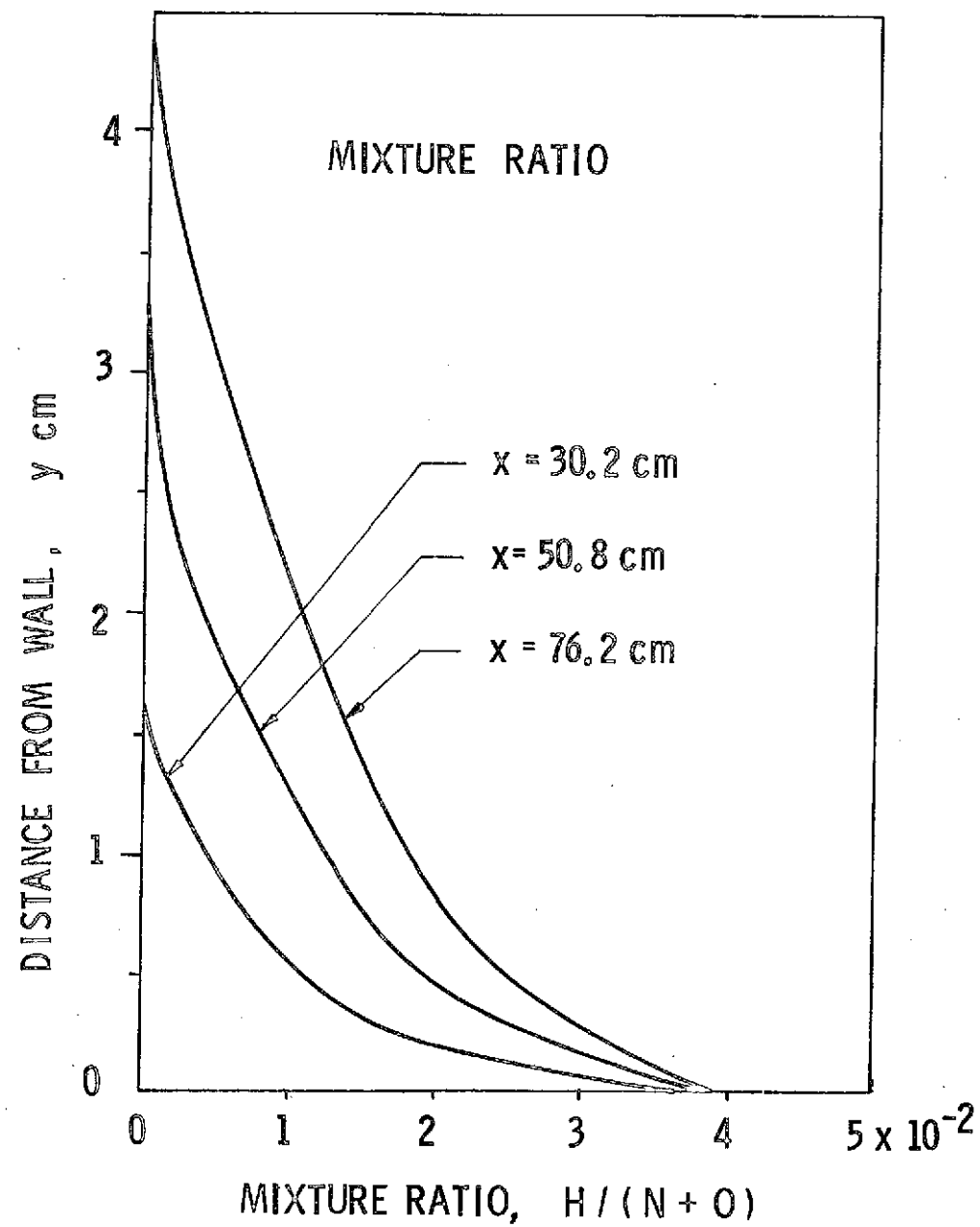


Figure 17. Mixture Ratio Profiles

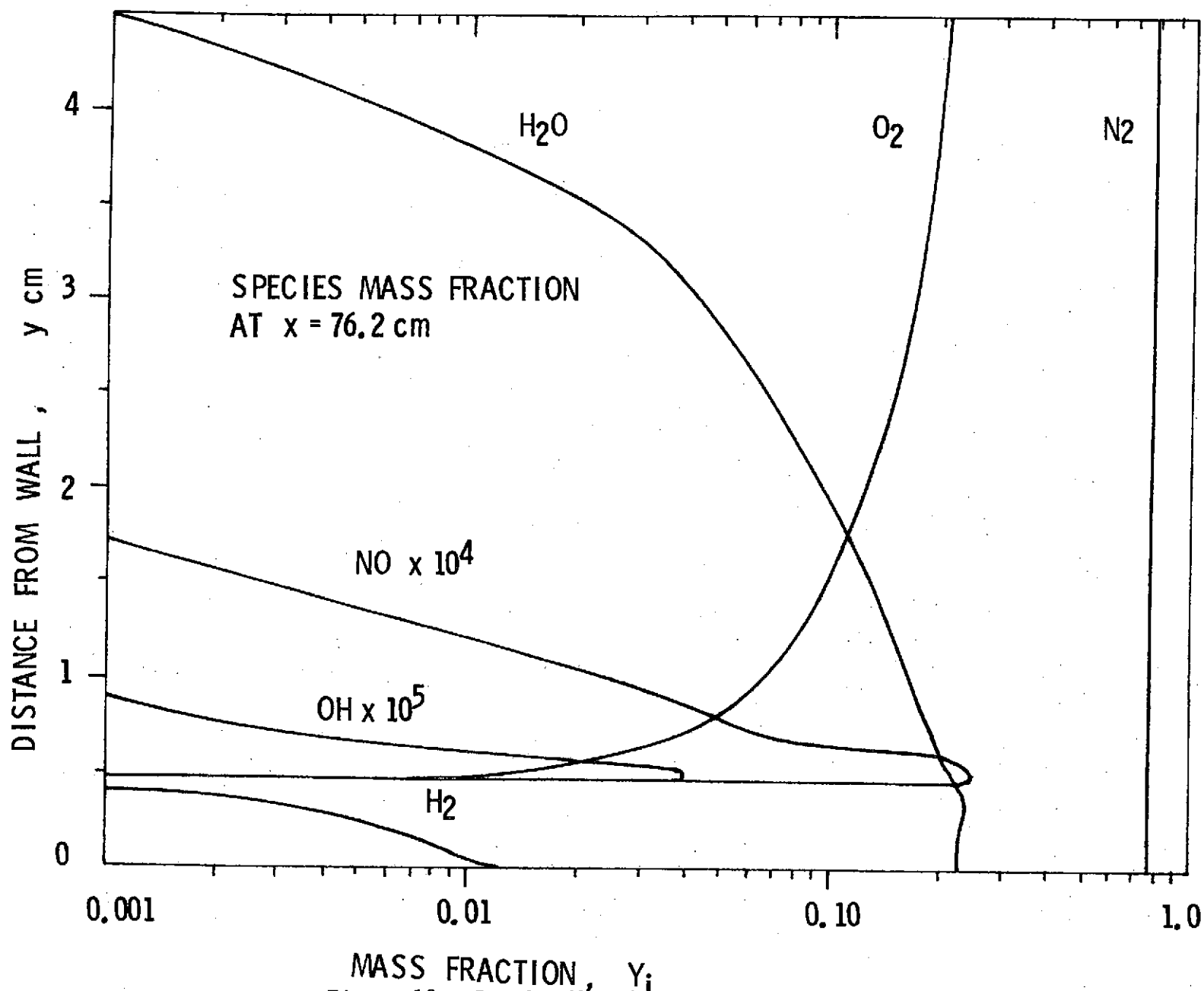


Figure 18. Species Mass Fraction Profiles

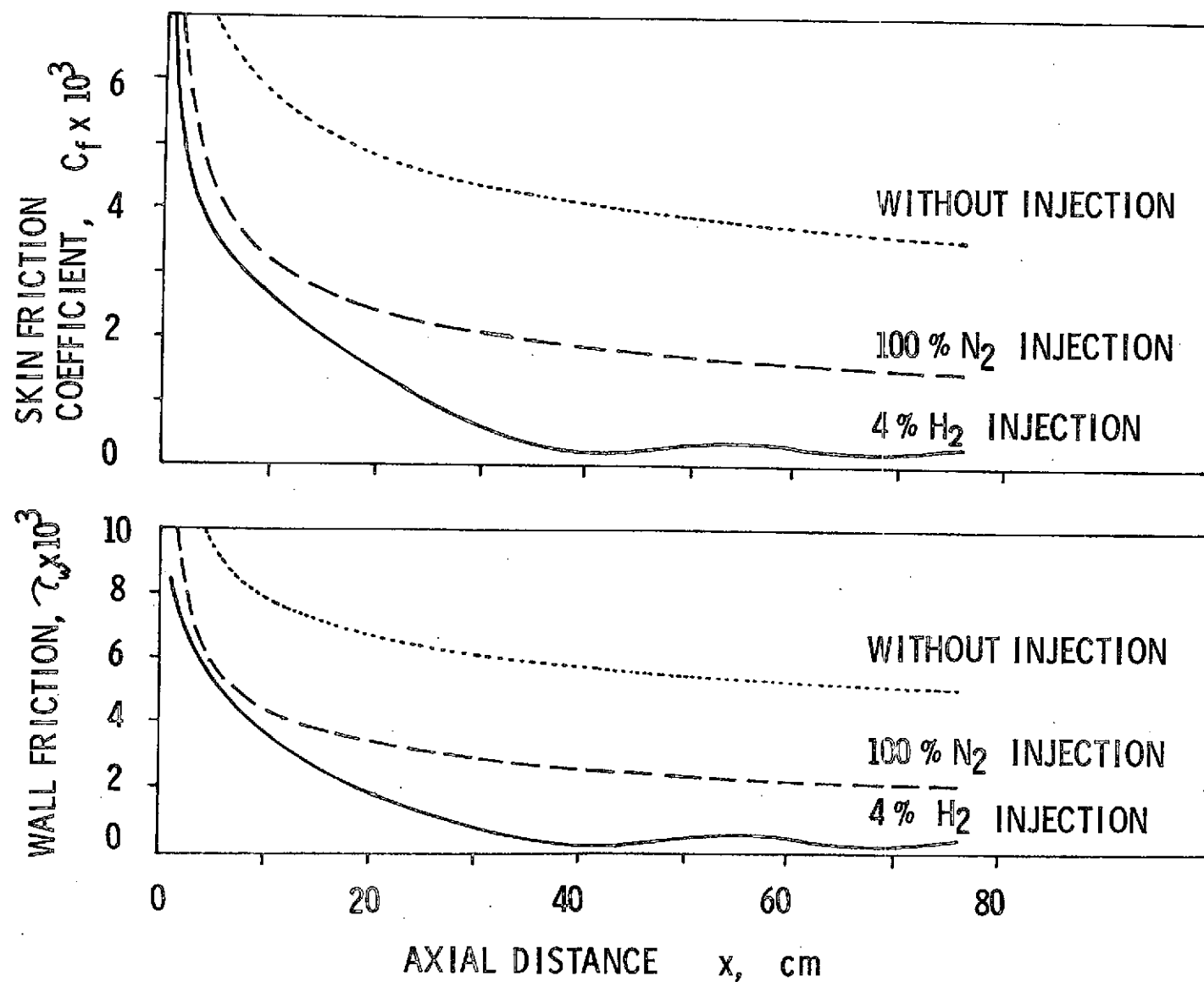


Figure 19. Distributions of Skin Friction and Its Coefficient

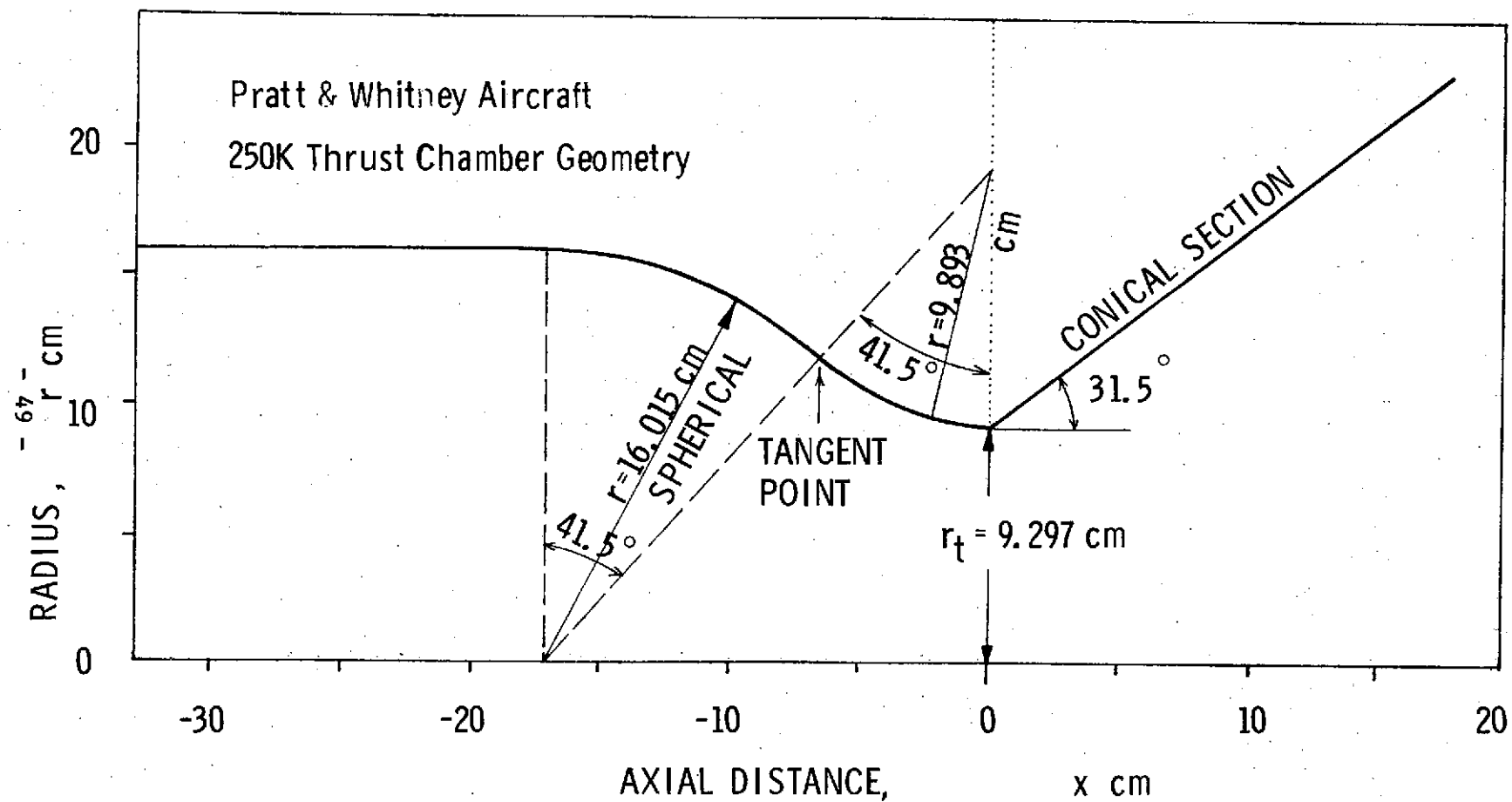


Figure 20. 250K Thrust Chamber Geometry of Pratt & Whitney Aircraft

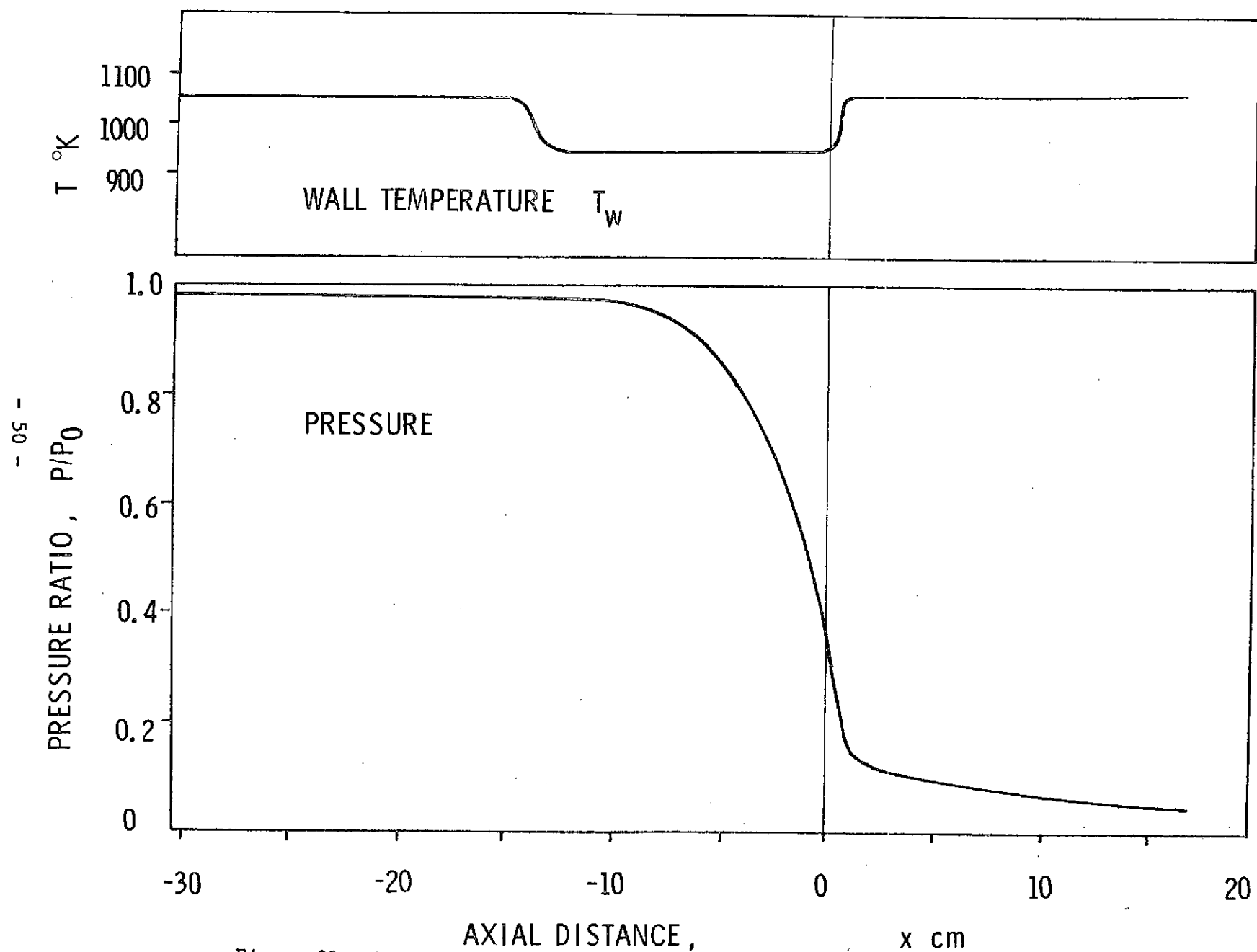


Figure 21. Input Distributions of Gas-side Wall Temperature and Pressure

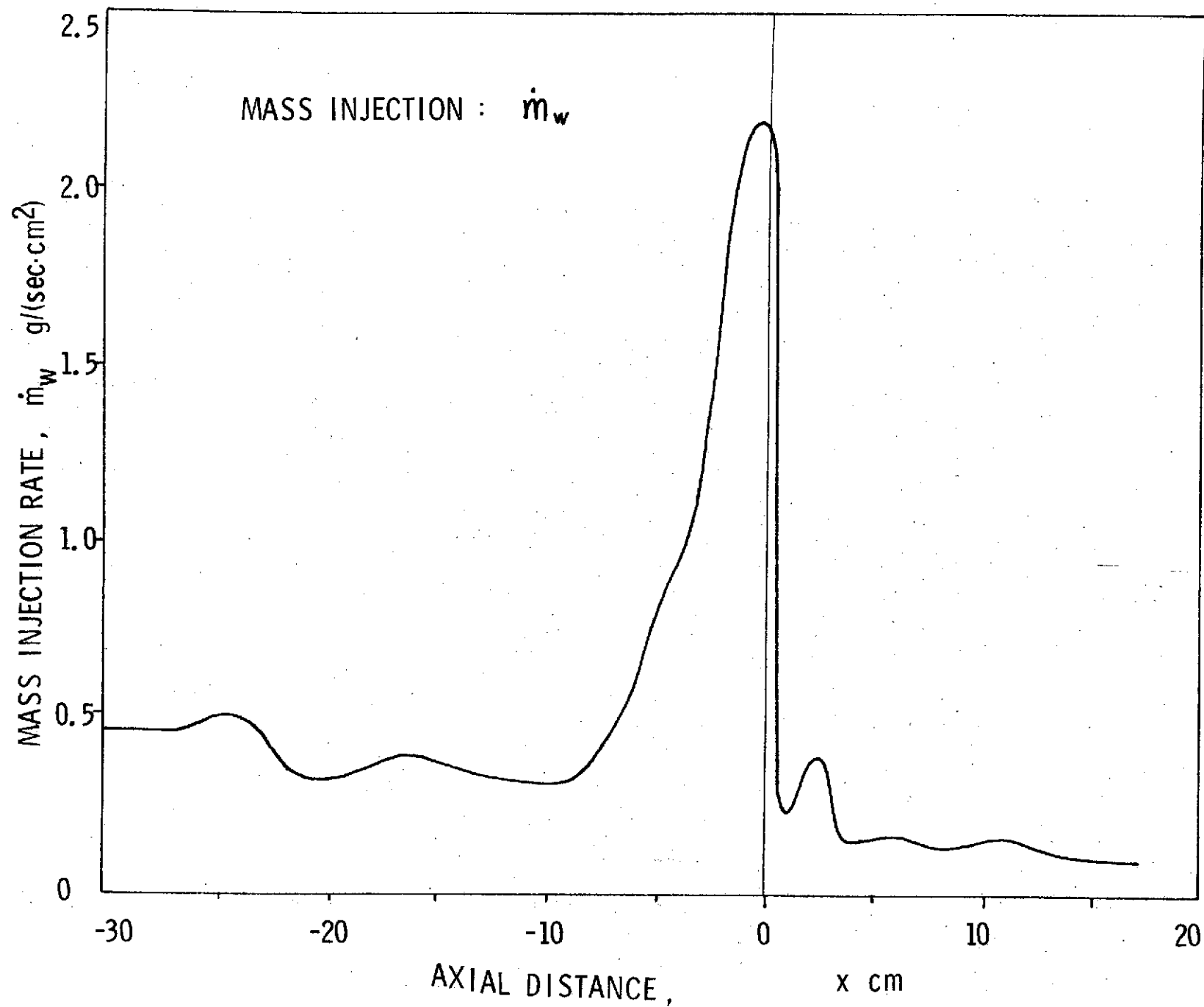


Figure 22. Input Distribution of Mass Injection Rate

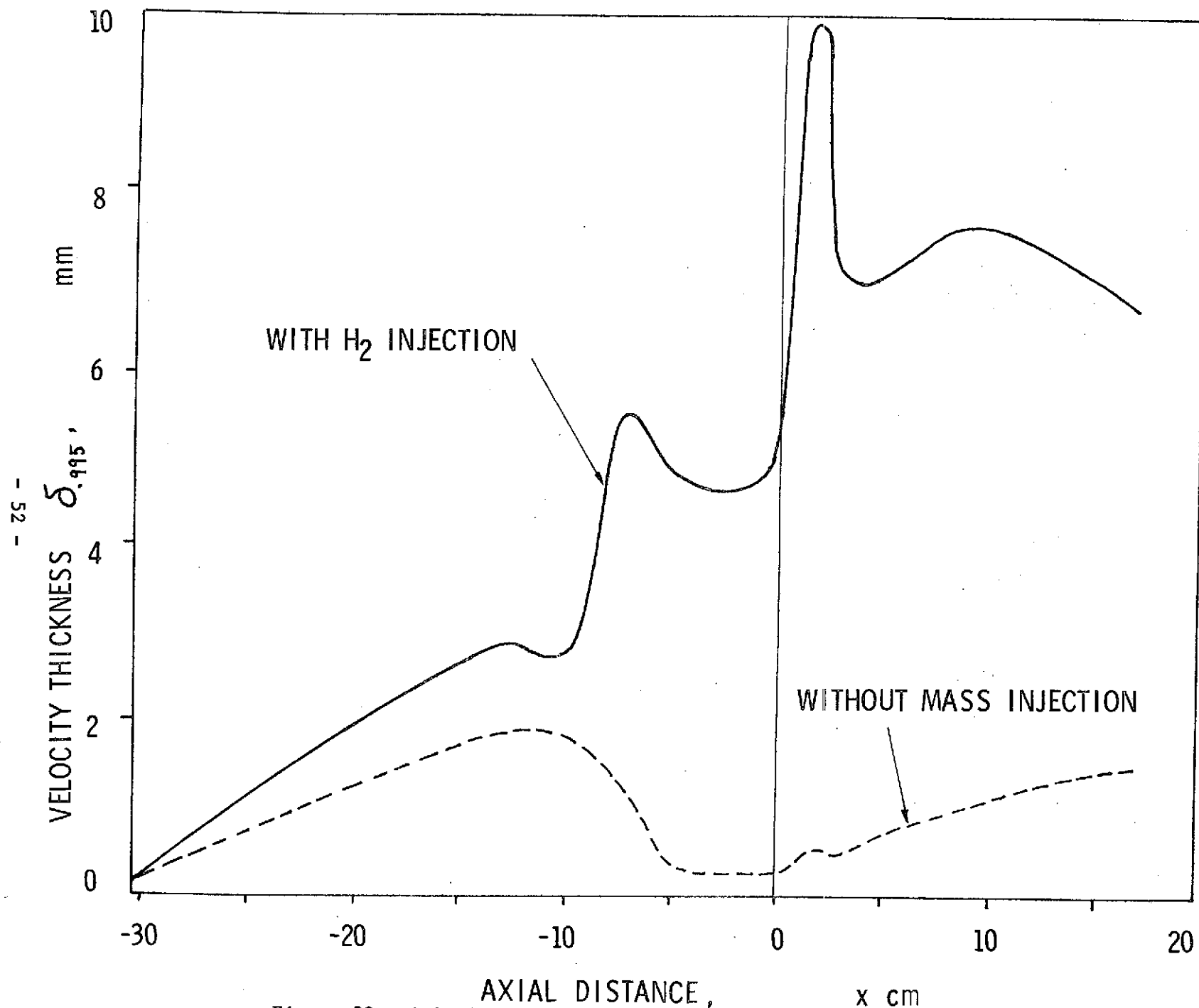


Figure 23. Calculated Distributions of Velocity Thickness

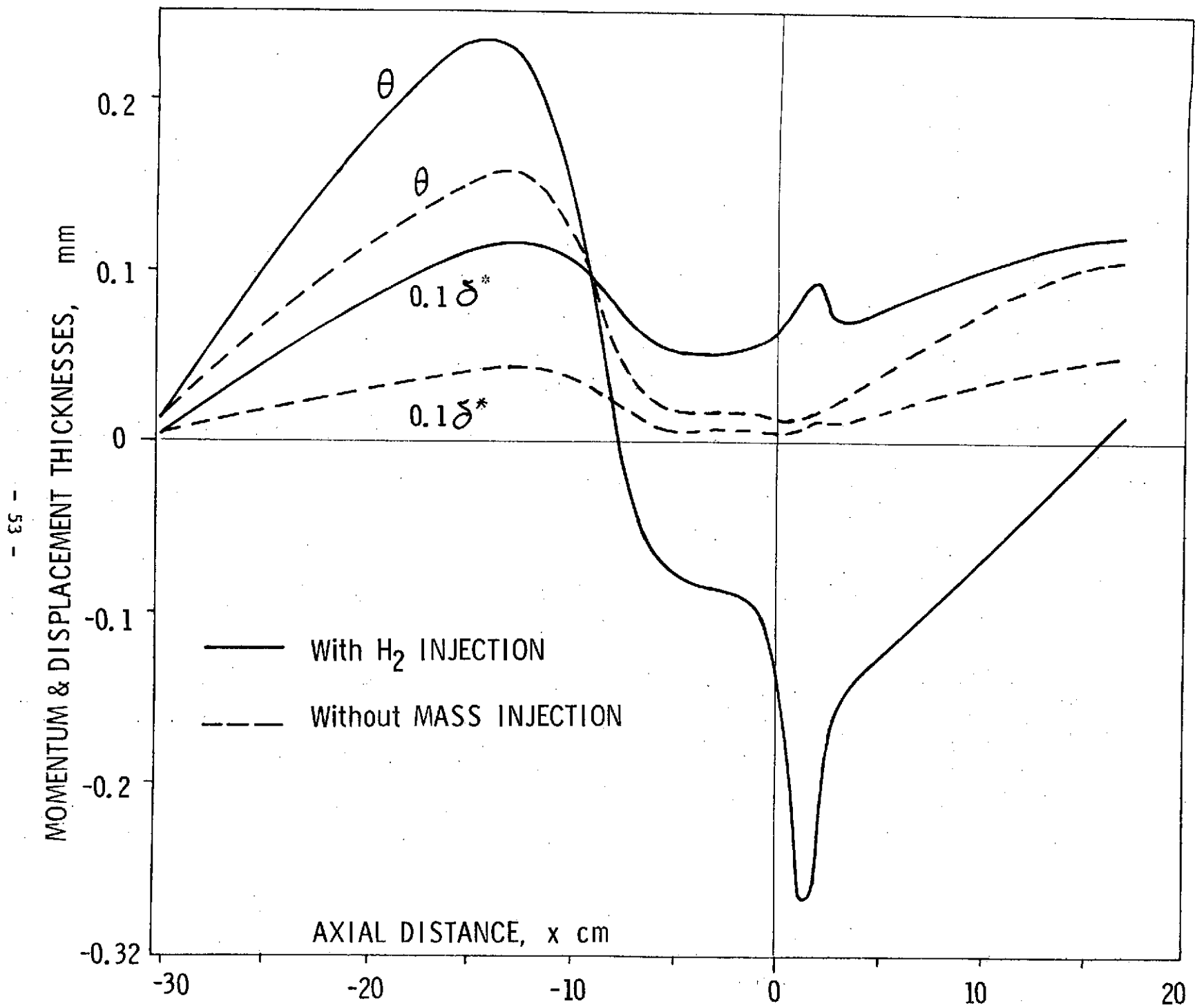


Figure 24. Calculated Distributions of Momentum and Displacement Thicknesses

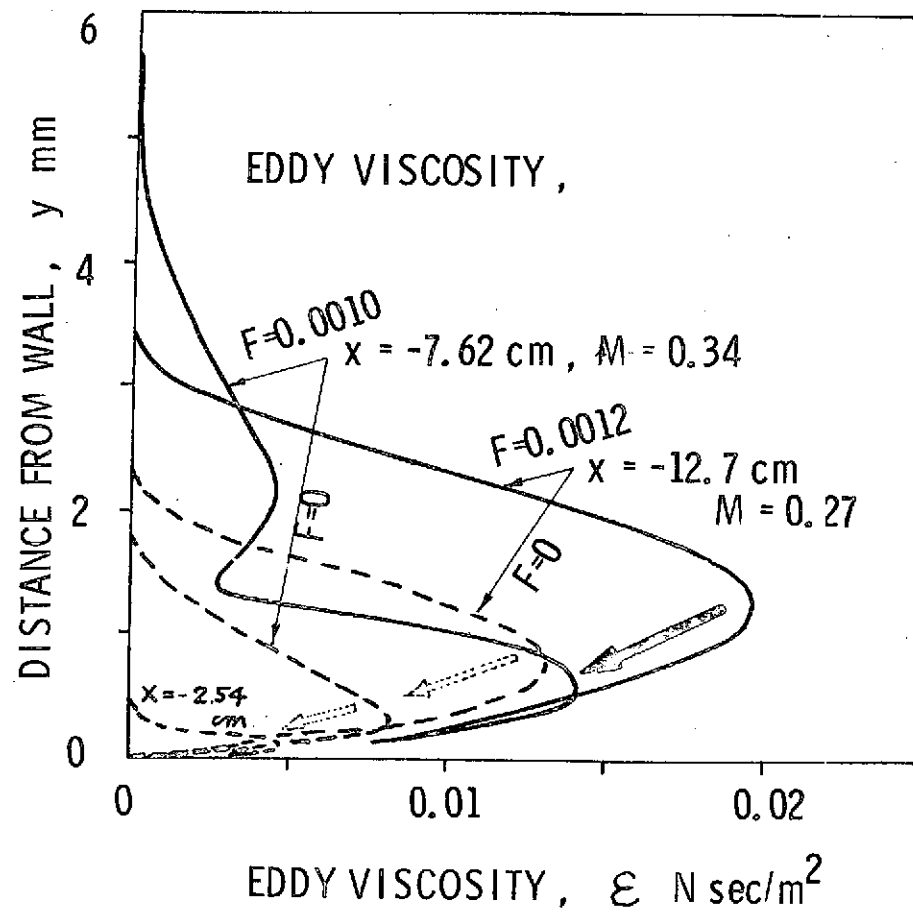


Figure 25. Comparison of Eddy Viscosities with and without Hydrogen Injection

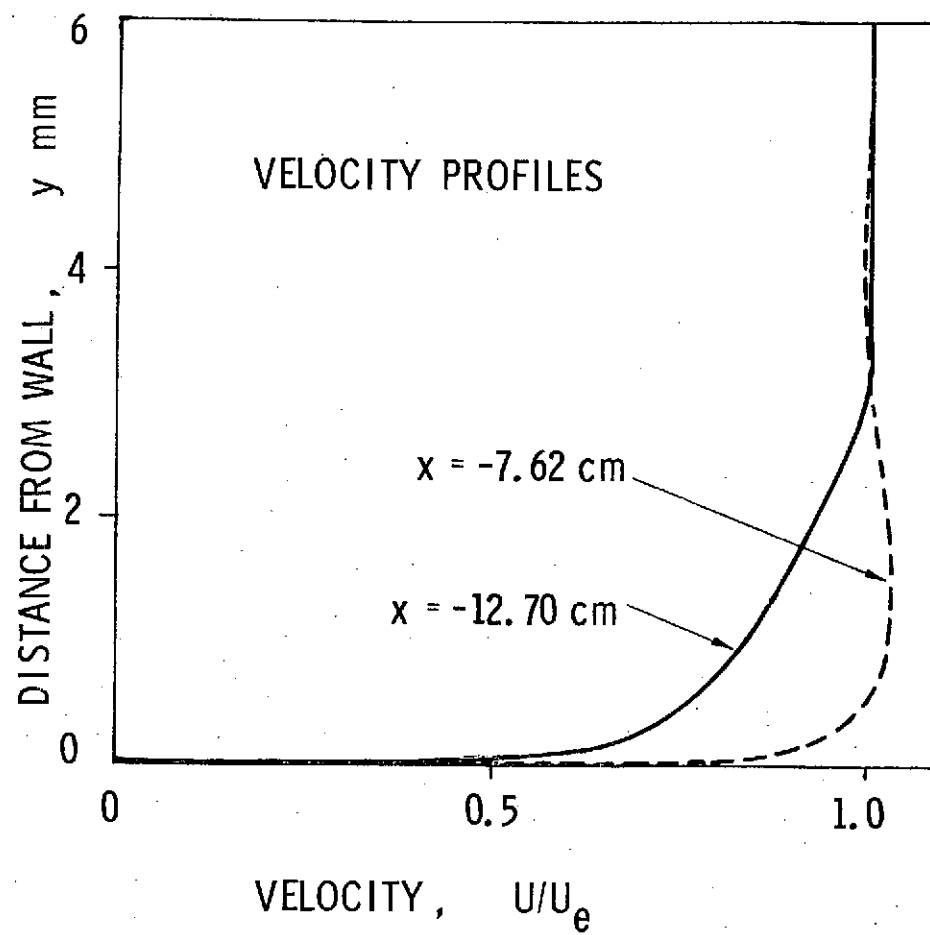


Figure 26. Velocity Profiles with Hydrogen Injection

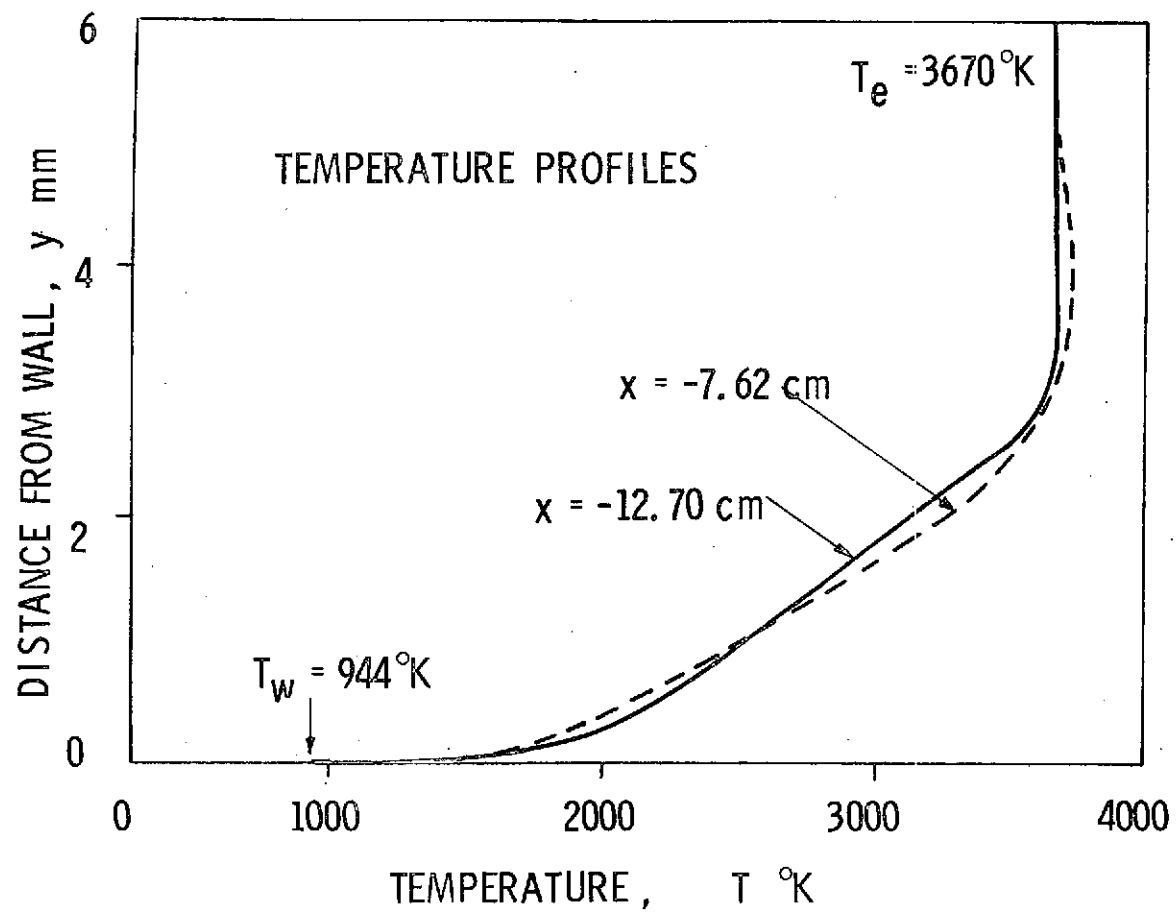


Figure 27. Temperature Profiles with Hydrogen Injection

\dot{m}_w g/sec cm ²	θ cm	δ^* cm	C_f
0.1182	-0.0025	0.1129	0.001228
0	0.0096	0.0429	0.001094

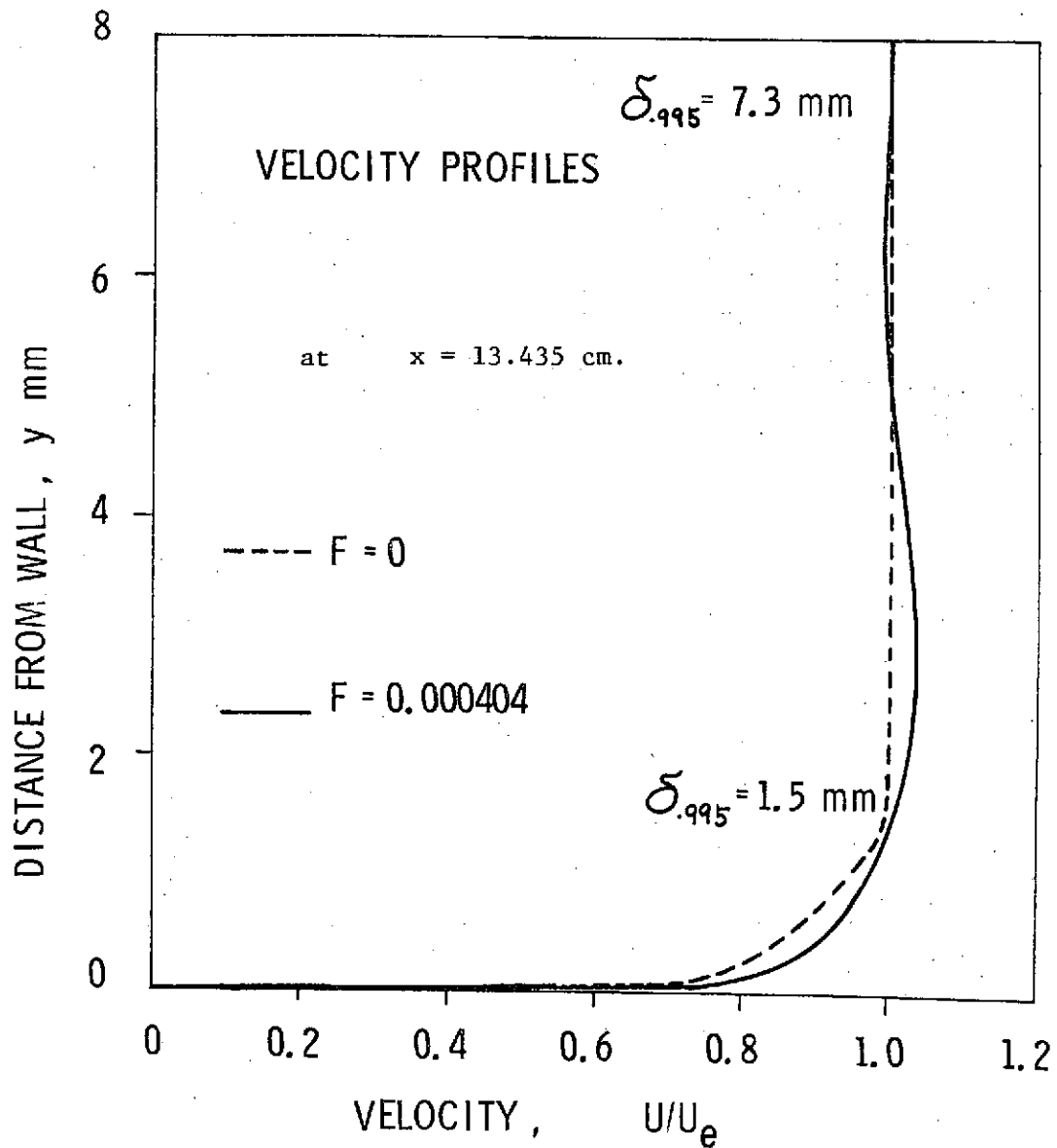


Figure 28. Comparison of Velocity Profiles with and without Hydrogen Injection at $M = 2.8$

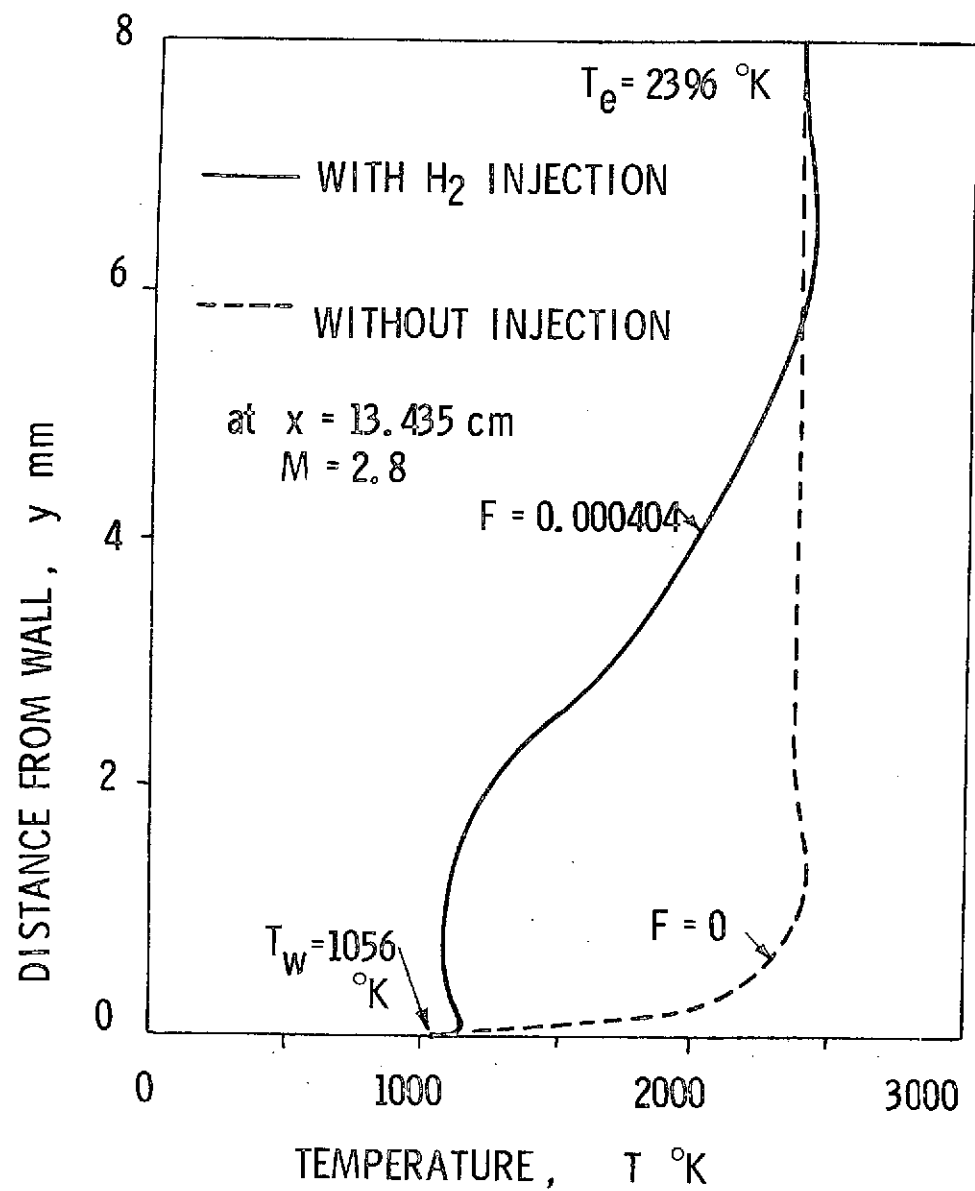


Figure 29. Comparison of Temperature Profiles with and without Hydrogen Injection at $M = 2.8$

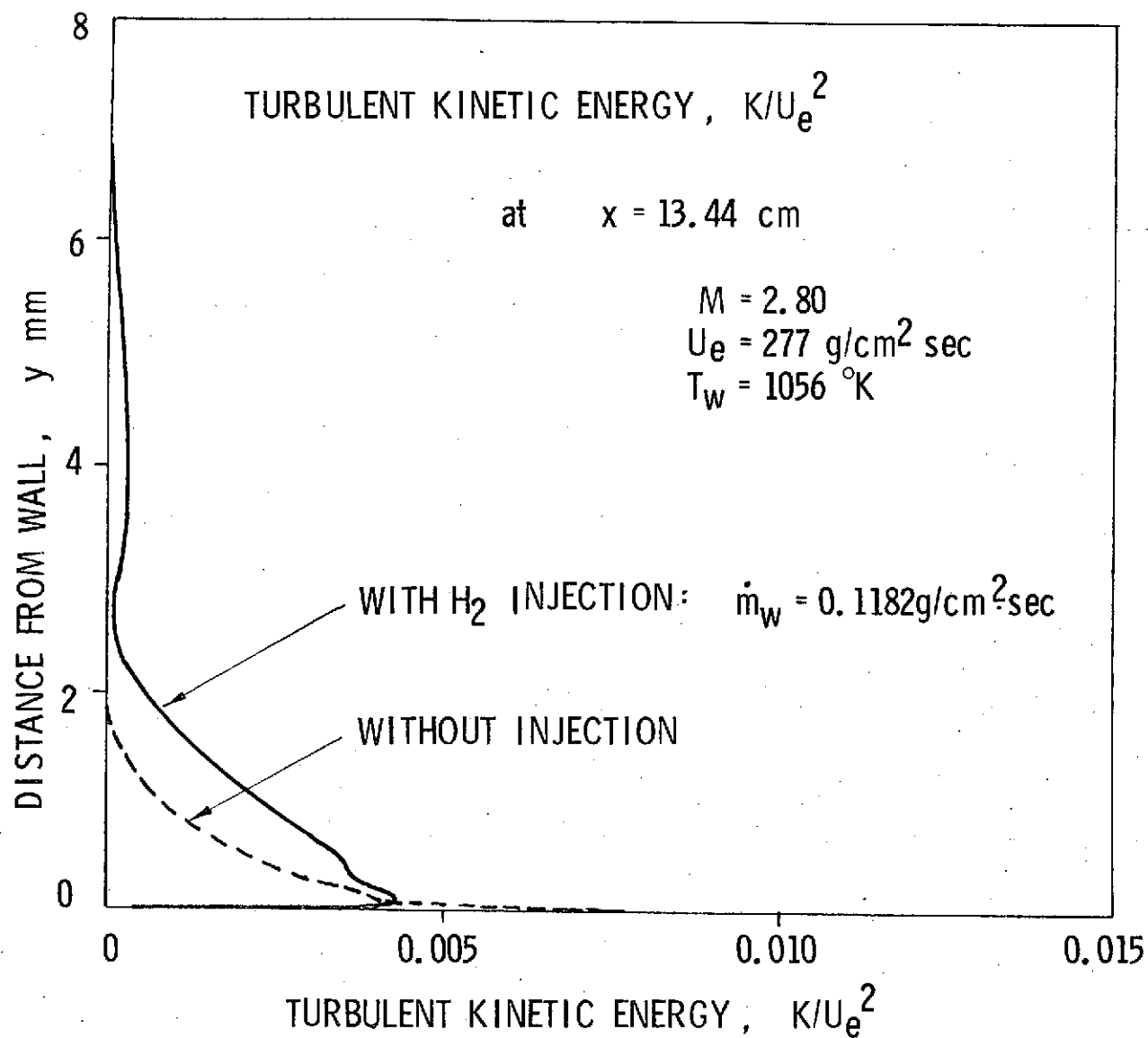


Figure 30. Comparison of Turbulent Kinetic Energy Profiles with and without Hydrogen at $M=2.35$ and 2.8

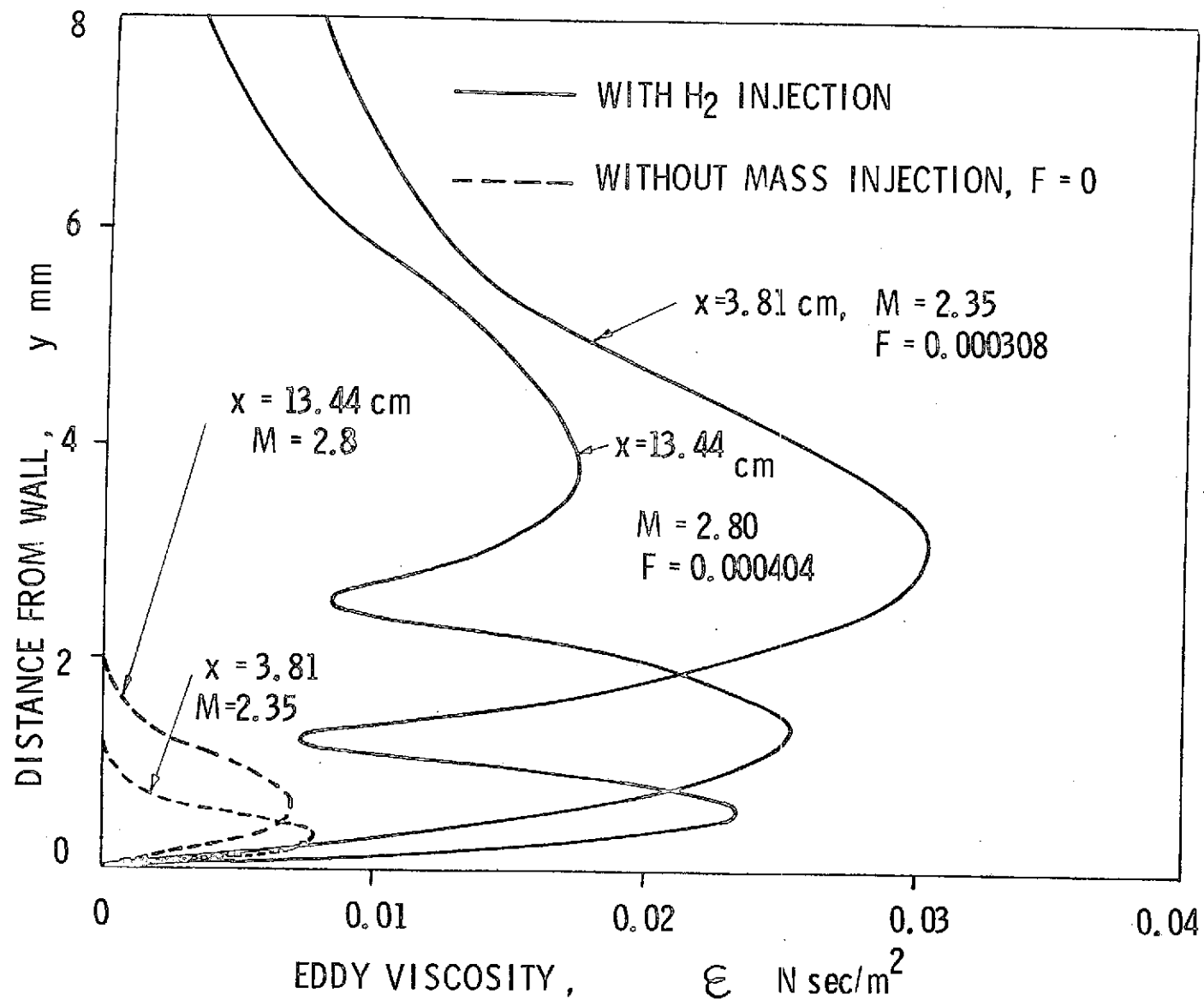


Figure 31. Comparison of Eddy Viscosity Profiles with and without Hydrogen Injection at $M=2.35$ and 2.8

Table I EFFECTS OF MASS INJECTION AND COMBUSTION
ON BOUNDARY LAYER CHARACTERISTICS AT $x = 76.2 \text{ cm}$

		$\delta_{990} \text{ cm}$	$\delta^* \text{ cm}$	$\theta \text{ cm}$	C_f	$\tau_w \text{ N/m}^2$	K_{\max}/U_e^2	$\epsilon_{\max} \frac{\text{N sec}}{\text{m}^2}$
WITHOUT INJECTION	COLD WALL $T_w = 150^\circ \text{K}$	1.234	0.131	0.191	0.00440	0.3103	0.0048	0.000661
	ISOTHERMAL $T_w = 295^\circ \text{K}$	1.387	0.271	0.183	0.00386	0.2586	0.0051	0.000656
	HOT WALL $T_w = 556^\circ \text{K}$	1.463	0.386	0.166	0.00356	0.2466	0.0054	0.000651
100 % N_2 INJECTION $\dot{m}_w = 0.0044 \text{ g/cm}^2 \cdot \text{s}$		2.484	1.096	0.332	0.00143	0.1010	0.0075	0.001317
4 % H_2 INJECTION $\dot{m}_w = 0.0044 \text{ g/cm}^2 \cdot \text{s}$		4.120	2.712	0.287	0.00034	0.0233	0.0129	0.001317

COLD WALL : WALL HAS A CONSTANT TEMPERATURE OF 150°K

ISOTHERMAL : WALL TEMPERATURE IS SAME AS MAIN FLOW TEMPERATURE

HOT WALL : WALL TEMPERATURE DISTRIBUTION IS AS SHOWN IN Fig. 6

APPENDIX A

TURBULENT BOUNDARY LAYER EQUATIONS

1. Continuity Equation

The overall continuity equation for steady flow reads

$$\frac{\partial (\rho u_i)}{\partial x_i} = 0 \quad (A-1)$$

in cartesian tensor notation.

In turbulent flows this equation must be true at any instant, but also on the average. The instantaneous quantities are replaced by the time average plus the fluctuating as follows:

$$\rho = \bar{\rho} + \rho' \quad (A-2)$$

and

$$u_i = \bar{u}_i + u_i' \quad (A-3)$$

Substitute these expressions in Eq. (A-1), then

$$\frac{\partial [(\bar{\rho} + \rho') (\bar{u}_i + u_i')] }{\partial x_i} = 0 \quad (A-4)$$

Since

$$(\bar{\rho} + \rho') (\bar{u}_i + u_i') = \bar{\rho} \bar{u}_i + \bar{\rho} u_i' + \rho' \bar{u}_i + \rho' u_i' \quad (A-5)$$

taking the time average of this equation and applying Reynolds' rule* of averages, we obtain

$$\begin{aligned} \overline{(\bar{\rho} + \rho') (\bar{u}_i + u_i')} &= \overline{\bar{\rho} \bar{u}_i} + \overline{\bar{\rho} u_i'} + \overline{\rho' \bar{u}_i} + \overline{\rho' u_i'} \\ &= \bar{\rho} \bar{u}_i + \bar{\rho} \overline{u_i'} + \overline{\rho' \bar{u}_i} + \overline{\rho' u_i'} \quad (A-6) \\ &= \bar{\rho} \bar{u}_i + \overline{\rho' u_i'} \end{aligned}$$

Therefore the continuity equation is written as

*Hughes, W. F., and Brighton, J. A., "Schaum's Outline of Theory and Problems of Fluid Dynamics," Schsum Publishing Co., 1964, p. 179.

$$\frac{\partial (\bar{\rho} \bar{u}_i + \overline{\rho' u_i'})}{\partial x_i} = 0 \quad (\text{A-7})$$

This equation is expressed for two-dimensional or axisymmetric flow in a curvilinear coordinate system as follows, in which s is the wetted length along the wall and y is measured normal to it*.

$$\frac{\partial}{\partial s} [(\bar{\rho} \bar{u} + \overline{\rho' u'}) r_w^j] + \frac{\partial}{\partial y} [(\bar{\rho} \bar{v} + \overline{\rho' v'}) r_w^j] = 0 \quad (\text{A-8})$$

where

$j = 0$ for two-dimensional planar flow

and $j = 1$ for axisymmetric flow.

Assuming

$$\frac{\partial (\overline{\rho' u'}) r_w^j}{\partial s} \ll \frac{\partial (\overline{\rho' v'}) r_w^j}{\partial y} \quad (\text{A-9})$$

Eq. (A-8) becomes

$$\frac{\partial (\bar{\rho} \bar{u} r_w^j)}{\partial s} + \frac{\partial [(\bar{\rho} \bar{v} + \overline{\rho' v'}) r_w^j]}{\partial y} = 0 \quad (\text{A-10})$$

The velocities, u and v , are those components along s and y , respectively.

2. Momentum Equation

The momentum equations are written in a cartesian notation as follows** for steady flow:

$$\rho u_i \frac{\partial u_i}{\partial x_i} = \frac{\partial \sigma_{ij}}{\partial x_i} \quad (\text{A-11})$$

where the stress tensor, σ_{ij} , is

$$\sigma_{ij} = -p \delta_{ij} + \mu \left(\frac{\partial u_i}{\partial x_j} + \frac{\partial u_j}{\partial x_i} - \frac{2}{3} \delta_{ij} \frac{\partial u_k}{\partial x_k} \right) + \zeta \delta_{ij} \frac{\partial u_k}{\partial x_k} \quad (\text{A-12})$$

*Schlichting, H., "Boundary-Layer Theory", McGraw-Hill Book Co., 1968, p. 223.

**Landau, L.D., and Lifshitz, E. M., "Fluid Mechanics," Pergamon Press, 1959, p. 48.

The quantities μ and ζ are called the molecular (or dynamic) viscosity and the bulk viscosity, and are functions of pressure and temperature. Neglecting the bulk viscosity term in Eq. (A-11) according to the Shvab-Zeldovich formulation[†], we can write Eq. (A-11) in cartesian coordinates as

$$\begin{aligned} \rho u_1 \frac{\partial u_1}{\partial x_1} + \rho u_2 \frac{\partial u_1}{\partial x_2} = & - \frac{\partial p}{\partial x_1} + \frac{\partial}{\partial x_1} \left\{ \mu \left[\left(\frac{\partial u_1}{\partial x_1} + \frac{\partial u_1}{\partial x_1} \right) - \frac{2}{3} \left(\frac{\partial u_1}{\partial x_1} + \frac{\partial u_2}{\partial x_2} \right) \right] \right\} \\ & + \frac{\partial}{\partial x_2} \left\{ \mu \left(\frac{\partial u_1}{\partial x_2} + \frac{\partial u_2}{\partial x_1} \right) \right\} \end{aligned} \quad (A-13)$$

and

$$\begin{aligned} \rho u_1 \frac{\partial u_2}{\partial x_1} + \rho u_2 \frac{\partial u_2}{\partial x_2} = & - \frac{\partial p}{\partial x_2} + \frac{\partial}{\partial x_1} \left\{ \mu \left(\frac{\partial u_2}{\partial x_1} + \frac{\partial u_1}{\partial x_2} \right) \right\} \\ & + \frac{\partial}{\partial x_2} \left\{ \mu \left[\left(\frac{\partial u_2}{\partial x_2} + \frac{\partial u_2}{\partial x_2} \right) - \frac{2}{3} \left(\frac{\partial u_1}{\partial x_1} + \frac{\partial u_2}{\partial x_2} \right) \right] \right\} \end{aligned} \quad (A-14)$$

Because of the boundary layer assumption^{††} Eqs. (A-13) and (A-14) reduce to

$$\rho u_1 \frac{\partial u_1}{\partial x_1} + \rho u_2 \frac{\partial u_1}{\partial x_2} = - \frac{\partial p}{\partial x_1} + \frac{\partial}{\partial x_2} \left(\mu \frac{\partial u_1}{\partial x_2} \right) \quad (A-15)$$

and

$$\frac{\partial p}{\partial x_2} = 0 \quad (A-16)$$

multiplying u_1 by Eq. (A-1), we obtain

[†]Williams, F. A., "Combustion Theory," Addison-Wesley Publishing Co., Inc., 1965, p. 9.

^{††}Schlichting, H., "Boundary-Layer Theory," McGraw-Hill Book Co., 1968, p. 223.

$$u_1 \frac{\partial (\rho u_1)}{\partial x_1} + u_1 \frac{\partial (\rho u_2)}{\partial x_2} = 0 \quad (A-17)$$

Adding Eqs. (A-15) and (A-17) gives

$$\frac{\partial (\rho u_1 u_1)}{\partial x_1} + \frac{\partial (\rho u_1 u_2)}{\partial x_2} = - \frac{\partial p}{\partial x_1} + \frac{\partial}{\partial x_2} \left(\mu \frac{\partial u_1}{\partial x_2} \right) \quad (A-18)$$

Substituting the following relations into the above equation,

$$\begin{aligned} \rho &= \bar{\rho} + \rho' \\ u_i &= \bar{u}_i + u_i' \\ p &= \bar{p} + p' \end{aligned} \quad (A-19)$$

and taking the time averages, we obtain

$$\begin{aligned} & \frac{\partial}{\partial x_1} \left\{ \overline{(\bar{\rho} + \rho') (\bar{u}_1 + u_1') (\bar{u}_1 + u_1')} \right\} + \frac{\partial}{\partial x_2} \left\{ \overline{(\bar{\rho} + \rho') (\bar{u}_1 + u_1') (\bar{u}_2 + u_2')} \right\} \\ &= - \frac{\partial \overline{(\bar{p} + p')}}{\partial x_1} + \frac{\partial}{\partial x_2} \left\{ \mu \frac{\partial \overline{(\bar{u}_1 + u_1')}}{\partial x_2} \right\} \end{aligned} \quad (A-20)$$

According to the Reynolds rule of averages,

$$\begin{aligned} \overline{(\bar{\rho} + \rho') (\bar{u}_1 + u_1') (\bar{u}_1 + u_1')} &= \overline{(\bar{\rho} + \rho') (\bar{u}_1 \bar{u}_1 + 2 u_1' \bar{u}_1 + u_1' u_1')} \\ &= \bar{\rho} \bar{u}_1 \bar{u}_1 + 2 \bar{\rho} \overline{u_1' \bar{u}_1} + \bar{\rho} \overline{u_1' u_1'} \\ &+ \bar{\rho}' \bar{u}_1 \bar{u}_1 + 2 \bar{\rho}' \overline{u_1' \bar{u}_1} + \bar{\rho}' \overline{u_1' u_1'} \\ &= \bar{\rho} \bar{u}_1 \bar{u}_1 + \bar{\rho} \overline{u_1' u_1'} + 2 \bar{\rho}' \overline{u_1' \bar{u}_1} + \bar{\rho}' \overline{u_1' u_1'} \end{aligned} \quad (A-21)$$

$$\begin{aligned}
(\bar{\rho} + \rho') (\bar{u}_1 + u_1') (\bar{u}_2 + u_2') &= (\bar{\rho} + \rho') (\bar{u}_1 \bar{u}_2 + \bar{u}_1 u_2' + u_1' \bar{u}_2 + u_1' u_2') \\
&= \overline{\bar{\rho} \bar{u}_1 \bar{u}_2} + \overline{\bar{\rho} \bar{u}_1 u_2'} + \overline{\bar{\rho} u_1' \bar{u}_2} + \overline{\rho u_1' u_2'} \\
&\quad + \overline{\rho' \bar{u}_1 \bar{u}_2} + \overline{\rho' \bar{u}_1 u_2'} + \overline{\rho' u_1' \bar{u}_2} + \overline{\rho' u_1' u_2'} \\
&= \overline{\bar{\rho} \bar{u}_1 \bar{u}_2} + \overline{\bar{\rho} u_1' u_2'} + \overline{\rho' u_2' \bar{u}_1} + \overline{\rho' u_1' \bar{u}_2} + \overline{\rho' u_1' u_2'}
\end{aligned} \tag{A-22}$$

$$\bar{p} + p' = \bar{p} \tag{A-23}$$

and

$$\overline{\bar{u}_1 + u_1'} = \bar{u}_1 \tag{A-24}$$

Thus Eq. (A-20) reduces to

$$\begin{aligned}
&\frac{\partial (\bar{\rho} \bar{u}_1 \bar{u}_1 + \bar{\rho} \overline{u_1' u_1'} + 2\overline{\rho' u_1' \bar{u}_1} + \overline{\rho' u_1' u_1'})}{\partial x_1} \\
&+ \frac{\partial (\bar{\rho} \bar{u}_1 \bar{u}_2 + \bar{\rho} \overline{u_1' u_2'} + \overline{\rho' u_2' \bar{u}_1} + \overline{\rho' u_1' \bar{u}_2} + \overline{\rho' u_1' u_2'})}{\partial x_2} \\
&= - \frac{\partial \bar{p}}{\partial x_1} + \frac{\partial}{\partial x_2} \left(\mu \frac{\partial \bar{u}_1}{\partial x_2} \right)
\end{aligned} \tag{A-25}$$

Substituting Eq. (A-7) into the above equation, then

$$\begin{aligned}
&(\rho \bar{u}_1 + \overline{\rho' u_1'}) \frac{\partial \bar{u}_1}{\partial x_1} + (\bar{\rho} \bar{u}_2 + \overline{\rho' u_2'}) \frac{\partial \bar{u}_1}{\partial x_2} \\
&= - \frac{\partial \bar{p}}{\partial x_1} + \frac{\partial}{\partial x_2} \left(\mu \frac{\partial \bar{u}_1}{\partial x_2} \right) - \frac{\partial (\bar{\rho} \overline{u_1' u_1'} + \overline{\rho' u_1' u_1'} + \overline{\rho' u_1' u_1'})}{\partial x_1}
\end{aligned}$$

$$- \frac{\partial (\bar{\rho} \overline{u_1' u_2'} + \overline{\rho' u_1' u_2} + \overline{\rho' u_1' u_2'})}{\partial x_2} \quad (\text{A-26})$$

Since

$$\overline{\rho u_1' u_1'} + \overline{\rho' u_1' u_1} + \overline{\rho' u_1' u_1'} = \overline{(\rho u_1)' u_1'} \quad (\text{A-27})$$

and

$$\overline{\rho u_1' u_2'} + \overline{\rho' u_1' u_2} + \overline{\rho' u_1' u_2'} = \overline{(\rho u_2)' u_1'} \quad (\text{A-28})$$

Eq. (A-26) is written in a cleaner form as

$$\begin{aligned} & (\bar{\rho} \overline{u_1} + \overline{\rho' u_1'}) \frac{\partial \bar{u}_1}{\partial x_1} + (\bar{\rho} \overline{u_2} + \overline{\rho' u_2'}) \frac{\partial \bar{u}_1}{\partial x_2} \\ & = - \frac{\partial \bar{p}}{\partial x_1} + \frac{\partial}{\partial x_2} \left\{ \mu \frac{\partial \bar{u}_1}{\partial x_2} - \overline{(\rho u_2)' u_1'} \right\} - \frac{\partial}{\partial x_1} \left\{ \overline{(\rho u_1)' u_1'} \right\} \end{aligned} \quad (\text{A-29})$$

This equation is expressed in a curvilinear coordinate system for two-dimensional or axisymmetric flow,* when the transverse-curvature effect can be neglected, as

$$\begin{aligned} & (\bar{\rho} \overline{u} + \overline{\rho' u'}) \frac{\partial \bar{u}}{\partial s} + (\bar{\rho} \overline{v} + \overline{\rho' v'}) \frac{\partial \bar{u}}{\partial y} \\ & = - \frac{\partial \bar{p}}{\partial s} + \frac{\partial}{\partial y} \left\{ \mu \frac{\partial \bar{u}}{\partial y} - \overline{(\rho v)' u'} \right\} - \frac{\partial}{\partial s} \left\{ \overline{(\rho u)' u'} \right\} \end{aligned} \quad (\text{A-30})$$

Assuming

$$\overline{\rho' u'} \frac{\partial \bar{u}}{\partial s} \ll \overline{\rho' v'} \frac{\partial \bar{u}}{\partial y} \quad (\text{A-31})$$

and

$$\frac{\partial}{\partial s} \left\{ \overline{(\rho u)' u'} \right\} \ll \frac{\partial}{\partial y} \left\{ \overline{(\rho v)' u'} \right\} \quad (\text{A-32})$$

*Schlichting, H., "Boundary-Layer Theory," McGraw-Hill Book Co., 1968, p. 223.

we finally obtain the momentum equation in s- direction.

$$\bar{\rho} \bar{u} \frac{\partial \bar{u}}{\partial s} + (\bar{\rho} \bar{v} + \bar{\rho}' v') \frac{\partial \bar{u}}{\partial y} = -\frac{d\bar{p}}{ds} + \frac{\partial}{\partial y} \left\{ \mu \frac{\partial \bar{u}}{\partial y} - \overline{(\rho v)' u'} \right\} \quad (A-33)$$

The y- direction momentum equation (A-16) yields

$$\bar{p} + p' = \text{constant} \quad (A-34)$$

across the boundary layer at each station.

3. Energy Equation

The general energy equation*,** for steady state is written for two-dimensional or axisymmetric flow in cartesian tensor coordinates as

$$\begin{aligned} \rho u_1 \frac{\partial H}{\partial x_1} + \rho u_2 \frac{\partial H}{\partial x_2} = \frac{\partial}{\partial x_2} \left[\frac{\mu}{Pr} \frac{\partial H}{\partial x_2} + \mu \left(1 - \frac{1}{Pr} \right) u \frac{\partial u}{\partial x_2} \right. \\ \left. + \frac{\mu}{Pr} (Le - 1) \sum_{i=1}^n h_i \frac{\partial Y_i}{\partial x_2} \right] \end{aligned} \quad (A-35)$$

where

$$H = h + \frac{U^2}{2}$$

$$h = \sum_{i=1}^n h_i Y_i$$

$$h_i = \int_{T^0}^T C_{pi} dT + h_i^0 \quad (A-36)$$

*Hughes, W.F., and Brighton, J.A., "Schaum's Outline of Theory and Problems of Fluid Dynamics," Schaum Publishing Co., p 196

**Lees, L., "Convective Heat Transfer with Mass Addition and Chemical Reactions," 3rd AGARD, 1950, p457.

$$Pr = \mu \bar{c}_p / \lambda$$

$$\bar{c}_p = \sum_{i=1}^n c_{p_i} Y_i$$

$$Le = \rho D \bar{c}_p / \lambda$$

$$\mu = \mu(T) \quad (A-36)$$

$$\lambda = \lambda(T)$$

Adding Eq. (A-1) multiplied by the total enthalpy, H, and Eq. (A-35), then we obtain

$$\begin{aligned} \frac{\partial(\rho u_1 H)}{\partial x_1} + \frac{\partial(\rho u_2 H)}{\partial x_2} &= \frac{\partial}{\partial x_2} \left[\frac{\mu}{Pr} \frac{\partial H}{\partial x_2} + \mu \left(1 - \frac{1}{Pr}\right) u_1 \frac{\partial u_1}{\partial x_2} \right. \\ &\quad \left. + \frac{\mu}{Pr} (Le-1) \sum_{i=1}^n h_i \frac{\partial Y_i}{\partial x_2} \right] \end{aligned} \quad (A-37)$$

Substitute the following relations

$$u_j = \bar{u}_j + u_j'$$

$$\rho = \bar{\rho} + \rho'$$

$$H = \bar{H} + H'$$

$$Y = \bar{Y}_1 + Y_1'$$

$$h_i = \bar{h}_i + h_i'$$

into Eq. (A-37), and take the time average, then

$$\begin{aligned}
& \frac{\partial [(\bar{\rho} + \rho')(\bar{u}_1 + u_1')(\bar{H} + H')]}{\partial x_1} + \frac{\partial [(\bar{\rho} + \rho')(\bar{u}_2 + u_2')(\bar{H} + H')]}{\partial x_2} \\
&= \frac{\partial}{\partial x_2} \left[\frac{\mu}{P_r} \frac{\partial (\bar{H} + H')}{\partial x_2} + \mu \left(1 - \frac{1}{P_r}\right) (\bar{u}_1 + u_1') \frac{\partial (\bar{u}_1 + u_1')}{\partial x_2} \right. \\
&\quad \left. + \frac{\mu}{P_r} (L_e - 1) \sum_{i=1}^n (\bar{h}_i + h_i') \frac{\partial (\bar{Y}_i + Y_i')}{\partial x_2} \right]
\end{aligned} \tag{A-39}$$

The left-hand side of the above equation is simplified using the turbulent continuity equation (A-7) as

$$\begin{aligned}
& \frac{\partial [(\bar{\rho} + \rho')(\bar{u}_1 + u_1')(\bar{H} + H')]}{\partial x_1} + \frac{\partial [(\bar{\rho} + \rho')(\bar{u}_2 + u_2')(\bar{H} + H')]}{\partial x_2} \\
&= \frac{\partial (\bar{\rho} \bar{u}_1 \bar{H} + \bar{\rho}' u_1' \bar{H} + \bar{\rho} \bar{u}_1' H' + \bar{\rho}' H' \bar{u}_1 + \bar{\rho}' u_1' H')}{\partial x_1} \\
&\quad + \frac{\partial (\bar{\rho} \bar{u}_2 \bar{H} + \bar{\rho}' u_2' \bar{H} + \bar{\rho} \bar{u}_2' H' + \bar{\rho}' H' \bar{u}_2 + \bar{\rho}' u_2' H')}{\partial x_2} \\
&= (\bar{\rho} \bar{u}_1 + \bar{\rho}' u_1') \frac{\partial \bar{H}}{\partial x_1} + (\bar{\rho} \bar{u}_2 + \bar{\rho}' u_2') \frac{\partial \bar{H}}{\partial x_2} \\
&\quad + \frac{\partial (\bar{\rho} \bar{u}_1' H' + \bar{\rho}' H' \bar{u}_1 + \bar{\rho}' u_1' H')}{\partial x_1} + \frac{\partial (\bar{\rho} \bar{u}_2' H' + \bar{\rho}' H' \bar{u}_2 + \bar{\rho}' u_2' H')}{\partial x_2}
\end{aligned} \tag{A-40}$$

where

$$\begin{aligned}\overline{\rho} \overline{u_1' H'} + \overline{\rho' H'} \overline{u_1} + \overline{\rho' u_1' H'} &= \overline{(\rho u_1)' H'} \\ \overline{\rho} \overline{u_2' H'} + \overline{\rho' H'} \overline{u_2} + \overline{\rho' u_2' H'} &= \overline{(\rho u_2)' H'}\end{aligned}\quad (A-41)$$

Assuming

$$\frac{\partial [(\rho u_1)' H']}{\partial x_1} \ll \frac{\partial [(\rho u_2)' H']}{\partial x_2} \quad (A-42)$$

and

$$\overline{\rho'} \overline{u_1'} \ll \overline{\rho} \overline{u_1} \quad (A-43)$$

Eq. (A-39) is simplified to

$$\begin{aligned}& \overline{\rho_1} \overline{u_1} \frac{\partial \overline{H}}{\partial x_1} + (\overline{\rho} \overline{u_2} + \overline{\rho' u_2'}) \frac{\partial \overline{H}}{\partial x_2} \\ &= \frac{\partial}{\partial x_2} \left[\frac{\mu}{P_r} \frac{\partial \overline{H}}{\partial x_2} - \{(\rho u)' H'\} + \mu \left(1 - \frac{1}{P_r}\right) \left\{ \overline{u} \frac{\partial \overline{u}}{\partial x_2} + \frac{1}{2} \frac{\partial (\overline{u' u'})}{\partial x_2} \right\} \right. \\ & \quad \left. + \frac{\mu}{P_r} (Le-1) \sum_{i=1}^n \left\{ \overline{h_i} \frac{\partial \overline{Y_i}}{\partial x_2} + (\overline{h_i'}) \frac{\partial \overline{Y_i'}}{\partial x_2} \right\} \right] \quad (A-44)\end{aligned}$$

Since

$$\begin{aligned}H &= h + \frac{u_1^2}{2} \\ &= \overline{h} + h' + \frac{(\overline{u_1} + u_1')^2}{2} \\ &= \overline{h} + \frac{\overline{u_1}^2}{2} + h' + \overline{u_1} u_1' + \frac{u_1'^2}{2} \\ &= \overline{H} + H'\end{aligned}\quad (A-45)$$

Thus

$$H' = h' + \bar{u}_1 u_1' + \frac{u_1'^2}{2} \quad (A-46)$$

The fluctuating term, $(\rho u_2)'$, is expressed as

$$\begin{aligned} (\rho u_2)' &= \rho u_2 - \overline{(\rho u_2)} \\ &= (\bar{\rho} + \rho')(\bar{u}_2 + u_2') - \overline{(\bar{\rho} + \rho')(\bar{u}_2 + u_2')} \\ &= \bar{\rho} \bar{u}_2 + \rho' \bar{u}_2 + \bar{\rho} u_2' + \rho' u_2' - \bar{\rho} \bar{u}_2 - \overline{\rho' u_2'} \\ &= \rho' \bar{u}_2 + \bar{\rho} u_2' + \rho' u_2' - \overline{\rho' u_2'} \end{aligned} \quad (A-47)$$

Therefore

$$\begin{aligned} -\overline{(\rho u_2)' H'} &= -(\rho' \bar{u}_2 + \bar{\rho} u_2' + \rho' u_2' - \overline{\rho' u_2'}) \left(h' + \bar{u}_1 u_1' + \frac{u_1'^2}{2} \right) \\ &= -(\overline{\rho' h'} \bar{u}_2 + \overline{\rho' u_1'} \bar{u}_1 \bar{u}_2 + \frac{\overline{\rho' u_1' u_1' u_2}}{2} + \bar{\rho} \overline{u_2' h'}) \\ &\quad + \bar{\rho} \bar{u}_1 \overline{u_1' u_2'} + \frac{\overline{\rho u_1' u_1' u_2'}}{2} + \overline{\rho' u_2' h'} + \overline{\rho' u_1' u_2'} \bar{u}_1 \\ &\quad + \frac{\overline{\rho' u_1' u_1' u_2'}}{2} - \frac{\overline{\rho' u_2' u_1' u_1'}}{2}) \end{aligned} \quad (A-48)$$

Neglecting the terms which include three or four correlations, we

simplify Eq. (A-48) as

$$-\overline{(\rho u_2)' H'} = -(\overline{\rho' h'} \bar{u}_2 + \overline{\rho' u_1'} \bar{u}_1 \bar{u}_2 + \overline{\rho u_2' h'} + \bar{\rho} \bar{u}_1 \overline{u_1' u_2'}) \quad (A-49)$$

The fluctuating term of static enthalpy, h' , is expressed as

$$\begin{aligned}
 h' &= h - \bar{h} = \sum_{i=1}^n h_i Y_i - \overline{\sum_{i=1}^n h_i Y_i} \\
 &= \sum_{i=1}^n (\bar{h}_i + h_i') (\bar{Y}_i + Y_i') - \overline{\sum_{i=1}^n (\bar{h}_i + h_i') (\bar{Y}_i + Y_i')} \\
 &= \sum_{i=1}^n (\bar{h}_i \bar{Y}_i + \bar{h}_i Y_i' + h_i' \bar{Y}_i + h_i' Y_i') \\
 &= \sum_{i=1}^n (\bar{h}_i \bar{Y}_i + \overline{h_i' Y_i'}) \\
 &= \sum_{i=1}^n (\bar{h}_i Y_i' + h_i' \bar{Y}_i + h_i' Y_i' - \overline{h_i' Y_i'})
 \end{aligned}$$

(A-50)

Substitute the above equation into Eq. (A-49), and neglect third correlation terms, then

$$\begin{aligned}
 -(\rho u_2)' H' &\approx - \sum_{i=1}^n \{ \bar{u}_2 (\rho' Y_i' \bar{h}_i + \rho' h_i' \bar{Y}_i) + \bar{\rho} (\bar{h}_i \overline{u_2' Y_i'} + \overline{u_2' h_i' Y_i'}) \} \\
 &= - (\overline{\rho' u_1' u_1} \bar{u}_2 + \bar{\rho} \overline{u_1 u_1' u_2'}) \\
 &= - \sum_{i=1}^n \{ (\overline{\rho' h_i' u_2} + \bar{\rho} \overline{u_2' h_i'}) \bar{Y}_i + (\overline{\rho' Y_i' u_2} + \bar{\rho} \overline{u_2' Y_i'}) \bar{h}_i \} \\
 &= - \bar{u}_1 (\overline{\rho' u_1' u_2} + \bar{\rho} \overline{u_1' u_2'})
 \end{aligned}$$

(A-51)

where

$$\overline{\rho' h_1'} \overline{u_2} + \overline{\rho u_2' h_1'} = \overline{(\rho u_2)' h_1'} - \overline{\rho' u_2' h_1'} \quad (A-52)$$

$$\overline{\rho' Y_1'} \overline{u_2} + \overline{\rho u_2' Y_1'} = \overline{(\rho u_2)' Y_1'} - \overline{\rho' u_2' Y_1'} \quad (A-53)$$

$$\overline{\rho' u_1'} \overline{u_2} + \overline{\rho u_1' u_2'} = \overline{(\rho u_2)' u_1'} - \overline{\rho' u_1' u_2'} \quad (A-54)$$

Eq. (A-51) is rewritten as

$$\begin{aligned} -\overline{(\rho u_2)' h_1'} = & -\sum_{i=1}^n \{ [\overline{(\rho u_2)' h_1'} - \overline{\rho' u_2' h_1'}] \overline{Y_1} + [\overline{(\rho u_2)' Y_1'} \\ & - \overline{\rho' u_2' Y_1'}] \overline{h_1} \} - \overline{u_1} [\overline{(\rho u_2)' u_1'} - \overline{\rho' u_1' u_2'}] \end{aligned} \quad (A-55)$$

Let us define the turbulent thermal conductivity, λ_T , and diffusivity, D_T , as

$$-\sum_{i=1}^n [\overline{(\rho u_2)' h_1'} - \overline{\rho' u_2' h_1'}] \overline{Y_1} = \lambda_T \frac{\partial \overline{T}}{\partial x_2} \quad (A-56)$$

$$- [\overline{(\rho u_2)' Y_1'} - \overline{\rho' u_2' Y_1'}] = \overline{\rho} D_T \frac{\partial \overline{Y_1}}{\partial x_2} \quad (A-57)$$

and assume

$$\overline{(\rho u_2)' u_1'} \gg \overline{\rho' u_1' u_2'} \quad (A-58)$$

$$\frac{\partial}{\partial x_2} \left(\overline{u_1} \frac{\partial \overline{u_1}}{\partial x_2} \right) \gg \frac{1}{2} \frac{\partial^2 \overline{(u_1' u_1')}}{\partial x_2^2} \quad (A-59)$$

and

$$\frac{\partial}{\partial x_2} \left(\overline{h_1} \frac{\partial \overline{Y_1}}{\partial x_2} \right) \gg \frac{\partial}{\partial x_2} \left(\overline{h_1'} \frac{\partial \overline{Y_1'}}{\partial x_2} \right) \quad (A-60)$$

then, Eq. (A-44) becomes

$$\begin{aligned}
 & (\bar{\rho} \bar{u}_1 + \bar{\rho}' u_1') \frac{\partial \bar{H}}{\partial x_1} + (\bar{\rho} \bar{u}_2 + \bar{\rho}' u_2') \frac{\partial \bar{H}}{\partial x_2} \\
 & = \frac{\partial}{\partial x_2} \left[\frac{\mu}{P_r} \frac{\partial \bar{H}}{\partial x_2} + \lambda_T \frac{\partial \bar{T}}{\partial x_2} + \bar{\rho} D_T \sum_{i=1}^n (\bar{h}_i \frac{\partial \bar{Y}_i}{\partial x_2}) - \bar{u} (\bar{\rho} u_2)' u_1' \right. \\
 & \quad \left. + \mu (1 - \frac{1}{P_r}) \bar{u}_1 \frac{\partial \bar{u}_1}{\partial x_2} + \frac{\mu}{P_r} (Le-1) \sum_{i=1}^n (\bar{h}_i \frac{\partial \bar{Y}_i}{\partial x_2}) \right] \quad (A-61)
 \end{aligned}$$

In order to replace the temperature, \bar{T} , in the above equation to the static enthalpy, h and h_i , and the species mass fraction Y_i , consider the definition of the averaged specific heat, \tilde{C}_p .

$$\begin{aligned}
 \tilde{C}_p & = \sum_{i=1}^n C_{p_i} Y_i = \sum_{i=1}^n \left(\frac{\partial h_i}{\partial T} \right) Y_i \\
 & = \sum_{i=1}^n \left[\frac{\partial (h_i Y_i)}{\partial T} - h_i \frac{\partial Y_i}{\partial T} \right] \\
 & = \frac{\partial h}{\partial T} - \sum_{i=1}^n h_i \frac{\partial Y_i}{\partial T} \quad (A-62)
 \end{aligned}$$

Thus

$$\tilde{C}_p \frac{\partial \bar{T}}{\partial x} = \frac{\partial h}{\partial x_2} - \sum_{i=1}^n h_i \frac{\partial Y_i}{\partial x_2} \quad (A-63)$$

Taking the time mean of the above equation considering Eq. (A-60),

then

$$\frac{\partial \bar{T}}{\partial x_2} = \frac{1}{\tilde{C}_p} \left(\frac{\partial \bar{h}}{\partial x_2} - \sum_{i=1}^n \bar{h}_i \frac{\partial \bar{Y}_i}{\partial x_2} \right) \quad (A-64)$$

Now the eddy viscosity, ϵ , the turbulent Lewis and Prandtl numbers,

Le_T and Pr_T , are defined as follows:

$$\epsilon = -(\rho u_2)' u_1' \frac{\partial \bar{u}}{\partial x_2} \quad (A-65)$$

$$Le_T = \frac{\bar{\rho} \tilde{C}_p}{\lambda_T} \quad (A-66)$$

and

$$Pr_T = \frac{\epsilon \tilde{C}_p}{\lambda_T} \quad (A-67)$$

Considering Eqs. (A-64) through (A-67), Eq. (A-61) is written in a curvilinear coordinate system as

$$\begin{aligned} \bar{\rho} \bar{u} \frac{\partial \bar{H}}{\partial s} + (\bar{\rho} v + \bar{\rho}' v') \frac{\partial \bar{H}}{\partial y} = \frac{\partial}{\partial y} \left\{ \left(\frac{\mu}{Pr} + \frac{\epsilon}{Pr_T} \right) \frac{\partial \bar{H}}{\partial y} + \right. \\ \left. \left[\mu \left(1 - \frac{1}{Pr} \right) + \epsilon \left(1 - \frac{1}{Pr_T} \right) \right] \bar{u} \frac{\partial \bar{u}}{\partial y} + \left[\frac{\mu}{Pr} (Le - 1) + \frac{\epsilon}{Pr_T} (Le_T - 1) \right] \sum_{i=1}^R \bar{h}_i \frac{\partial \bar{Y}_i}{\partial y} \right\} \end{aligned} \quad (A-68)$$

where the assumption below was made.

$$\frac{\bar{\rho}' u'}{\bar{\rho}} \frac{\partial \bar{H}}{\partial s} \ll \frac{\bar{\rho}' v'}{\bar{\rho}} \frac{\partial \bar{H}}{\partial y} \quad (A-69)$$

4. Element Equation

Since there is no generation nor disappearance of atoms in the system considered, the continuity conservation equation of each atom, m , is written as

$$\text{div} (\rho m u_m) = 0 \quad (A-70)$$

where

$$\rho_m = \rho \alpha_m \quad (A-71)$$

$$u_m = u_{m,dif} + u \quad (A-72)$$

$$\left(\begin{array}{ll} u_m & : \text{Velocity of element } m \\ u_{dif} & : \text{Diffusion velocity of element } m \\ u & : \text{Mean velocity} \end{array} \right.$$

Thus

$$\text{div} [\rho \alpha_m (u_{m,dif} + u)] = 0 \quad (A-73)$$

This equation is rewritten as

$$(\rho u \text{ grad}) \alpha_m + \text{div} (\rho \alpha_m u_{m,dif}) + \alpha_m \text{div} (\rho u) = 0 \quad (A-74)$$

Considering the overall continuity equation, Eq. (A-1), and

Fick's Law

$$\rho u_{m,dif} = - (\rho D \text{ grad}) \alpha_m \quad (A-75)$$

Eq. (A-74) becomes

$$(\rho u \text{ grad}) \alpha_m = \text{div} [(\rho D \text{ grad}) \alpha_m] \quad (A-76)$$

For two-dimensional or axisymmetric flow, this equation is expressed

in a curvilinear coordinate with the boundary layer assumption.

$$\rho u \frac{\partial \alpha_m}{\partial s} + \rho v \frac{\partial \alpha_m}{\partial y} = \frac{\partial}{\partial y} \left(\rho D \frac{\partial \alpha_m}{\partial y} \right) \quad (A-77)$$

Multiply d_m to Eq. (A-1), then

$$\alpha_m \frac{\partial(\rho u)}{\partial s} + \alpha_m \frac{\partial(\rho v)}{\partial y} = 0$$

Add the above two equations, and we obtain

$$\frac{\partial(\rho u \alpha_m)}{\partial s} + \frac{\partial(\rho v \alpha_m)}{\partial y} = \frac{\partial}{\partial y} (\rho D \frac{\partial \alpha_m}{\partial y}) \quad (A-79)$$

Substituting Eqs. (A-2) and (A-3), and

$$\alpha_m = \bar{\alpha}_m + \alpha_m' \quad (A-80)$$

into Eq. (A-79), Eq. (A-79) becomes

$$\begin{aligned} \frac{\alpha [(\bar{\rho} + \rho') (\bar{u} + u') (\bar{\alpha} + \alpha_m')]}{\partial s} + \frac{\alpha [(\bar{\rho} + \rho') (\bar{v} + v') (\bar{\alpha}_m + \alpha_m')]}{\partial y} \\ = \frac{\partial}{\partial y} [(\bar{\rho} + \rho') D \frac{\partial (\bar{\alpha}_m + \alpha_m')}{\partial y}] \end{aligned} \quad (A-81)$$

Taking the time average of this equation yields

$$\begin{aligned} \bar{\rho} \bar{u} \frac{\partial \bar{\alpha}_m}{\partial s} + (\bar{\rho} \bar{v} + \rho' v') \frac{\partial \bar{\alpha}_m}{\partial y} \\ = \frac{\partial}{\partial y} (\bar{\rho} D \frac{\partial \bar{\alpha}_m}{\partial y}) - \frac{\partial [(\rho v)' \alpha_m']}{\partial y} \end{aligned} \quad (A-82)$$

where the following left hand side terms have been omitted in deriving Eq. (A-82) because of their smallnesses compared with the remaining terms.

$$\overline{\rho' u'} \frac{\partial \bar{\alpha}_m}{\partial s} \ll \overline{\rho' v'} \frac{\partial \bar{\alpha}_m}{\partial y} \quad (\text{A-83})$$

and

$$\frac{\partial [(\rho u)' \alpha_m']}{\partial s} \ll \frac{\partial [(\rho v)' \alpha_m']}{\partial y} \quad (\text{A-84})$$

APPENDIX B

TURBULENT KINETIC ENERGY EQUATION

The momentum equation for compressible fluid flow reads

$$\begin{aligned}
 (\bar{\rho} + \rho') \frac{\partial (\bar{u}_i + u_i')}{\partial t} + (\bar{\rho} + \rho') (\bar{u}_k + u_k') \frac{\partial (\bar{u}_i + u_i')}{\partial x_k} \\
 = - \frac{\partial (\bar{p} + p')}{\partial x_i} + \frac{\partial (\bar{\tau}_{ik} + \tau_{ik}')}{\partial x_k}
 \end{aligned}
 \tag{B-1}$$

where

$$\begin{aligned}
 \tau_{ik} &= \bar{\tau}_{ik} + \tau_{ik}' \\
 &= \underbrace{\mu \left(\frac{\partial u_i}{\partial x_k} + \frac{\partial u_k}{\partial x_i} \right)}_{\text{molecular viscosity}} - \frac{2}{3} \delta_{ik} \underbrace{\frac{\partial u_l}{\partial x_l}}_{\text{bulk viscosity}} + \zeta \delta_{ik} \frac{\partial u_l}{\partial x_l}
 \end{aligned}
 \tag{B-2}$$

The continuity equation is

$$\frac{\partial (\bar{\rho} + \rho')}{\partial t} + \frac{\partial (\bar{\rho} + \rho') (\bar{u}_k + u_k')}{\partial x_k} = 0
 \tag{B-3}$$

thus

$$\frac{\partial (\bar{\rho} + \rho')}{\partial t} + \frac{\partial (\bar{\rho} \bar{u}_k + \bar{\rho} u_k' + \rho' \bar{u}_k + \rho' u_k')}{\partial x_k} = 0
 \tag{B-4}$$

Subtract from Eq. (B-4) its time averaged equation, that is,

$$\frac{\partial \bar{\rho}}{\partial t} + \frac{\partial (\bar{\rho} \bar{u}_k + \overline{\rho' u_k'})}{\partial x_k} = 0
 \tag{B-5}$$

and we obtain

$$\frac{\partial \rho'}{\partial t} + \frac{\partial (\overline{\rho u_k'} + \rho' \overline{u_k} + \rho' u_k' - \overline{\rho' u_k'})}{\partial x_k} = 0 \quad (B-6)$$

Multiplying u_1' by the above equation (B-6), and adding this and Eq. (B-1), we obtain

$$\begin{aligned} & \overline{\rho} \frac{\partial \overline{u_1}}{\partial t} + \overline{\rho} \frac{\partial u_1'}{\partial t} + \rho' \frac{\partial \overline{u_1}}{\partial t} + \rho' \frac{\partial u_1'}{\partial t} + u_1' \frac{\partial \rho'}{\partial t} \\ & + (\overline{\rho} \overline{u_k} + \overline{\rho} u_k' + \rho' \overline{u_k} + \rho' u_k') \frac{\partial (\overline{u_1} + u_1')}{\partial x_k} \\ & + u_1' \frac{\partial (\overline{\rho} u_k' + \rho' \overline{u_k} + \rho' u_k' - \overline{\rho' u_k'})}{\partial x_k} \\ & = - \frac{\partial (\overline{p} + p')}{\partial x_1} + \frac{\partial (\overline{\tau_{1k}} + \tau_{1k}')}{\partial x_k} \end{aligned} \quad (B-7)$$

Subtract from this Eq. (B-7) the time average equation, then

$$\begin{aligned} & \overline{\rho} \frac{\partial u_1'}{\partial t} + \rho' \frac{\partial \overline{u_1}}{\partial t} + \frac{\partial (\rho' u_1' - \overline{\rho' u_1'})}{\partial t} + (\overline{\rho} u_k' + \rho' \overline{u_k} + \rho' u_k' - \overline{\rho' u_k'}) \frac{\partial \overline{u_1}}{\partial x_k} \\ & + (\overline{\rho} \overline{u_k} + \overline{\rho} u_k' + \rho' \overline{u_k} + \rho' u_k') \frac{\partial u_1'}{\partial x_k} - (\overline{\rho} u_k' + \rho' \overline{u_k} + \rho' u_k') \frac{\partial u_1'}{\partial x_k} \\ & + u_1' \frac{\partial (\overline{\rho} u_k' + \rho' \overline{u_k} + \rho' u_k' - \overline{\rho' u_k'})}{\partial x_k} - u_1' \frac{\partial (\overline{\rho u_k'} + \rho' \overline{u_k} + \rho' u_k' - \overline{\rho' u_k'})}{\partial x_k} \\ & = - \frac{\partial p'}{\partial x_1} - \frac{\partial \tau_{1k}'}{\partial x_k} \end{aligned} \quad (B-8)$$

Write the same equation for the velocity component u_j' . Multiply Eq. (B-8) by u_j' and the equation for u_j' by u_1' , and add these two equations obtained, then

$$\begin{aligned}
& \frac{\rho}{\rho} \frac{\partial u_1' u_j'}{\partial t} + \rho' \left(u_j' \frac{\partial \bar{u}_1}{\partial t} + u_1' \frac{\partial \bar{u}_j}{\partial t} \right) + \frac{\partial (\rho' u_1' u_j')}{\partial t} - u_j' \frac{\partial (\rho' u_1')}{\partial t} - u_1' \frac{\partial (\rho' u_j')}{\partial t} \\
& + u_j' (\bar{\rho} u_k' + \rho' \bar{u}_k + \rho' u_k' - \overline{\rho' u_k'}) \frac{\partial \bar{u}_1}{\partial x_k} \\
& + u_1' (\bar{\rho} u_k' + \rho' \bar{u}_k + \rho' u_k' - \overline{\rho' u_k'}) \frac{\partial \bar{u}_j}{\partial x_k} \\
& + (\bar{\rho} \bar{u}_k + \bar{\rho} u_k' + \rho' \bar{u}_k + \overline{\rho' u_k'}) \frac{\partial (u_1' u_j')}{\partial x_k} + 2 u_1' u_j' \frac{\partial (\bar{\rho} u_k' + \rho' \bar{u}_k + \rho' u_k' - \overline{\rho' u_k'})}{\partial x_k} \\
& - u_j' [(\bar{\rho} u_k' + \rho' \bar{u}_k + \rho' u_k') \frac{\partial \bar{u}_1'}{\partial x_k}] - u_1' [(\bar{\rho} u_k' + \rho' \bar{u}_k + \rho' u_k') \frac{\partial \bar{u}_j'}{\partial x_k}] \\
& - u_j' \left[u_1' \frac{\partial (\bar{\rho} u_k' + \rho' \bar{u}_k + \rho' u_k' - \overline{\rho' u_k'})}{\partial x_k} \right] - u_1' \left[u_j' \frac{\partial (\bar{\rho} u_k' + \rho' \bar{u}_k + \rho' u_k' - \overline{\rho' u_k'})}{\partial x_k} \right] \\
& = - u_j' \frac{\partial P'}{\partial x_1} + u_1' \frac{\partial P'}{\partial x_j} + u_j' \frac{\partial \tau_{1k}'}{\partial x_k} + u_1' \frac{\partial \tau_{jk}'}{\partial x_k} \tag{B-9}
\end{aligned}$$

After time averaging Eq. (B-9), the result is written as

$$\begin{aligned}
& \frac{\rho}{\rho} \frac{\partial \overline{(u_1' u_j')}}{\partial t} + \overline{\rho' u_j'} \frac{\partial \bar{u}_1}{\partial t} + \overline{\rho' u_1'} \frac{\partial \bar{u}_j}{\partial t} + \frac{\partial (\rho' u_1' u_j')}{\partial t} \\
& + (\bar{\rho} \overline{u_j' u_k'} + \overline{\rho' u_j' u_k'} + \overline{\rho' u_j' u_k'}) \frac{\partial \bar{u}_1}{\partial x_k}
\end{aligned}$$

$$\begin{aligned}
& + (\overline{\rho u_1' u_k'} + \overline{\rho' u_1' u_k} + \overline{\rho' u_1' u_k'}) \frac{\partial u_j}{\partial x_k} \\
& + \left[\overline{(\rho u_k' + \rho' \bar{u}_k + \rho' u_k')} \frac{\partial (u_1' u_j')}{\partial x_k} \right] + \overline{\rho' u_k} \frac{\partial (\rho_1' u_j')}{\partial x_k} \\
& + 2 \left[u_1' u_j' \frac{\partial (\overline{\rho u_k'} + \rho' \bar{u}_k + \rho' u_k' - \rho' u_k')} {\partial x_k} \right] \\
= & - \left[u_j' \frac{\partial P'}{\partial x_1} + u_1' \frac{\partial P'}{\partial x_j} \right] + \left[u_j' \frac{\partial \tau_{1k}'}{\partial x_k} + u_1' \frac{\partial \tau_{1k}'}{\partial x_k} \right]
\end{aligned}
\tag{B-10}$$

where

$$\begin{aligned}
& \overline{\rho u_k' \frac{\partial (u_1' u_j')}{\partial x_k}} + 2 u_1' u_j' \frac{\partial (\overline{\rho u_k'})}{\partial x_k} \\
= & u_1' u_j' \frac{\partial (\overline{\rho u_k'})}{\partial x_k} + \frac{\partial (\overline{\rho u_1' u_j' u_k'})}{\partial x_k}
\end{aligned}
\tag{B-11}$$

\uparrow
 Diffusion of the correlation $u_1' u_j'$
 by the turbulent motion itself

This term is dropped for the incompressible flow, since

$$\frac{\partial (\overline{u_k} + u_k')}{\partial x_k} = 0, \quad (A) \qquad \frac{\partial (\overline{u_k} + u_k')}{\partial x_k} = 0 \quad (B)$$

$$(A) - (B) \Rightarrow \frac{\partial u_k'}{\partial x_k} = 0$$

Substitute Eq. (B-6) into Eq. (B-11), we obtain

$$\begin{aligned}
 & \overline{\rho} \left[\overline{u_k'} \frac{\partial(u_1' u_j')}{\partial x_k} \right] + 2 \left[\overline{u_1' u_j'} \frac{\partial(\rho u_k')}{\partial x_k} \right] \\
 & = - \left[\overline{u_1' u_j'} \left\{ \frac{\partial(\rho' \overline{u_k} + \rho' u_k' - \overline{\rho' u_k'})}{\partial x_k} \right\} + \frac{\partial \rho'}{\partial t} \right] + \frac{\partial(\overline{\rho u_1' u_j' u_k'})}{\partial x_k}
 \end{aligned}
 \tag{B-12}$$

Thus Eq. (B-10) is rewritten as follows:

$$\begin{aligned}
 & \overline{\rho} \frac{\partial(u_1' u_j')}{\partial t} + \overline{\rho' u_j'} \frac{\partial \overline{u_1}}{\partial t} + \overline{\rho' u_1'} \frac{\partial \overline{u_j}}{\partial t} + \frac{\partial(\rho' u_1' u_j')}{\partial t} \\
 & + \overline{(\rho u_k)'} u_j' \frac{\partial \overline{u_1}}{\partial x_k} + \overline{(\rho u_k)'} u_1' \frac{\partial \overline{u_j}}{\partial x_k} + \frac{\partial(\overline{\rho u_1' u_j' u_k'})}{\partial x_k} \\
 & + \left[\overline{(\rho' \overline{u_k} + \rho' u_k')} \frac{\partial(u_1' u_j')}{\partial x_k} \right] + \overline{\rho' u_k} \frac{\partial(u_1' u_j')}{\partial x_k} \\
 & + \left[\overline{u_1' u_j'} \frac{\partial(\rho' \overline{u_k} + \rho' u_k' - \overline{\rho' u_k'})}{\partial x_k} \right] - \overline{u_1' u_j'} \frac{\partial \rho'}{\partial t} \\
 & = - \left[\frac{\partial(\overline{\rho' u_j'})}{\partial x_i} + \frac{\partial(\overline{\rho' u_1'})}{\partial x_j} \right] + \left[\overline{p'} \left(\frac{\partial u_j'}{\partial x_i} \frac{\partial u_1'}{\partial x_j} \right) \right] + \left[\overline{u_j' \frac{\partial \tau_{ik}'}{\partial x_k} + u_1' \frac{\partial \tau_{jk}'}{\partial x_k}} \right]
 \end{aligned}$$

\uparrow
 The general pressure
diffusion terms

\uparrow
 The tendency-
towards isotropy
term

(B-13)

Since

$$\begin{aligned}
 & \overline{(\rho' u_k + \rho' u_k')} \frac{\partial (\overline{u_1' u_j'})}{\partial x_k} + \overline{u_1' u_j'} \frac{\partial (\overline{\rho' u_k'})}{\partial x_k} + \overline{u_1' u_j'} \frac{\partial (\overline{\rho' u_k'})}{\partial x_k} \\
 & = \frac{\partial (\overline{\rho' u_k u_1' u_j'})}{\partial x_k} + \frac{\partial (\overline{\rho' u_k' u_1' u_j'})}{\partial x_k} \quad (B-14)
 \end{aligned}$$

Eq. (B-13) is written for steady flow as

$$\begin{aligned}
 & \overline{(\rho u_k)' u_1'} \frac{\partial \overline{u_j'}}{\partial x_k} + \overline{(\rho u_k)' u_1' \frac{\partial u_j'}{\partial x_k}} + \frac{\partial (\overline{\rho u_1' u_j' u_k'})}{\partial x_k} \\
 & + \frac{\partial (\overline{\rho' u_k u_1' u_j'})}{\partial x_k} + \frac{\partial (\overline{\rho' u_1' u_j' u_k'})}{\partial x_k} + \overline{\rho u_k} \frac{\partial (\overline{u_1' u_j'})}{\partial x_k} - \overline{u_1' u_j'} \frac{\partial \overline{\rho' u_k'}}{\partial x_k} \\
 & = \left[\frac{\partial (\overline{p' u_j'})}{\partial x_1} + \frac{\partial (\overline{p' u_1'})}{\partial x_j} \right] + \left[p' \left(\frac{\partial u_j'}{\partial x_1} \frac{\partial u_1'}{\partial x_j} \right) + \left[u_j' \frac{\partial \tau_{1k}'}{\partial x_k} + u_1' \frac{\partial \tau_{jk}'}{\partial x_k} \right] \right] \quad (B-15)
 \end{aligned}$$

where

$$\frac{\partial (\overline{\rho u_1' u_j' u_k'})}{\partial x_k} + \frac{\partial (\overline{\rho' u_k u_1' u_j'})}{\partial x_k} + \frac{\partial (\overline{\rho' u_1' u_j' u_k'})}{\partial x_k} = \frac{\partial [(\overline{\rho u_k})' u_1' u_j']}{\partial x_k} \quad (B-16)$$

and

$$\overline{-u_1' u_j'} \frac{\partial \overline{\rho' u_k'}}{\partial x_k} = - \frac{\partial [(\overline{\rho' u_k'}) (\overline{u_1' u_j'})]}{\partial x_k} + \overline{\rho' u_k'} \frac{\partial \overline{u_1' u_j'}}{\partial x_k} \quad (B-17)$$

Thus Eq. (B-15) is

$$\begin{aligned}
 & \overline{(\rho u_k)' u_j'} \frac{\partial \bar{u}_i}{\partial x_k} + \overline{(\rho u_k)' u_i'} \frac{\partial \bar{u}_j}{\partial x_k} + \frac{\partial [(\rho u_k)' u_i' u_j']}{\partial x_k} - \frac{\partial [(\rho' u_k') (\overline{u_i' u_j'})]}{\partial x_k} \\
 & + (\bar{\rho} \bar{u}_k + \overline{\rho' u_k'}) \frac{\partial (\overline{u_i' u_j'})}{\partial x_k} \\
 = & - \left[\frac{\partial (\overline{p' u_j'})}{\partial x_i} + \frac{\partial (\overline{p' u_i'})}{\partial x_j} \right] + \left[\overline{p' \left(\frac{\partial u_j'}{\partial x_i} + \frac{\partial u_i'}{\partial x_j} \right)} \right] + \left[\overline{u_j' \frac{\partial \tau_{ik}'}{\partial x_k} + u_i' \frac{\partial \tau_{jk}'}{\partial x_k}} \right]
 \end{aligned}
 \tag{B-18}$$

Let us assume

$$\frac{\partial [(\rho u_k)' u_i' u_j']}{\partial x_k} - \frac{\partial [(\rho' u_k') (\overline{u_i' u_j'})]}{\partial x_k} = \frac{\partial (\overline{\rho u_i' u_j' u_k'})}{\partial x_k}
 \tag{B-19}$$

then we have a system of turbulent fluctuation equation in a simple form as

$$\begin{aligned}
 & \overline{(\rho u_k)' u_j'} \frac{\partial \bar{u}_i}{\partial x_k} + \overline{(\rho u_k)' u_i'} \frac{\partial \bar{u}_j}{\partial x_k} + \frac{\partial (\overline{\rho u_i' u_j' u_k'})}{\partial x_k} + (\bar{\rho} \bar{u}_k + \overline{\rho' u_k'}) \frac{\partial (\overline{u_i' u_j'})}{\partial x_k} \\
 = & - \left[\frac{\partial (\overline{p' u_j'})}{\partial x_i} + \frac{\partial (\overline{p' u_i'})}{\partial x_j} \right] + \left[\overline{p' \left(\frac{\partial u_j'}{\partial x_i} + \frac{\partial u_i'}{\partial x_j} \right)} \right] + \left[\overline{u_j' \frac{\partial \tau_{ik}'}{\partial x_k} + u_i' \frac{\partial \tau_{jk}'}{\partial x_k}} \right]
 \end{aligned}
 \tag{B-20}$$

As Eq. (B-2) showed

$$\begin{aligned}\tau_{ik} &= \bar{\tau}_{ik} + \tau_{ik}' \\ &= \mu \left(\frac{\partial u_i}{\partial x_k} + \frac{\partial u_k}{\partial x_i} - \frac{2}{3} \delta_{ik} \frac{\partial u_l}{\partial x_l} \right) + \zeta \delta_{ik} \frac{\partial u_l}{\partial x_l}\end{aligned}$$

thus neglecting the bulk viscosity term, we have

$$\tau_{ik}' = \mu \left(\frac{\partial u_i'}{\partial x_k} + \frac{\partial u_k'}{\partial x_i} - \frac{2}{3} \delta_{ik} \frac{\partial u_l'}{\partial x_l} \right) \quad (B-21)$$

Let us assume

$$u_j' \frac{\partial}{\partial x_k} \left[\mu \left(\frac{\partial u_i'}{\partial x_j} - \frac{2}{3} \delta_{ij} \frac{\partial u_l'}{\partial x_l} \right) \right] + u_i' \frac{\partial}{\partial x_k} \left[\mu \left(\frac{\partial u_i'}{\partial x_j} - \frac{2}{3} \delta_{jk} \frac{\partial u_l'}{\partial x_l} \right) \right] = 0 \quad (B-22)$$

then the last term on the left hand side of Eq. (B-20) becomes

$$\begin{aligned}\left[u_j' \frac{\partial \tau_{ik}'}{\partial x_k} + u_i' \frac{\partial \tau_{jk}'}{\partial x_k} \right] &= u_j' \frac{\partial}{\partial x_k} \left(\mu \frac{\partial u_i'}{\partial x_k} \right) + u_i' \frac{\partial}{\partial x_k} \left(\mu \frac{\partial u_j'}{\partial x_k} \right) \\ &= \frac{\partial}{\partial x_k} \left(\mu \frac{\partial u_i' u_j'}{\partial x_k} \right) - 2\mu \frac{\partial u_i'}{\partial x_k} \frac{\partial u_j'}{\partial x_k} \\ &\quad - \frac{\partial}{\partial x_k} \left(\mu \frac{\partial u_i' u_j'}{\partial x_k} \right) - 2\mu \frac{\partial u_i'}{\partial x_k} \frac{\partial u_j'}{\partial x_k}\end{aligned} \quad (B-23)$$

Therefore Eq. (B-20) is simplified to

[Turbulent Fluctuation Equations]

$$\begin{aligned} & \overline{(\rho u_k)' u_j'} \frac{\partial \bar{u}_i}{\partial x_k} + \overline{(\rho u_k)' u_i'} \frac{\partial \bar{u}_j}{\partial x_k} + \frac{\partial (\rho u_i' u_j' u_k')}{\partial x_k} + (\bar{\rho} \bar{u}_k + \overline{\rho' u_k'}) \frac{\partial \overline{u_i' u_j'}}{\partial x_k} \\ &= - \left(\frac{\partial \overline{P' u_j'}}{\partial x_i} + \frac{\partial \overline{P' u_i'}}{\partial x_j} \right) + \overline{P'} \left(\frac{\partial u_j'}{\partial x_i} + \frac{\partial u_i'}{\partial x_j} \right) \frac{\partial}{\partial x_k} \left(\mu \frac{\partial u_i' u_j'}{\partial x_k} \right) - 2\mu \frac{\partial u_i'}{\partial x_k} \frac{\partial u_j'}{\partial x_k} \end{aligned}$$

(B-24)

Add three equations above for $i=j=1, 2, \text{ and } 3$ considering the boundary layer assumption, then we obtain the following turbulent kinetic energy equation:

[Turbulent Kinetic Energy Equation]

$$\begin{aligned} \bar{\rho} \bar{u} \frac{\partial K}{\partial x} + (\bar{\rho} \bar{v} + \overline{\rho' v'}) \frac{\partial K}{\partial y} &= - 2 \overline{(\rho v)' u'} \frac{\partial \bar{u}}{\partial y} \\ &+ \frac{\partial}{\partial y} \left[\mu \frac{\partial K}{\partial y} - \overline{(\rho K_0 + 2P') v'} - 2 \mu \left(\overline{\frac{\partial u'}{\partial y} \frac{\partial u'}{\partial y}} + \overline{\frac{\partial v'}{\partial y} \frac{\partial v'}{\partial y}} + \overline{\frac{\partial w'}{\partial y} \frac{\partial w'}{\partial y}} \right) \right] \end{aligned}$$

(B-25)

where

$$K_0 = \overline{u' u'} + \overline{v' v'} + \overline{w' w'}$$

and

$$K = \overline{u' u'} + \overline{v' v'} + \overline{w' w'}$$